ACTA PROTOZOOLOGICA

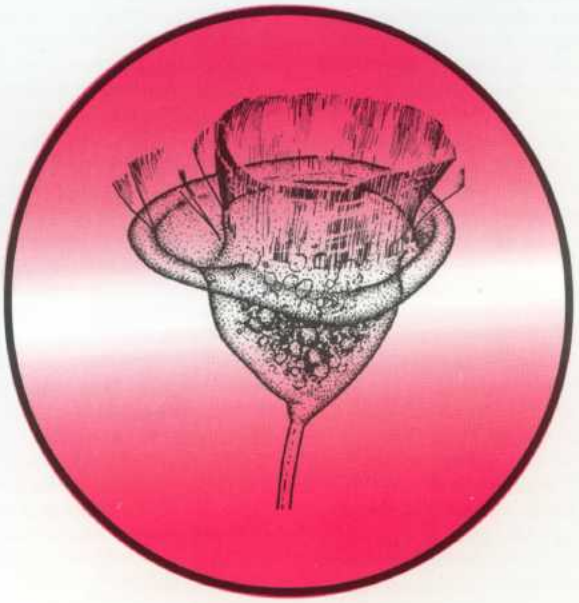

NENCKI INSTITUTE OF EXPERIMENTAL BIOLOGY
WARSAW, POLAND
2001
VOLUME 40 NUMBER 4
ISSN 0065-1583

Polish Academy of Sciences
Nencki Institute of Experimental Biology
and
Polish Society of Cell Biology

ACTA PROTOZOOLOGICA
International Journal on Protistology

ACTA PROTOZOOLOGICA appears quarterly.

The price (including Air Mail postage) of subscription to ACTA PROTOZOOLOGICA at 2002 is: US $ 200.- by institutions and US $ 120.- by individual subscribers. Limited numbers of back volumes at reduced rate are available. TERMS OF PAYMENT: check, money oder or payment to be made to the Nencki Institute of Experimental Biology account: 111-01053-401050001074 at Państwowy Bank Kredytowy XIII Oddz. Warszawa, Poland. For matters regarding ACTA PROTOZOOLOGICA, contact Editor, Nencki Institute of Experimental Biology, ul. Pasteura 3, 02-093 Warszawa, Poland; Fax: (4822) 822 53 42; E-mail: jurek@ameba.nencki.gov.pl For more information see Web page **http://www.nencki.gov.pl/ap.htm**).

Front cover: Song W. and Warren A. (2000) A redescription of *Pseudovorticella patellina* (O. F. Müller, 1776) nov. comb., a Peritrichous ciliate (Protozoa: Ciliophora: Peritrichida) isolated from mariculture biotopes in North China. *Acta Protozool.* **39:** 43-50

This publication is supported by the State Committee for Scientific Research

Desktop processing: Justyna Osmulska, Data Processing Laboratory of the Nencki Institute
Printed at the MARBIS, ul. Kombatantów 60, 05-070 Sulejówek, Poland

Acta Protozool. (2001) 40: 235 - 247

ACTA
PROTOZOOLOGICA

Minipodia, the Adhesive Structures Active in Locomotion and Endocytosis of Amoebae

Andrzej GRĘBECKI, Lucyna GRĘBECKA and Anna WASIK

Department of Cell Biology, Nencki Institute of Experimental Biology, Warszawa, Poland

Summary. *Amoeba proteus* cells, strains A and C_t, with well pronounced motor polarity (the polytactic and orthotactic forms) develop dense coats of discrete minipodia which anchor them to the glass substratum. The scanning electron microscopy demonstrates that minipodia are surface microprotrusions about 0.5 μm thick and up to 8 μm long, covering mainly the middle-anterior area of the ventral cell surface. They are few at the frontal zone and absent at the tail region. It means that the dense felt of discrete minipodia is located in the same region which has been earlier described as the zone of most efficient adhesion of a directionally moving amoeba. The cells without stable motor polarity and those which adhere to the glass without moving, or just start locomotion, lack areas covered by discrete minipodia; instead, minipodia are grouped in rosette contacts, which have the form of papillae composed of supporting platforms with crones of minipodia projected from them. The cells detached from the substratum by simple experimental procedures: radiate heterotactic forms produced by mechanical shocks, anucleate fragments obtained by microdissection, and amoebae in course of cation-induced pinocytosis, neither have separate minipodia nor rosette contacts. In contrast, during phagocytosis amoebae strongly adhere and produce dense sheaths of discrete minipodia extending along the whole surface up to the tail, except the naked front enclosing the phagosome. It was demonstrated by staining with the fluorescein-conjugated phalloidin that both types of adhesive structures: the discrete minipodia as well as the rosette contacts are very rich in the cytoskeletal F-actin.

Key words: adhesive organelles, *Amoeba proteus,* amoeboid movement, minipodia, rosette contacts.

INTRODUCTION

The discovery that *Amoeba proteus* cells are not flatly spread over the substratum, but contact with it at discrete points, is due to side-view observations of their movement in a horizontally mounted classical light microscope. Dellinger (1906) in his pioneer work concluded that amoebae do not creep but "walk", supported by vertical pseudopods similar to those seen in the horizontal plane, but growing downwards. *A. proteus* has been studied again in side-view by Bell and Jeon (1963) and Grębecki (1976), while Haberey (1971) and Opas (1978) examined its contacts with the substratum in the reflection interference microscope (devised by Curtis 1964).

The cell-to-substratum attachment sites seen in side-view, called contact pseudopods or supporting knobs (Bell and Jeon 1963, Grębecki 1976), are stable in reference to the substratum in the firm adhesion zone,

Address for correspondence: Andrzej Grębecki, Department of Cell Biology, Nencki Institute of Experimental Biology, ul. Pasteura 3, 02-093 Warszawa, Poland; Fax: (04822) 8225342; E-mail: grebecki@nencki.gov.pl

but the "young" ones which are frontally located and are not yet attached, as well as the "old" ones being gradually detached in the rear, may glide over the glass surface. The fixed and gliding contact sites were also discerned at the same positions by reflection interference microscopy (Opas 1978). The most efficient adhesion zone in *A. proteus* was localised, by frame-by-frame analysis of time lapse motion pictures taken in side-view, at the middle-anterior region of the ventral cell surface, approximately at $^1/_3$ of the cell length behind the leading edge (Grębecki 1976). As a result, the posterior $^2/_3$ of amoeba body decrease in size during locomotion, while the anterior $^1/_3$ grows up (Grębecka and Grębecki 1975). Another consequence of such position of the firm adhesion zone is a centripetal retraction of the whole contractile cortical cytoskeleton of amoeba toward these attachment sites (Grębecki 1984).

A smaller species of amoeba, *Naegleria gruberi,* has been more intensely studied by reflection interference microscopy than *A. proteus* (Preston and King 1978 a, b; King *et al.* 1979, 1983 a, b). In *Naegleria* small spots of "close contact" with a 20 nm separation gap between the cell and the substratum are linked to much larger platforms of more loose "associated contact" with about 100 nm separation gaps.

However, neither the reflection interference maps of cell-to-substratum distance, nor the low resolution side-view pictures taken under poor optical conditions, cannot provide information about the fine morphology of the contact sites of amoebae at the ultrastructural level. In the present study we have applied in this purpose the scanning electron microscopy, and have examined the cell surface of *A. proteus* inside and outside its adhesive areas, under conditions allowing or excluding the attachment of these cells to the substratum. Since in a precedent paper (Grębecka *et al.* 1997) we have described the punctate distribution of F-actin at the lower surface of *A. proteus* and demonstrated by confocal microscopy connections of the cortical actin cytoskeleton of amoeba with the substratum contact sites, in the present research we have also tested the revealed adhesive structures for F-actin, by phalloidin staining.

Preliminary findings were reported elsewhere (Grębecki *et al.* 2001).

MATERIALS AND METHODS

Amoeba proteus cells belonged to two strains: the most common strain A originating from Edinburgh (Jeon and Lorch 1973), and the clone C_t of the strain C originating from Sankt Petersburg, isolated by Nikolajeva *et al.* (1980), which is almost transparent because of the absence of crystalic inclusions and apparently better adheres to glass substratum. Cultures were grown in unmodified Pringsheim medium, at room temperature, and fed twice a week on *Tetrahymena pyriformis.* The cell samples were fixed in 3.5% paraformaldehyde with 0.5% acrolein, dissolved in phosphate buffered Pringsheim medium.

For scanning electron microscopy (SEM) the fixed amoebae were dehydrated through a graded series of ethanol and acetone, dried by the CO_2 critical point technique, and then coated with carbon and gold. They were examined in a Jeol 1200 EX transmission electron microscope with an ASID 19 scanning attachment, operating at 80 KV and original magnification ranging from x250 to x20 000.

F-actin filaments were stained, after the same fixation as described above, with 1% phalloidin labelled with fluorescein isothiocyanate (Sigma, St. Louis) and examined in a fluorescence microscope (FLM), Nikon Diaphot with an epifluorescence device.

Living amoebae were observed in a PZO Biolar microscope with differential interference contrast (DIC). Microdissections were performed with a de Fonbrune micromanipulator. Pinocytosis was induced by 100 mM KCl solution, and phagocytosis by introducing heliozoa (*Actinophrys sol*) and/or ciliates (*Tetrahymena pyriformis*).

RESULTS

Amoebae which were unidirectionally moving at the moment of fixation (Figs 1-3, 14) have a distinct motor polarity, expressed by differentiation of distended frontal regions (F) which produce advancing pseudopods (AP), and the corrugated retracting tails (T) with many membrane folds and wrinkles (W). The specimens seen from the upper side, in the strain A (Fig. 1) as well as in the strain C_t (not shown) look naked, without any more delicate protrusions at the surface. Other strain A amoebae, which presumably expose their bottom sides up (Figs 2, 3), display at low magnification a dense pattern of miniature protuberances along frontal advancing pseudopods and between them. This difference between the two opposite cell sides, one of them being smooth and another producing microprotrusions, could be in several instances examined in the same amoeba by rotating it in SEM at 45° in two directions.

We adopt for these microprotuberances beneath the ventral surface of amoebae, the name of "minipodia", which was given by Cheng (1992) to adhesive microprotrusions revealed by him by video-enhanced DIC light microscopy under lamellipodia of living 3T3 fibroblasts.

Minipodia are absent from the surface of folds and wrinkles at the posterior regions of normally polarized strain A amoebae (Figs 2, 3, 5). In such locomoting cells

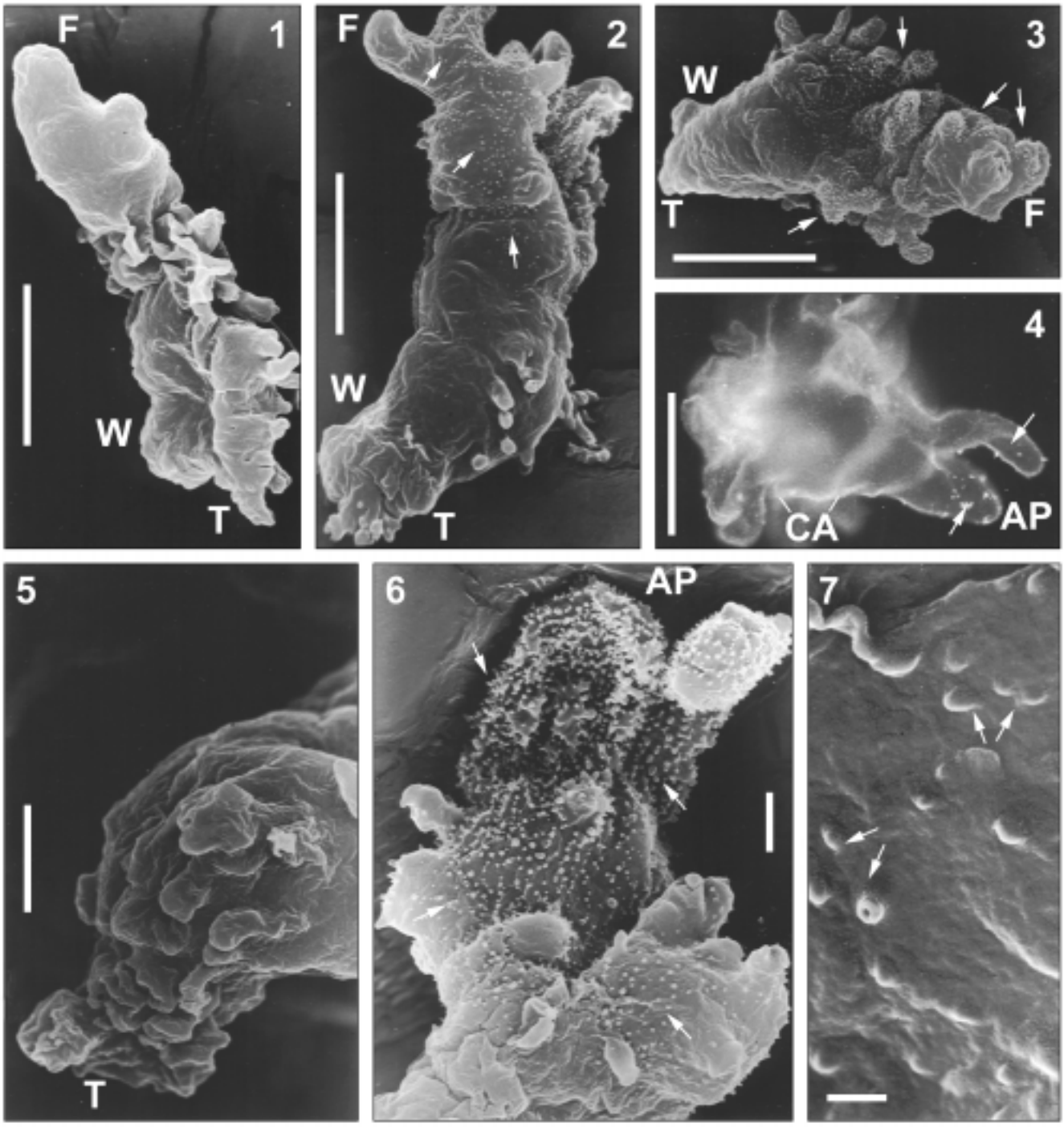

Figs 1-7. *Amoeba proteus,* strain A, cells with the established motor polarity: well differentiated fronts (F) with smooth growing pseudopods (AP), and retracting tails (T) with folds and wrinkles (W); SEM (1-3, 5-7) and FLM (4) pictures. **1** - dorsal side of a locomoting specimen; **2, 3** - two moving amoebae shown from the ventral side; minipodia (arrows) are seen as small nodules dispersed at the frontal region and on the advancing pseudopods; **4** - punctated F-actin fluorescence (arrows) at the walls of advancing pseudopods and the continuous cortical actin layer along the cell body (CA); **5** - absence of any surface microprotrusions at the corrugated tail; **6** - profusion of minipodia (arrows) at the anterior region, pseudopods included; **7** - a higher magnification demonstrating that minipodia really are three-dimensional microprojections of the cell surface. Scale bars - **1-4** - 100 μm; **5, 6** - 20 μm; **7** - 2 μm

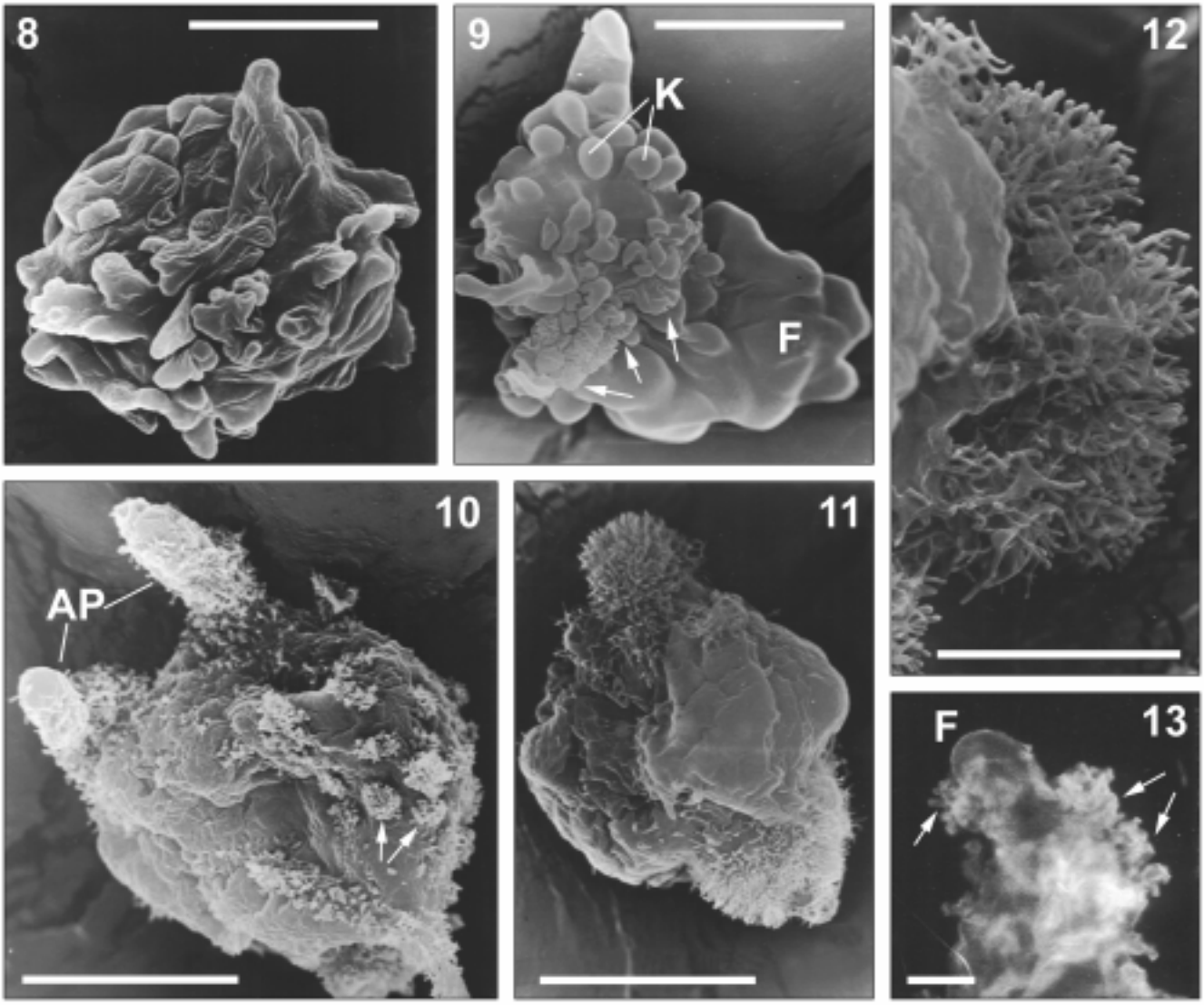

Figs 8-13. *Amoeba proteus,* strain A, cells recovering the motor polarity and the substratum attachment; SEM (8-12) and FLM (13) pictures. **8** - non-polarized amoeba in form of a corrugated sphere, unattached to the substratum; **9** - amoeba beginning to develop the frontal zone (F), supporting knobs (K) which probably extend to the substratum, and presumable precursors of minipodia (arrows); **10** - a smooth spherical form producing two pseudopods (AP) with randomly spread minipodia, and other minipodia grouped in adhesive papillae (arrows); **11, 12** - two magnifications of prominent bunches of branched minipodia larger than the typical adhesive papillae; **13** - fluorescent F-actin aggregations (arrows), just behind the frontal pseudopodium (F), corresponding in shape to the adhesive papillae with minipodia shown in SEM. Scale bars - **8-11** - 100 μm; **12, 13** - 20 μm

minipodia are merely produced on the smooth surface of the anterior $^{1}/_{3}$ - $^{1}/_{2}$ part of the ventral area (Fig. 2) and often also on the frontal pseudopods (Figs 3, 6). Dots of F-actin stained with fluorescein-conjugated phalloidin are similar in shape, size and localisation on the walls of advancing pseudopods (Fig. 4). Figure 7 demonstrates in a higher SEM magnification that in the strain A minipodia of normal locomoting forms represent short microprotuberances emerging directly from the cell surface, and are spread beneath the middle-anterior body regions at random. Probably, the zone of efficient adhesion is in reality more restricted, than the area occupied by minipodia (Figs 2, 3), because the first minipodia at the front may be not yet attached and those in the rear already detached from the substratum.

In normal cultures one can always find some strongly corrugated spherical cells, non-polarized and unattached. Such spheres (Fig. 8) do not have any minipodia. How-

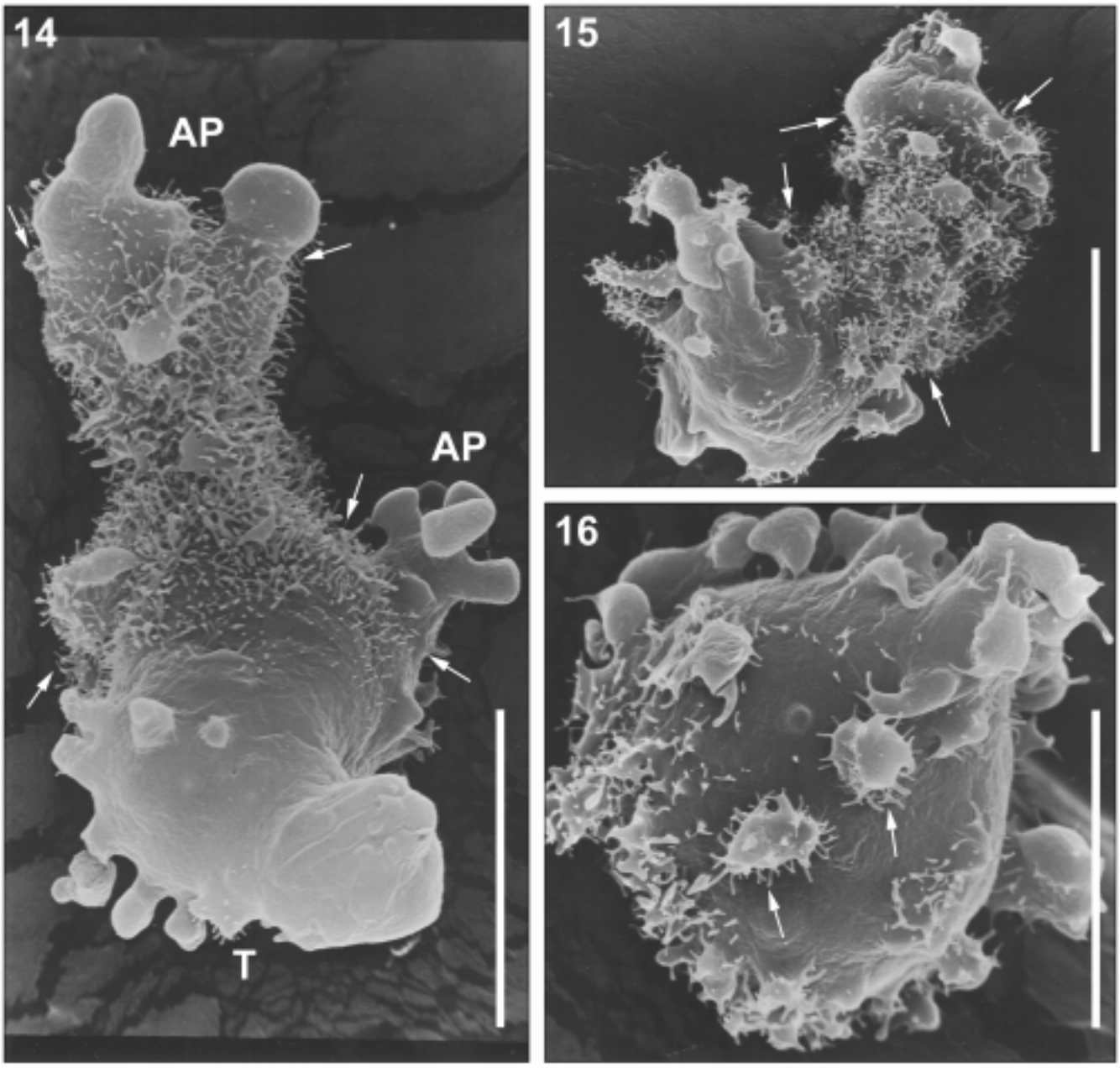

Figs 14-16. Distribution and configuration of minipodia in the strain C_t of *A. proteus*; SEM. **14** - a locomoting cell without microprotrusions on the frontal and lateral advancing pseudopods (AP) and on the posterior region (T), but with sharply delimited adhesion zone randomly covered by hair-like minipodia (between arrows); **15** - abundance of adhesive papillae (arrows) at the ventral surface of a specimen with uncertain direction of locomotion; **16** - composition of adhesive papillae (arrows) in a non-polarized amoeba; note the basal platforms and crones of minipodia projected around from them. Scale bars - 100 μm

ever, they are capable of spontaneously re-attaching to the substratum, re-establishing the antero-posterior polarity and resuming locomotion. Simultaneously with the recovery of motor polarity of amoeba by reconstruction of the frontal zone (Fig. 9) some supporting knobs leaning against the substratum form cauliflower-like papillae with strongly folded surface (arrows). Possibly, they are precursors of minipodia. The corrugated spheres may also smoothen and start producing pseudopods (Fig. 10). In such specimens minipodia are well developed, and are also grouped in papillae (arrows) on the cell body surface and randomly spread on the advancing pseudopods. Figures 11 and 12 show that sometimes minipodia are aggregated in massive bunches much larger than the

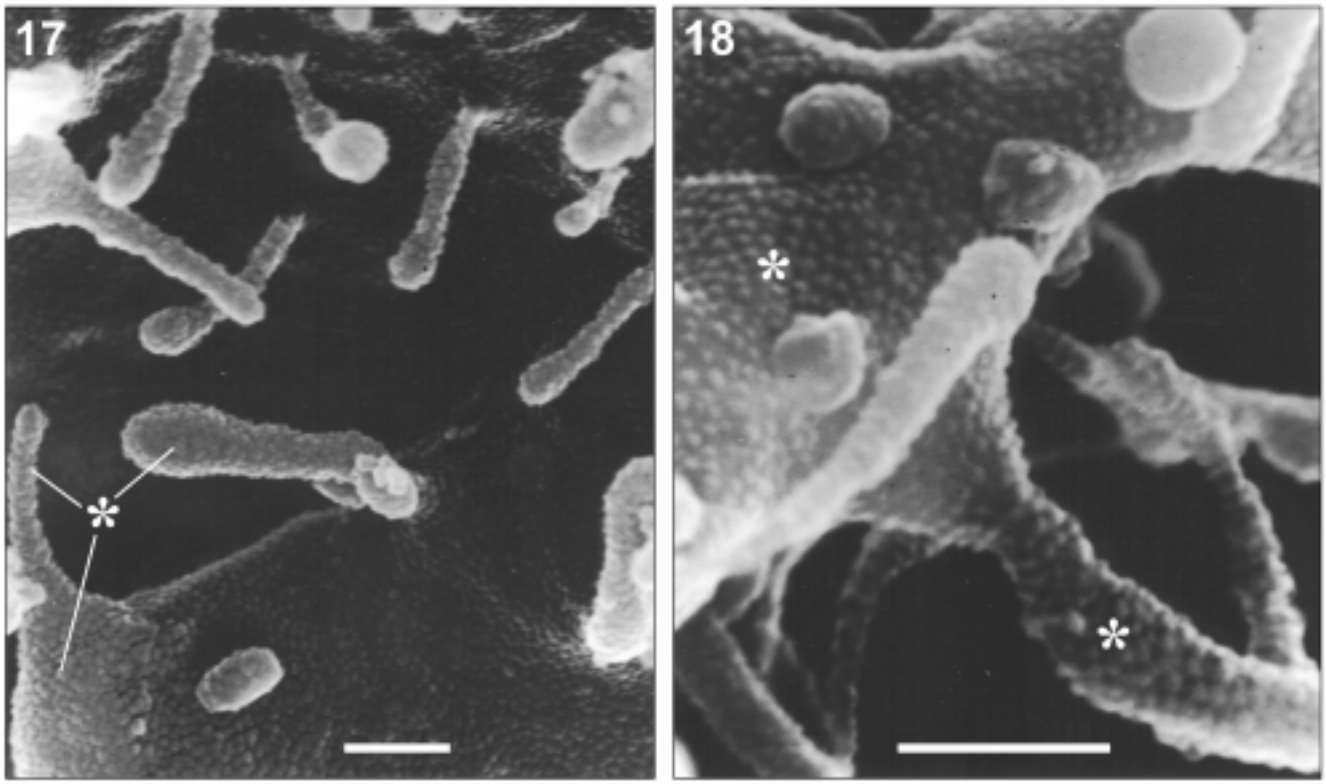

Figs 17, 18. High magnification of minipodia of *A. proteus,* strain C_t; SEM. Note the same external texture of minipodia and of the cell surface from which they emerge (asterisks); further explanations in the text. Scale bars - 1 μm

typical papillae; wrinkling of the whole surface around these bunches suggests that such strong aggregations may result from general contraction of some cells, either spontaneous or provoked by fixation. The typical cauliflower-like papillae with microprotrusions were detected behind the fronts of normal locomoting amoebae also by staining F-actin with fluorescent phalloidin (Fig. 13).

The papillae producing minipodia may be alternatively called ”rosette contacts”. This name introduced by David-Pfeuty and Singer (1980) was later applied (e.g. by Chen 1989) to composite surface protrusions of transformed cells equivalent to the podosomes.

In the strain C_t of *A. proteus* the minipodia, spread at random or grouped in rosette contacts, are better developed and it is easier to examine their structure and distribution, than in the common strain A. In directionally moving specimens with distinct antero-posterior polarity (Fig. 14) the discrete long minipodia densely cover middle-anterior zone of the ventral surface, rather sharply delimited (arrows) from the naked walls of the advancing pseudopods and of the retracted posterior body regions. It is exactly this position, which is commonly indicated by experiments in living material, as the cell-to-substratum adhesion zone in a locomoting *A. proteus.* In some forms with unclear motor polarity (Fig. 15) and spherical ones (Fig. 16) the rosette contacts (arrows) are the dominating type of adhesive structures, and their conformation may be distinctly seen: they are composed each of a supporting platform with the emerging hair-like minipodia.

The separate minipodia and the rosette contacts emerge not only from the surface directly facing the substratum, but are produced as well by both lateral edges of amoeba (Figs 14, 15), where they are seen in side-view (compare Fig. 6 in Gręb ecki *et al.* 2001). These lateral projections may pull amoeba to the sides over the substratum, which explains cell spreading and flattening with the increase of adhesion.

At higher magnifications (Figs 17, 18) the minipodia of *A. proteus* belonging to the strain C_t appear as clavate projections about 0.5 μm thick and up to 8 μm long, often expanded at the tips. Their surface has the same ”lizard

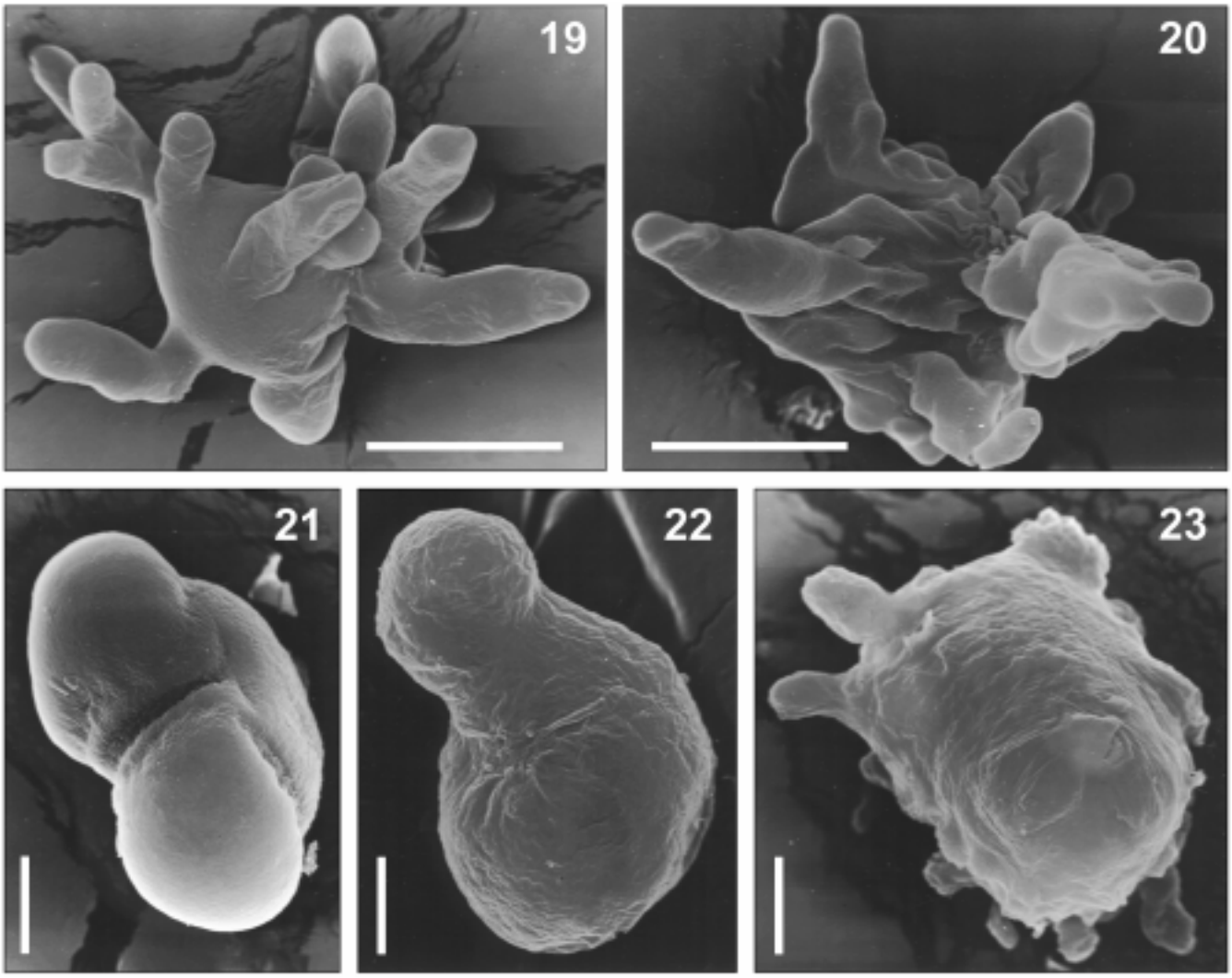

Figs 19-23. Absence of minipodia on the surface of experimentally produced non-adhesive forms of *A. proteus*; SEM. **19** - heterotactic specimen belonging to the strain C_t; **20** - heterotactic specimen belonging to the strain A; **21** - rounded and smooth anucleate fragment of amoeba belonging to the strain C_t; **22** - rounded and slightly wrinkled anucleate fragment of amoeba belonging to the strain A; **23** - another anucleate fragment of a strain A amoeba, transiently contracting and producing short pseudopods. Scale bars - **19, 20, 23** - 100 μm; **21, 22** - 20 μm

skin" texture as the cell surface from which they derive (asterisks). Exactly the same texture of the surface was seen in a SEM micrograph of *A. proteus* pinocytising egg albumin, published by Klein *et al.* (1988), and attributed to absorption of this protein by the external mucopolysaccharide sheet; in our experiments however, the "lizard skin" appeared without exposing the surface of amoebae to any coagulating agent, except coating it with gold and carbon.

All amoebae of both strains, shown in Figs 1-7 and 9-18, were at the moment of fixation either migrating on the surface of a cover slip or at least steadily attached to it. At the next step in contrast, we have examined in SEM, as a control, amoebae subjected to some simple experimental procedures, which deprive them of adhesiveness to the substratum.

Mechanical shocks (e.g., shaking the culture or strong pipetting a sample) produce the forms called heterotactic (Grębecki and Grębecka 1978) which have a radial symmetry and extend very long pseudopods in all directions; heterotactic amoebae freely float in the medium or loosely settle on the bottom without attachment. In fact, we never found any minipodia in these forms, neither in the strain C_t (Fig. 19) nor A (Fig. 20).

It is known from a long time (see e.g., Clark 1942, Lorch 1969, Grębecka 1977) that the anucleate frag-

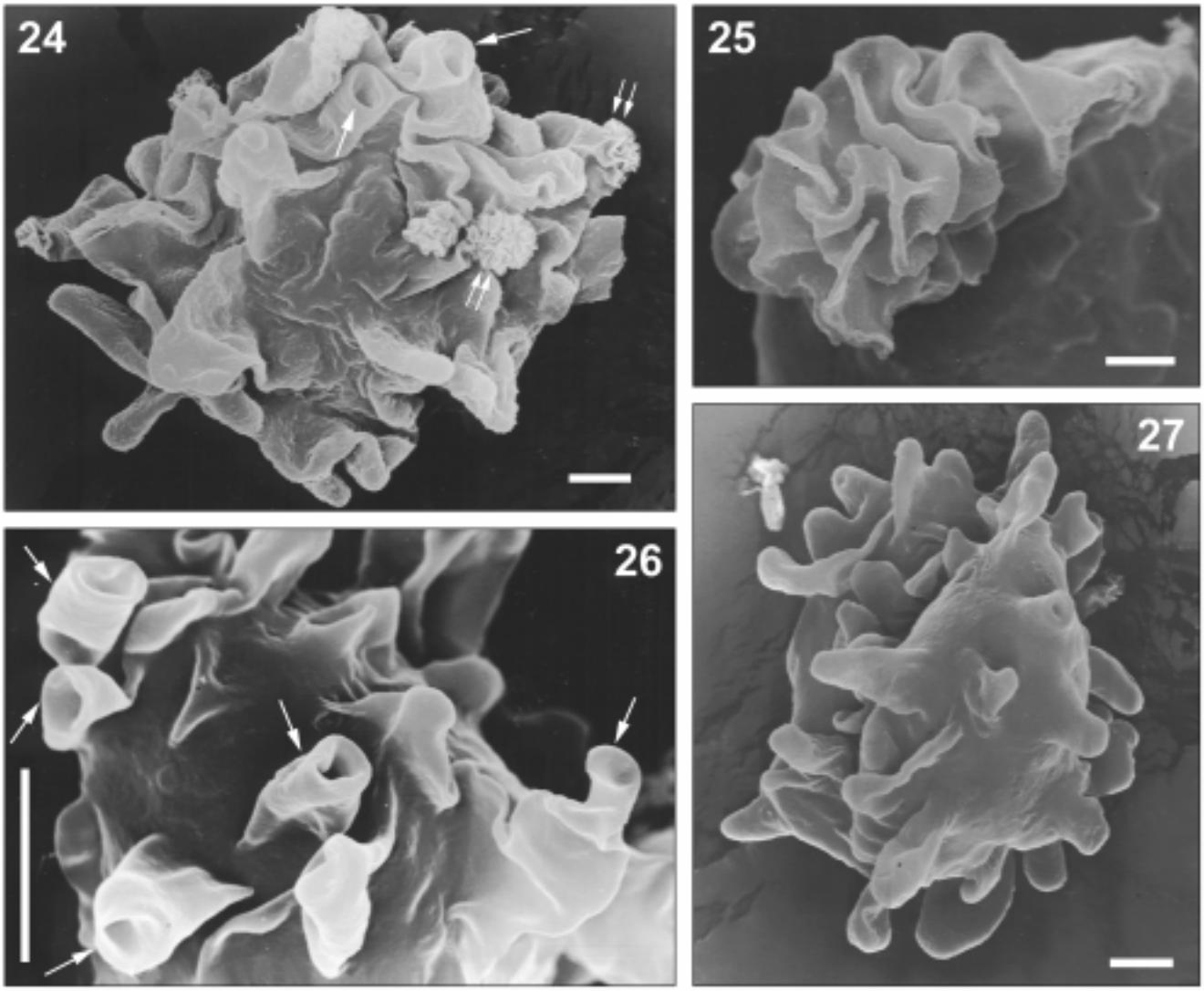

Figs 24-27. Absence of adhesive structures in *A. proteus,* strain C_t, during pinocytosis; SEM. **24** - the rosette-shaped amoeba with some active pinocytotic pseudopods forming channels (arrows) and some others retracted and convoluted (double-arrows); **25** - tip of a retracted pinocytotic pseudopod composed of membrane folds, without microprotrusions; **26** - absence of minipodia between pseudopods with channels (arrows) at the culmination of pinocytosis; **27** - absence of minipodia on the surface of a postpinocytotic rosette. Scale bars - **24, 26, 27** - 20 μm; **25** - 2 μm

ments of *A. proteus* produced by microdissection are rounded, motionless and unattached to the substratum; only sporadically they can resume for brief periods of time some contractile and protrusive activity. No kind of adhesive structures could be detected by SEM in such anucleate fragments, up to 96 h after dissection, independently of the strain of amoebae and of their either smooth or slightly wrinkled surface (Figs 21, 22). Even the fragments transiently contracting and protruding short pseudopods had no minipodia (Fig. 23).

Amoebae lose their contact with the substratum also during cation-induced pinocytosis, whereas during phagocytosis they are strongly attached (Opas 1981); the de-adhesion during pinocytosis is not related to membrane internalisation but to cells' shape change into the rosette form (Kłopocka *et al.* 1996). In the present experiments amoebae were fixed 10 min after addition of 100 mM KCl, when the large majority of them had pinocytotic pseudopods with channels (arrows; Figs 24, 26). In many specimens the structures appeared, which

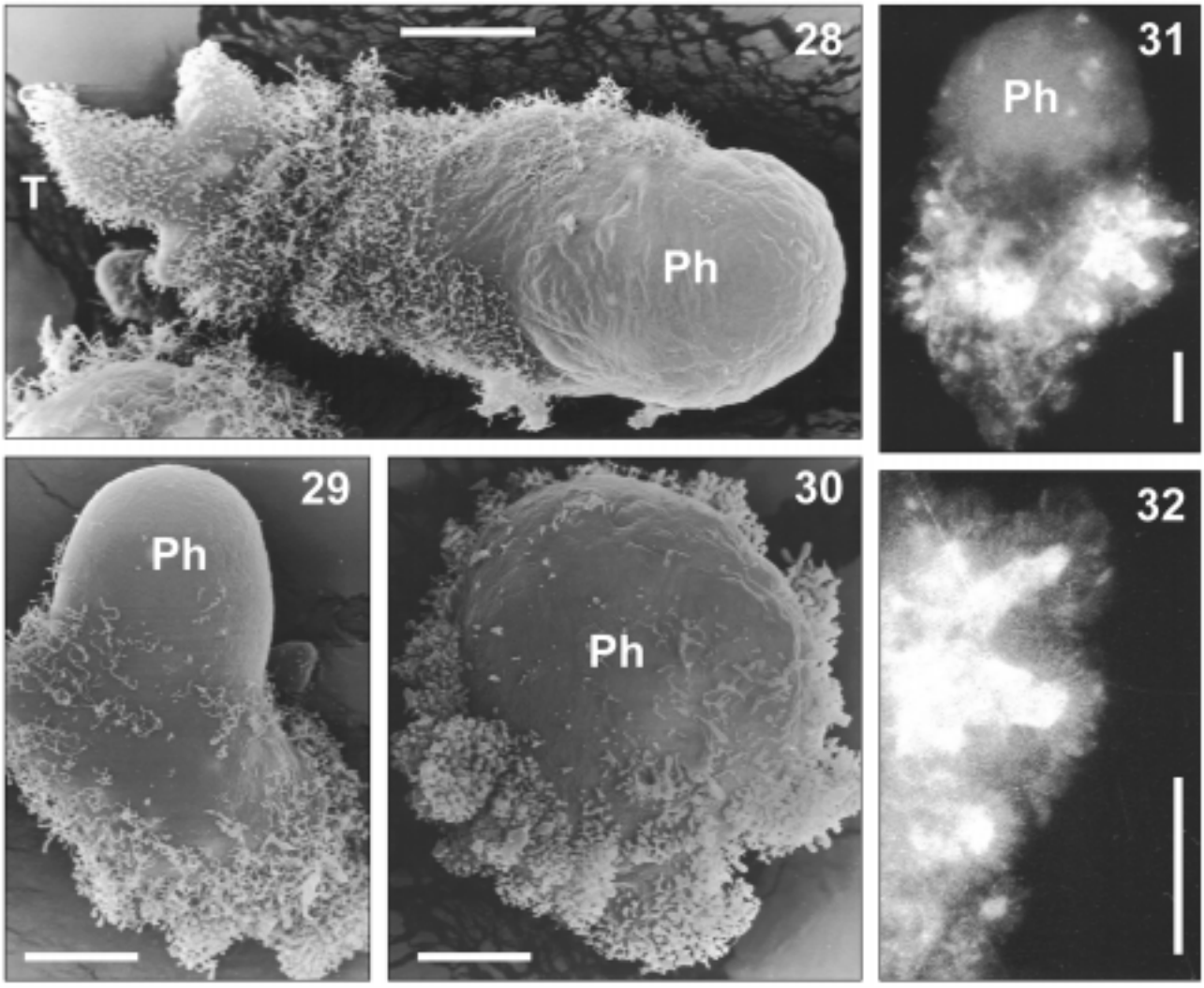

Figs 28-32. Abundant development of adhesive structures in *A. proteus,* strain C_t, during phagocytosis; SEM (28-30) and FLM (31, 32). **28** - amoeba soon after swallowing a heliozooon; very dense minipodia at the posterior body regions (T) and the naked anterior swollen part which contains the phagosome (Ph); **29** - later stage of ingesting the prey; **30** - a spherical cell during food digestion, still attached to the substratum with bunches of minipodia; **31** - F-actin localisation in amoeba at an early stage after ingesting a heliozoon, detected by fluorescein-conjugated phalloidin; it coincides with distribution of minipodia shown by SEM; **32** - enlarged fragment of the same specimen demonstrating that the F-actin pattern is the same as the composition of rosette contacts seen in SEM. Scale bars - 50 μm

at low magnification looked similar to the adhesive papillae (double-arrows; Fig. 24). A higher magnification (Fig. 25) demonstrated however that they are not composed of minipodia but of membrane folds and coils. *In vivo* observation in a DIC microscope proved that these structures arise by strong contraction of formerly active pinocytotic pseudopods. We conclude therefore that at the culmination of pinocytosis amoebae lack any minipodia or adhesive papillae. Those of them who have finished pinocytosis keep the rosette shape (without channels) and are also devoid of any adhesive structures (Fig. 27).

In contrast, amoebae which have phagocytised a heliozoon (or a ciliate) produce at the posterior regions of their ventral surface very prominent coats of discrete minipodia and rosette contacts, soon after the ingestion of prey (Fig. 28), as well as at the later stages (Figs 29, 30). The characteristic distribution and shape of the adhesive projections of *A. proteus* during phagocytosis were not well seen in SEM at lower magnifications in an

early study of Jeon and Jeon (1976). The fluorescence of the labelled phalloidin at the surface of amoebae in course of phagocytosis (Fig. 31) demonstrates that F-actin distribution is exactly the same as the position of minipodia and rosette contacts. The enlarged fragment in Fig. 32 shows the strong fluorescence of actin in the basal knobs of rosette contacts surrounded by a more subtle layer of bright hairs corresponding to the minipodia.

DISCUSSION

Amoebae processed for SEM are detached from their former substratum and are examined in haphazard positions, which makes impossible a direct recognition which cell side was the ventral and which the dorsal one before fixation. However, a number of indirect evidence makes reasonable the presumption, that discrete minipodia and their rosette-like aggregations are specifically located on the ventral cell surface: (1) they always appeared unilaterally distributed in those well polarized amoebae which could be rotated in SEM about their axis of locomotion; (2) the frequencies of specimens exposing at different angles either the microprojections or the naked side, were random; (3) minipodia and their aggregations reappeared in non-polarized and unattached specimens occurring in cultures, when they began to recover the polarity; (4) they were never found in amoebae experimentally deprived of attachment to the substratum, either by mechanical shocks, amputation of the cell part containing the nucleus, or by induction of pinocytosis; (5) they are rich in F-actin, and the dots of accumulated F-actin were earlier localised by us in a confocal microscope at the cell-substratum contact level (Grębecka *et al.* 1997).

According to the classic protistological terminology the minipodia of *A. proteus* fall into the category of filopodia, which are usually defined as filiform pseudopods, sometimes branching but never anastomosing, composed of ectoplasmic actin gel without fluid endoplasm and without microtubules. They occur in many, but not all taxa of amoebae. In the order Euamoebida they are present in the families Paramoebidae and Vexilliferidae, but considered to be absent in Amoebidae, Hartmannelidae, Thecamoebidae and Vannellidae (Page 1988). The present description of the minipodia of *A. proteus* is therefore the first finding of filopodia in the family of Amoebidae. The excellent term "subpseudopodia" introduced also by Page, but not commonly used, might be applied to those minipodia of *A. proteus,* which arise from the supporting knobs in the rosette contacts or from the surface of frontal lobopodia.

We have chosen for the adhesive structures revealed by us in *A. proteus* the descriptive names: minipodia and rosette contacts, among many others given in the literature to the specialised adhesion sites of protozoan and metazoan cells, because these two terms refer merely to their morphology and function in cell-to-substratum attachment, without anticipating their molecular composition and other features which, in the case of *A. proteus,* may be different or less known than in some motile tissue cells.

Similar actin-rich microprotrusions directed toward the substratum (or actin patches at the substratum contact sites) were earlier found in two categories of metazoan cells, both highly motile and invasive in nature: the metastatic transformed cells and normal cells of monocytic origin in the immune system. Their adhesive structures were described under different names. For example, adhesive microprotrusions of human fibrosarcoma cells penetrating endothelial cells monolayer were called microvilli (Kramer and Nicolson 1981), although this term is traditionally reserved rather to microprojections performing absorptive, but not adhesive functions. Recently the actin-rich protuberances formed at the substratum contact sites of the invasive transformed cells are most often called podosomes (Tarone *et al.* 1985, Marchisio *et al.* 1987, Nermut *et al.* 1991) or invadopodia (Chen 1989, Mueller *et al.* 1992). Podosome-like microprotrusions and F-actin nodules at the cell-to-substratum contact sites were also described in polymorphonuclear leukocytes (Boyles and Bainton 1979, Wolosewick 1984, Yürüker and Niggli 1992), macrophages (Trotter 1981, Amato *et al.* 1983, Ono *et al.* 1993), and osteoclasts (Marchisio *et al.* 1984).

Surprisingly little is known about the micromorphology and molecular composition of adhesive organelles produced in the third category of highly motile cells: the free-living amoebae (see Introduction). They were described not long ago, only in myxamoebae of *Dictyostelium discoideum* by Fukui and Inoué (1997) under the name of eupodia. The eupodia studied in the living material, in a very high aperture DIC microscope with focal plain depth reduced to 0.3 μm, appear at the ventral surface of migrating cells as "knobby foot-like structures". They develop behind the leading edge, at the basis of each advancing pseudopod, anchor the cell by penetrating transiently into the agar gel substratum, and

are retracted when a new pseudopod, formed in another cell region, re-orients locomotion of the myxamoeba. Indirect immunofluorescence revealed in them accumulation of F-actin, myosin I and α-actinin, but not talin.

Minipodia revealed in the present study in *Amoeba* by SEM seem to be in several aspects homologous with eupodia of *Dictyostelium.* Both structures have the shape of protrusions of the cell surface and are comparable in diameters (0.5-1μm), whereas their difference in length is roughly proportional to the size difference between these two amoebae. They occupy a similar middle-anterior zone at the ventral cell side, behind the advancing edge. This is the position which exactly corresponds to the zone of the most stable adhesion in locomoting giant amoebae, as it was earlier demonstrated by side-view observations and reflection interference microscopy, and concluded from retraction pattern of the contractile cell cortex (c.f. Introduction). It is worthy to add, that the present results revealed a shift of the substratum adhesion sites of *A. proteus* during phagocytosis, from the middle-anterior to the posterior location in the cells (compare Figs 14 and 28). Minipodia of *Amoeba* as well as eupodia of *Dictyostelium* are rich in F-actin. This is demonstrated in Figs 4, 13, 31 and 32 in the present paper; moreover, the concentration of F-actin in minipodia fits well with the distribution pattern of F-actin dots demonstrated by us earlier in *A. proteus* by confocal microscopy at the cell-substratum contact level (Grębecka *et al.* 1997). The α-actinin in *A. proteus* is evenly distributed everywhere between cell membrane and cortical actin network, and the vinculin at the middle-anterior zone (Brix *et al.* 1990); therefore, these two components of the molecular bridge between the adhesion site and the cytoskeleton probably may be at least present, if not accumulated, in the minipodia of *Amoeba.* No information is available about the presence of talin in *Amoeba*; in *Dictyostelium* a talin homologue was found in the leading edge (Kreitmeier *et al.* 1995), but not in eupodia (Fukui and Inoué 1997).

Common features of minipodia and eupodia should be further studied by examining morphology of the ventral surface of *Dictyostelium* in high-resolution SEM, and reciprocally, the dynamics of ventral projections of *Amoeba* in locomoting living cells, by confocal microscopy. It is possible, for example, that the largest knobs of *Dictyostelium* presumed by Fukui and Inoué (1997) to be formed by a close apposition of eupodia, are in fact the rosette contacts, as those described by us in *Amoeba.* The rosette contacts in *A. proteus* certainly correspond well to the platforms of more loose "associated contact" linked to "close contact" spots, which were revealed long ago in *Naegleria gruberi* by reflection interference microscopy (Preston and King 1978 a, b).

Preston and King (1978 b), and Preston and O'Dell (1980) treat the close contact sites of *Naegleria* as equivalent of focal contacts. However, the homology between minipodia of *Amoeba* and eupodia of *Dictyostelium,* and probably the adhesive organelles of some other free-living amoebae, cannot be easily extended to focal contacts of fibroblasts for several reasons: (1) in the focal contacts actin cytoskeleton is linked to the integrins, whereas integrins are unknown in free-living amoebae; (2) this association is established by interactions of α-actinin, vinculin and talin, but the talin may be missing in the contact organelles of amoebae; (3) focal contacts provide attachments to the stress fibres, which are absent in amoebae; (4) cell-to-substratum attachments in amoebae are much more dynamic than focal contacts of the fibroblasts (see reviews of focal contacts structure and dynamics by Burridge *et al.* 1988, Petit and Thiery 2000, Sastry and Burridge 2000).

These differences do not depend only on the state of the knowledge, but in a large extent they may result from different conditions and mode of life of free-living amoebae and metazoan motile cells: (1) In metazoan tissues the cells migrate on protein substrata and in culture they adhere to artificial substrata in the presence of serum proteins, while free-living amoebae move in nature rather on fresh or degraded plant material, *i.e.*, mainly on the polysaccharides, in absence of proteins in the fluid medium as well; hence, the metazoan-type integrins may not be used by them; it seems significant in this context that *A. proteus* fails to adhere to the gelatin gel (Kołodziejczyk *et al.* 1995), although it well attaches to the agar gel; it is also symptomatic that integrin-like molecules in amoebae were found only in two parasitic species: *Neoparamoeba aestuarina* from sponges (Custodio *et al.* 1995) and *Entamoeba histolytica* (Talahás-Rohana *et al.* 1998) living in higher Metazoa. (2) Competition between the specific molecular bridges linking a cell to the substratum and non-specific physical repulsive forces between both surfaces (Bell *et al.* 1984) is strongly influenced by ionic strength of the medium (Curtis 1964; King *et al.* 1979, 1983 a; Gingell and Vince 1982); the ionic strength in the culture of *A. proteus* is 25 times lower than in a standard tissue culture. (3) The motile metazoan cells in the tissues penetrate three-dimensional substrata, whereas the fresh water amoebae as benthic organisms are adapted to moving on a flat surface. (4) In most cases not only the

absolute, but even the relative locomotion rates are much higher in amoebae than in the metazoan cells; for example a fibroblast needs $1^1/_2$-2 hours to cross the distance equal to its own length, while *A. proteus* covers it 40 times quicker, within 2-3 minutes; thus, the amoeba must much more promptly establish and destroy its contacts with the substratum. All these factors could contribute to some divergence of structures performing essentially the same function in protozoan and metazoan amoeboid cells: anchoring the contractile actomyosin cytoskeleton to the substratum by F-actin rich microprotrusions of the cell surface.

Acknowledgements. We thank Miss Anna Łopatowska for culturing the amoebae, and Miss Anna Mirgos, Miss Justyna Osmulska and the staff of the Electron Microscopy Laboratory for their very competent technical assistance.

REFERENCES

Amato P. A., Unanue E. R., Taylor D. R. (1983) Distribution of actin in spreading macrophages: A comparative study of living and fixed cells. *J. Cell Biol.* **96:** 750-761

Bell G. I., Dembo M., Bongrand P. (1984) Cell adhesion: Competition between nonspecific repulsion and specific bonding. *Biophys. J.* **45:** 1051-1064

Bell L. G. E., Jeon K. W. (1963) Locomotion of *Amoeba proteus*. *Nature* **198:** 675-676

Boyles J., Bainton D. F. (1979) Changing patterns of plasma membrane-associated filaments during the initial phases of polymorphonuclear leukocyte adherence. *Cell Biol.* **82:** 347-368

Brix K., Reinecke A., Stockem W. (1990) Dynamics of the cytoskeleton in *Amoeba proteus.* III. Influence of microinjected antibodies on the organization and function of the microfilament system. *Eur. J. Cell Biol.* **51:** 279-284

Burridge K., Fath K., Kelly T., Nuckolls G., Turner C. (1988) Focal adhesions: Transmembrane junctions between the extracellular matrix and the cytoskeleton. *Ann. Rev. Cell Biol.* **4:** 487-525

Chen W-T. (1989) Proteolytic activity of specialized surface protrusions formed at rosette contact sites of transformed cells. *J. exp. Zool.* **251:** 167-185

Cheng T. P. O. (1992) Minipodia, novel structures for extension of the lamella: A high-spatial-resolution video microscopic study. *Exp. Cell Res*. **203:** 25-31

Clark A. M. (1942) Some effects of removing the nucleus from amoebae. *Austral. J. Exp. Biol. Med. Sci.* **20:** 240-247

Curtis A. S. G. (1964) Mechanism of adhesion of cells to glass: A study by interference reflection microscopy. *J. Cell Biol*. **20:** 199-215

Custodio M. R., Imsiecke G., Borojevic R., Rinkevich B., Rogerson A., Mueller W. E. G. (1995) Evolution of cell adhesion systems: Evidence for Arg-Gly-Asp mediated adhesion in the protozoan *Neoparamoeba aestuarina. J. Euk. Microbiol.* **42:** 721-724

David-Pfeuty T., Singer S. J. (1980) Altered distributions of the cytoskeletal proteins vinculin and α-actinin in cultured fibroblasts transformed by Rous sarcoma virus. *Proc. Natl. Acad. Sci. USA.* **77:** 6687-6691

Dellinger O. P. (1906) Locomotion of amoebae and allied forms. *J. exp. Zool.* **3:** 337-358

Fukui Y., Inoué S. (1997) Amoeboid movement anchored by eupodia, new actin-rich knobby feet in *Dictyostelium*. *Cell Mot. Cytoskeleton* **36:** 339-354

Gingell D., Vince S. (1982) Substratum wettability and charge influence the spreading of *Dictyostelium* amoeba and the formation of ultrathin cytoplasmic lamellae. *J. Cell Sci.* **54:** 255-285

Grębecka L. (1977) Behaviour of anucleate anterior and posterior fragments of *Amoeba proteus. Acta Protozool*. **16:** 87-105

Grębecka L., Grębecki A. (1975) Morphometric study of moving *Amoeba proteus*. *Acta Protozool*. **14:** 337-361

Grębecka L., Pomorski P., Grębecki A., Łopatowska A. (1997) Adhesion-dependent F-actin pattern in *Amoeba proteus* as a common feature of amoebae and the metazoan motile cells. *Cell Biol. Int.* **21:** 565-573

Grębecki A. (1976) Co-axial motion of the semi-rigid cell frame in *Amoeba proteus*. *Acta Protozool*. **15:** 221-248

Grębecki A. (1984) Relative motion in *Amoeba proteus* in respect to the adhesion sites. I. Behavior of monotactic forms and the mechanism of fountain phenomenon. *Protoplasma* **123:** 116-134

Grębecki A., Grębecka L. (1978) Morphodynamic types of *Amoeba proteus:* A terminological proposal. *Protistologica* **14:** 349-358

Grębecki A., Grębecka L., Wasik A. (2001) Minipodia and rosette contacts are adhesive organelles present in free-living amoebae. *Cell Biol. Int.* **25:** (in press)

Haberey M. (1971) Bewegungsverhalten und Untergrundkontakt von *Amoeba proteus*. *Mikroskopie* **27:** 226-234

Jeon K. V., Jeon M. S. (1976) Scanning electron microscope observations of *Amoeba proteus* during phagocytosis. *J. Protozool.* **23:** 83-86

Jeon K. V., Lorch I. J. (1973) Strain specificity in *Amoeba proteus.* In: The Biology of Amoeba, (Ed. K. W. Jeon), Academic Press, New York and London, 549-567

King C. A., Cooper L., Preston T. M. (1983 a) Cell-substrate interactions during amoeboid locomotion of *Naegleria gruberi* with special reference to alterations in temperature and electrolyte concentration of the medium. *Protoplasma* **118:** 10-18

King C. A., Preston T. M., Miller R. H. (1983 b) Cell-substrate interactions in amoeboid locomotion - a matched reflection interference and transmission electron microscopy study. *Cell Biol. Int. Rep*. **7:** 641-649

King C. A., Westwood R., Cooper L., Preston T. M. (1979) Speed of locomotion of the soil amoeba *Naegleria gruberi* in media of different ionic compositions with special reference to interactions with the substratum. *Protoplasma* **99:** 323-334

Klein H. P., Köster B., Stockem W. (1988) Pinocytosis and locomotion of *Amoebae.* XVIII. Different morphodynamic forms of endocytosis and microfilament organization in *Amoeba proteus. Protoplasma* **2(Suppl.)** 76-87.

Kłopocka W., Kołodziejczyk J., Łopatowska A., Grębecki A. (1996) Relationship between pinocytosis and adhesion in *Amoeba proteus. Cell Biol. Int.* **20:** 635-641

Kołodziejczyk J., Kłopocka W., Łopatowska A., Grębecka L., Grębecki A. (1995) Resumption of locomotion by *Amoeba proteus* readhering to different substrata. *Protoplasma* **188:** 180-186

Kramer R. R., Nicolson G. L. (1981) Invasion of vascular endothelial cell monolayers and underlying matrix by metastatic human cancer cells. In: International Cell Biology 1980-1981, (Ed. H.G. Schweiger), Springer-Verlag, Berlin, Heidelberg, 794-799

Kreitmeier M., Gerisch G., Heizer C., Müller-Taubenberger A. (1995) A talin homologue of *Dictyostelium* rapidly assembles at the leading edge of cells in response to chemoattractants. *J. Cell Biol.* **129:** 179-188

Lorch I. J. (1969) The rate of attachment to the substratum: A study of nuclear-cytoplasmic relationship. *J. Cell Physiol.* **73:** 171-177

Marchisio P. C., Cirillo D., Naldini L., Primavera M. V., Teti A., Zambonin-Zallone A. (1984) Cell-substratum interaction of cultured avian osteoclasts is mediated by specific adhesion structures. *J. Cell Biol.* **99:** 1696-1705

Marchisio P. C., Cirillo D., Teti A., Zambonin-Zallone A., Tarone G. (1987) Rous sarcoma virus-transformed fibroblasts and cells of monocytic origin display a peculiar dot-like organization of cytoskeletal proteins involved in microfilament-membrane interactions. *Exp. Cell Res.* **169:** 202-214

Mueller S. C., Yeh Y., Chen W-T. (1992) Tyrosin phosphorylation of membrane proteins mediates cellular invasion by transformed cells. *J. Cell Biol.* **119:** 1309-1325

Nermut M. V., Eason P., Hirst E. M. A., Kellie S. (1991) Cell/substrate adhesions in RSV-transformed rat fibroblasts. *Exp. Cell Res.* **193:** 382-397

Nikolajeva G. V, Kalinina L. V., Sikora J. (1980) Transparent *Amoeba proteus* originated from the strain C. *Acta Protozool*. **19:** 327-332

Ono M., Murakami T., Tomita M., Ishikawa H. (1993) Association of the actin cytoskeleton with glass adherent proteins in mouse peritoneal macrophages. *Biol. Cell* **77:** 219-230

Opas M. (1978) Interference reflection microscopy of adhesion of *Amoeba proteus*. *J. Microscopy* **112:** 215-221

Opas M. (1981) Effects of induction of endocytosis on adhesiveness of *Amoeba proteus. Protoplasma* **107:** 161-169

Page F.C. (1988) A New Key to Freshwater and Soil Gymnamoebae. Freshwater Biological Association, Ambleside, U.K.

Petit V., Thiery J-P. (2000) Focal adhesions: structure and dynamics. *Biol. Cell* **92:** 477-494

Preston T. M., King C. A. (1978 a) Cell-substrate associations during the amoeboid locomotion of *Naegleria. J. Gen. Microbiol.* **104:** 347-351

Preston T. M., King C. A. (1978 b) An experimental study of the interaction between the soil amoeba *Naegleria gruberi* and a glass substrate during amoeboid locomotion. *J. Cell Sci.* **34:** 145-158

Preston T. M., O'Dell D. S. (1980) The cell surface in amoeboid locomotion: Behaviour of *Naegleria gruberi* on an adhesive lectin substrate. *J. Gen. Microbiol.* **116:** 515-520

Sastry S. K., Burridge K. (2000). Focal adhesions: A nexus for intracellular signaling and cytoskeletal dynamics. *Exp. Cell Res.* **261:** 25-36.

Talahás-Rohana P., Herández-Ramirez V. I., Perez-García J. N., Ventura-Juárez J. (1998) *Entamoeba histolytica* contains a b1 integrin-like molecule similar to fibronectin receptors from eukaryotic cells. *J. Euk. Microbiol.* **45:** 356-360

Tarone G., Cirillo D., Giancotti F. G., Comoglio P. M., Marchisio P. C. (1985) Rous sarcoma virus-transformed fibroblasts adhere primarily at discrete protrusions of the ventral membrane called podosomes. *Exp. Cell Res.* **159:** 141-157

Trotter J. A. (1981) The organization of actin in spreading macrophages. *Exp. Cell Res.* **132:** 235-248

Wolosewick J. J. (1984) Distribution of actin in migrating leukocytes in vivo. *Cell Tiss. Res.* **236:** 517-525

Yürüker B., Niggli V. (1992) Alpha-actinin and vinculin in human neutrophils: Reorganization during adhesion and relation to the actin network. *J. Cell Sci.* **101:** 403-414

Received on 15th May, 2001; accepted on 30th August, 2001

Acta Protozool. (2001) 40: 249 - 261

ACTA
PROTOZOOLOGICA

Nuclear Reorganization Variety in *Paramecium* (Ciliophora: Peniculida) and its Possible Evolution

Sergei I. FOKIN[1], Ewa PRZYBOŚ[3] and Sergei M. CHIVILEV[2]

Departments of [1]Invertebrates Zoology and [2]Hydrobiology of St. Petersburg State University, St. Petersburg, Russia; [3]Department of Experimental Zoology, Institute of Systematics and Evolution of Animals, Polish Academy of Sciences, Kraków, Poland

Summary. The nuclear reorganization pathway of *Paramecium* during conjugation was investigated for 12 morphospecies. For *P. woodruffi* and *P. schewakoffi* the nuclear reorganization was studied for the first time. Several key elements of the process were chosen for the analysis, including „crescent" or „parachute" stage of the micronucleus, number of nuclear products and time of their degradation, and behavior of the old macronucleus. The carried out analysis allowed making dendrogram and topogram of the nuclear reorganization similarity (UPGMA) of the investigated species. The constructed tree did not coincide with the results of our previous molecular-biological analysis in several ways. According to SSrRNA gene sequences, the basal branching pattern of *P. bursaria* and *P. duboscqui* is congruent with some peculiarities of their nuclear reorganization. As an ancient species, they diverged from each other and from *P. putrinum* quite long ago. It seems, the taxonomic species with shorter immaturity period and outbreeding strategy (*P. putrinum*) could show faster evolution rate. For the nuclear reorganization of that species and, probably, for it's mating type system we can expect secondarily modification. General direction of evolution for the old macronucleus changing in *Paramecium* is going, apparently, from the absence of any changing to the macronuclear fragmentation at the earlier nuclear reorganization steps.

Key words: conjugation, evolution, nuclear reorganization, *Paramecium.*

Abbreviations: Con - conjugation, Excon - exconjugants, Ma - macronucleus, Mi - micronucleus, MT - mating type, NR - nuclear reorganization.

INTRODUCTION

Genus *Paramecium* known for 250 years (Woodruff 1945, Wichterman 1986) and as one of the most investigated in ciliates it gave us the model organisms for numerous studies concerning different problems of protozoology, cytology, genetics, general biology and some other. Its wide distribution (for many species cosmopolitan), ease of cultivation, relative large dimensions (80-400 μm), allowed paramecia to become "universal laboratory animals".

Taxonomic species of *Paramecium* preserving similar shape show, however, significant polymorphism of morphology and several biologically important features, e.g. morphology of contractile vacuoles, micronuclei, mating type systems, type of nuclear apparatus, type of reorganization of nuclei during mating processes, and type of endocytobionts. Thus, they are group of organisms unique for comparative biological analysis. Such complex analysis with use of many *Paramecium* species was started not long ago (Fokin 1986, 1997, 2000; Fokin

Address for correspondence: Sergei. I. Fokin, Tuchkov 3, apt.6, 199053, St. Petersburg, Russia; E-mail: fokin@peterlink.ru

and Chivilev 1999, 2000; Fokin *et al.* 1999b; Strüder-Kypke *et al.* 2000a, b). It seems that the obtained data will help to solve some problems important for protozoology as well as for general cytology.

Diversity shown in the course of mating process - Con in different *Paramecium* species, till present, was not the object of comparative analysis, and in some species it was only a little studied or totally unknown. The NR process in the genus is very composed material, useful for studies of NR evolution in unicellular organisms. At present, some data obtained by molecular studies concerning phylogeny of the genus and its position in ciliate system (Strüder-Kypke *et al.* 2000a, b) brings new possibilities for such investigations.

Paramecia disclose amazing for one genus differentiation of several stages of NR in Con, though the general scheme of this process remains almost invariable (Wichterman 1953, 1986; Raikov 1972, 1982; Vivier 1974; Hiwatashi and Mikami 1989). NR contains progamic and metagamic phases. In the first phase, formation of pronuclei (haploid nuclei) takes place during three divisions of Mi (two first of them are meiosis). Exchange of migratory pronuclei and synkarion formation as a result of fusion of migratory pronuclei with the stationary ones end the progamic phase. Metagamic phase is connected with formation of new nuclear apparatus of the cell from products of synkarion divisions. Soon after starting metagamic phase, partners of Con separate, and the further stages of NR process, i.e. formation and development of Ma anlagen, Mi, and degeneration of the old Ma, take place already in Excon.

MATERIALS AND METHODS

The comparative analysis of the course of NR in majority of taxonomical species of *Paramecium* genus was carried out on the basis of the authors own studies (10 species among 12 taken into consideration) and literature data. Analysis was carried out in the following species: *P. bursaria*, *P. putrinum*, *P. duboscqui*, *P. nephridiatum*, *P. woodruffi*, *P. calkinsi*, *P. polycaryum*, *P. caudatum*, *P. multimicronucleatum*, *P. jenningsi*, *P. biaurelia* of the P. aurelia complex, and *P. schewiakoffi*.

Cultures of paramecia were kept in laboratory conditions according to the standard methods of Sonneborn (1970).

Con between individuals from clones representing complementary MT was obtained by mixing about 100 cells in one depression slide (capacity 2.5 ml), 10-12 h after last feeding (medium addition). Besides, self-conjugating pairs (obtained spontaneously or induced) were observed. Selfing was induced by washing paramecia twice in SMB buffer, Dryl's solution or others solutions used in that purpose (Shimomura and Takagi 1984, Yanagi and Haga 1996).

Conjugants and Excon were fixed in different time laps, mainly each 1 or 2 h depending on experiment, by the Bouin's or Carnoy's fixatives, the nuclear apparatus was stained by the Feulgen reaction. The slides were analyzed under magnification x400 to x1000 in microscope Axioscop, Zeiss, Germany, and Amplival, Zeiss, Germany. Alive conjugants and Excon were also observed using device for temporary immobilization (Skovorodkin 1990) under similar magnification and with the application of phase contrast. Data of the studied material (species, clonal, and geographical diversity) are presented in the Table 1.

For comparison of NR course in different species of *Paramecium,* the following characteristic (Jankowski 1972, Ossipov 1981, Raikov 1982) features were chosen: Mi shape in prophase of I-st meiotic division, number of degenerating products of Mi division in progamic phase as well as in metagamic phase, presence of the old Ma fragments, time of beginning of the old Ma fragmentation, time of conjugants separation, number of metagamic cycles, number of Ma anlagen, coordination of beginning of the old Ma fragmentation with time of partners separation (Table 2).

Data concerning NR in the studied *Paramecium* species were noted as presence or absence of the characteristic feature, and then elaborated with the application of cluster and multiple analysis (Fokin and Chivilev 1999, 2000). Classification and ordination of species using the data was made on the basis of Braverman (1965) recalculations of the Euclidean distance without transformation of primary data. The secondary matrix was graphically represented as dendrogram constructed by the using unweighted pair-group method with arithmetic averages (UPGMA) (Sneath and Sokal 1973). Ordination of *Paramecium* species was made by multidimensional scaling (MDS) (Kruskal and Wish 1978) resulting in the arrangement of the species in two-dimensional space (topogram) accounting for dissimilarity of the species' NR traits.

RESULTS AND DISCUSSION

The process of NR in conjugation was observed in the following species: *P. putrinum*, *P. duboscqui*, *P. nephridiatum*, *P. woodruffi*, *P. calkinsi*, *P. caudatum*, *P. multimicronucleatum*, *P. biaurelia* of the P. aurelia complex, *P. jenningsi* and *P. schewiakoffi* (Table 1), while data concerning the NR in Con and after its finishing in *P. bursaria*, *P. putrinum*, *P. polycaryum*, and other than *P. biaurelia* species of the P. aurelia complex - *P. triaurelia* (Przyboś *et al.* 1979) in majority were taken from literature. Literature data concerning NR in *P. caudatum* and *P. multimicronucleatum,* besides author's own observations, were also used for analysis of NR in the species. Rare literature data (usually 1 or 2 papers) concerning NR in *P. duboscqui*, *P. nephridiatum*, *P. calkinsi*, and *P. polycaryum* were also taken into analysis of the process.

As the main aim of the present paper was comparative analysis of basic stages of NR in *Paramecium* genus, the detailed description of the process in all studied species was neglected. Although, the data on NR in *P. woodruffi* and *P. schewiakoffi* are pioneering, and for *P. jenningsi* is it the first complete description of Con, only the short presentation of processes are given.

Paramecium woodruffi. Process of Con, described by Jankowski (1961), similarly as majority of papers on this species made before 1999, concerned really

Table 1. Cultures of *Paramecium* used for the experimental part of work

Species	Stock	Origin	Type of the nuclear reorganization	Method of *
P. putrinum	JS501-1	Japan, Sendai	conjugation	classical
	JS502-2	Japan, Sendai		
	GK1-1	Germany, Karlsruhe	selfing-conjugation	occasional
	GKz1-2	Germany, Konstanz		
P. woodruffi	BB2-1	Russia, Baltic Sea	conjugation	classical
	BB2-5			
	BB2-10	Russia, Baltic Sea	conjugation	classical
	BB2-12			
	KB3-3	Russia, White Sea	conjugation	classical
	KB3-6			
P. nephridiatum	DZ59-1	Russia, Barents Sea	conjugation	classical
	DZ59-4			
	KB1-5	Russia, White Sea	selfing-conjugation	occasional
P. calkinsi	GN1-4	Germany, North Sea	conjugation	classical
	GN1-9			
	JA1	Japan, Aio	conjugation	occasional
P. polycaryum	UK1-2	Ukraina, Kreimia	autogamy	occasional
	AN1-5	Namibia, Widhook	autogamy	occasional
P. biaurelia	MB3-3	Germany, Münster	selfing-conjugation	induced
	SK2-10	Germany, Stuttgart	selfing-conjugation	induced
P. caudatum	RO1-4	Russia, Lomonosov	conjugation	classical
	RO1-7			
	JY1-8	Japan, Yamaguchi	selfing-conjugation	induced
	BB3	Russia, St. Petersburg	conjugation	occasional
	AP-8	Armenia, Parzlich	conjugation	classical
	AP18			
P. multimicronucleatum	GA1-4	Germany, München	selfing-conjugation	induced
P. jenningsi	JYR-1	Japan, Yamaguchi	conjugation	classical
	JYR-3			
	Sh1-1	China, Shanghai	conjugation	classical
	Sh1-2			
	SA1-7	Saudi Arabia	selfing-conjugation	occasional
P. schewiakoffi	Sh1-37	China, Shanghai	selfing-conjugation	occasional
	Sh1-38			
	Sh1-40			
	Sh1-3		conjugation	classical
	Sh1-38			
	Sh1-40		autogamy	occasional

* - NR were analyzed in conjugants obtained by mixing cells representing complementary mating types (classical method) or in spontaneously received (occasional) or chemically induced self-conjugation (induced).

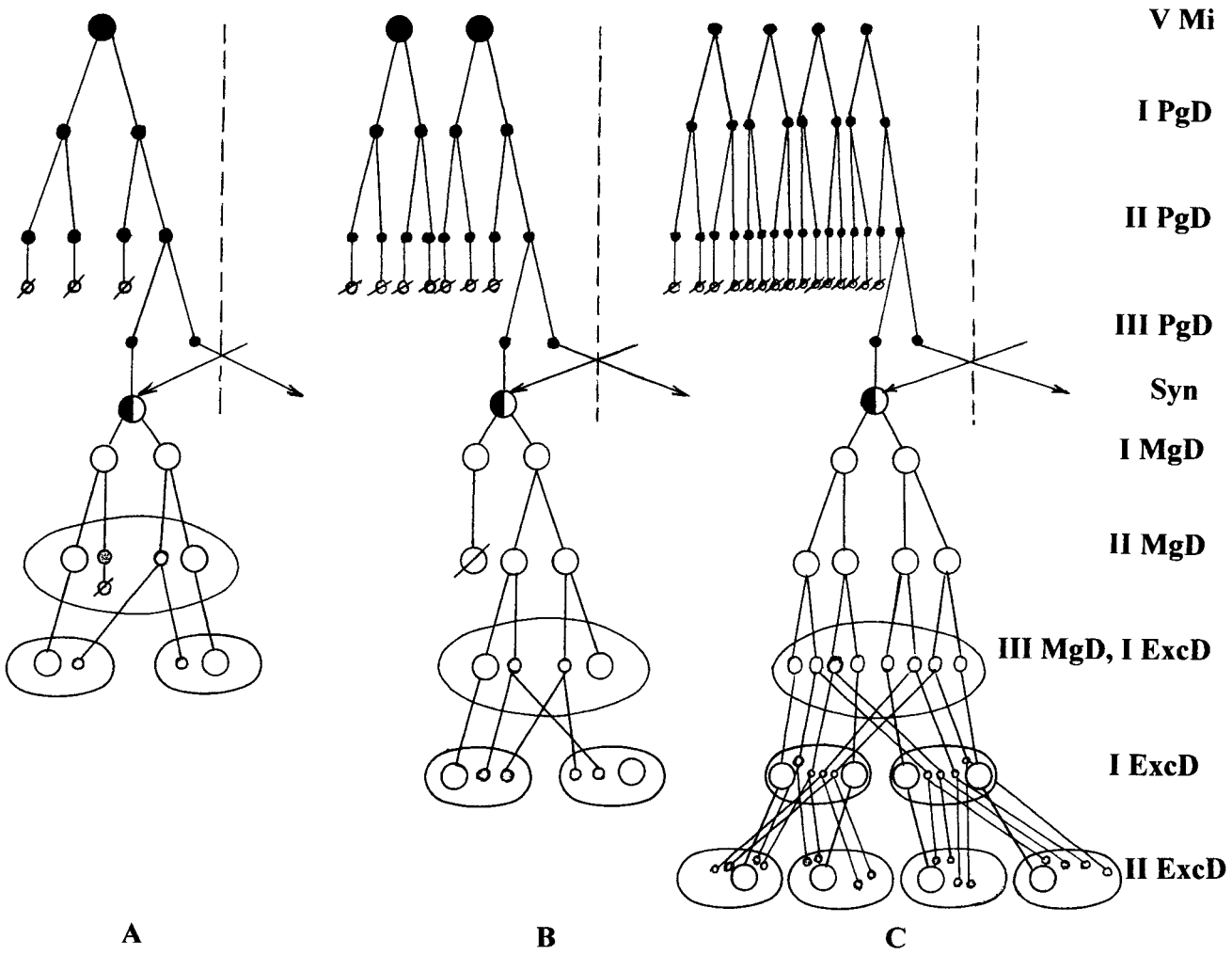

Figs 1A-C. Schemes of the nuclear reorganization process of *P. shewiakoffi* (**A**), *P. jenningsi* (**B**) and *P. woodruffi* (**C**). V Mi - vegetative micronuclei; I PgD - III PgD progamic divisions; I MgD - III MgD - metagamic divisions; Syn - synkarion; I ExcD, II ExcD - exconjugants divisions

P. nephridiatum (Fokin *et al.* 1999a). In that manner, *P. woodruffi* is one of the less studied species of *Paramecium* (Fokin and Chivilev 1999). Presented course of NR in the species was studied by the authors only in three pairs of clones (Table 1).

Two to five small (3-4 μm) Mi of endosomal type (Fokin 1997) enter I progamic division in synchronous manner. In its prophase „crescent" stage appears. Number of products of the II progamic division differs from 8 to 20 in partners of conjugation. Apparently only one nucleus participates in the III progamic division, and as a result of it two pronuclei are formed. Exchange of migratory pronuclei goes in paroral cone of partners; the stationary pronuclei are also nearby. Beginning of fragmentation of the old Ma starts between the end of II and beginning of III progamic divisions of Mi, and could be seen during exchange of pronuclei as ribbon. All cells observed at the stage of synkarion formation showed disintegrated Ma in ribbon form. Both products of I metagamic division enters II division. At that time, the old Ma appears as round fragments of different size in number 17 to 25 ($\bar{x}$ =20.6 ± 3.7, n=26). Separation of Con partners takes place during or shortly after I synkarion division, further NR goes in Excon. After III metagamic division, the Excon are shorter (about 15% of length), with 8 morphologically similar nuclei, and many fragments of the old Ma. The nuclei, however, are always grouped in 4 on the poles of the cell, in places

Table 2. Main stages of the nuclear reorganization in *Paramecium* species

Species	Nuclear dynamics in conjugants progamic phase, divisions nuclei and its peculiarities			Nuclear dynamics in exconjugants metagamic phase, divisions nuclei and its peculiarities				Ma number anlagen fragments		References
	I	II	III	I	II	III	IV			
P. bursaria	C, 2 (1)	2 (1)	2	2 (1)	2	4^x	-	2	-	Hamburger 1904, Chen 1940a, Wichterman 1948
P. putrinum	P, 2	4 (3)	2	2	4^x	8 (3)	-	4	85*	Diller 1948, Jankowski 1972
P. duboscqui	C, 4	8 (7)	2	2	4^x	8	-	4	2**	Watanabe *et al.* 1996, Fokin 1998
P. woodruffi	C, 4-10	8-20 (7-19)	2	2^x	4	8	-	4	20	Present study
P. nephridiatum	C, 6-8	8-16 (7-15)	2***	2 (1)	2	4	8^x	4	85*	Jankowski 1961
P. calkinsi	C, 4	8 (7)	2	2 (1)	2^x	4	-	2	12	Nakata 1958
P. polycaryum	C, 6-8	12-16 (11-15)	2	2	4^x	8	-	4	19	Diller 1954, 1958
P. caudatum	C, 2	4 (3)	2	2^x	4	8 (3)	-	4	55*	Calkins and Cull 1907
P. multimicronucleatum	C, 6-8	12-16 (11-15)	2	2	4^x	8	-	4	55*	Barnett 1964
P. jenningsi	C, 4	8 (7)	2	2 $(1)^x$	2	4	-	2	34	Mitchell 1962, Przyboś 1975
P. aurelia complex	C, 4	8 (7)	2	2^x	4	-	-	2	33	Jurand and Selman 1969
P. wichtermani	P, 4	8 (7)	2	2	4	8	-	4	?	Wichterman 1986
P. schewiakoffi	P, 2	4 (3)	2	2^x	4 (1)	-	-	2	25	Present study

* - Jankowski's data (1972); ** - products of additional division; *** - according to Jankowski (1961), higher number of pronuclei could appeared; P – the "parachute" stage; C- the „crescent" stage; (1) - number of pyknotic nuclei; 2^x - moment of mates separation; 2 - moment of beginning (skein formation) of the old Ma; ? - absent data

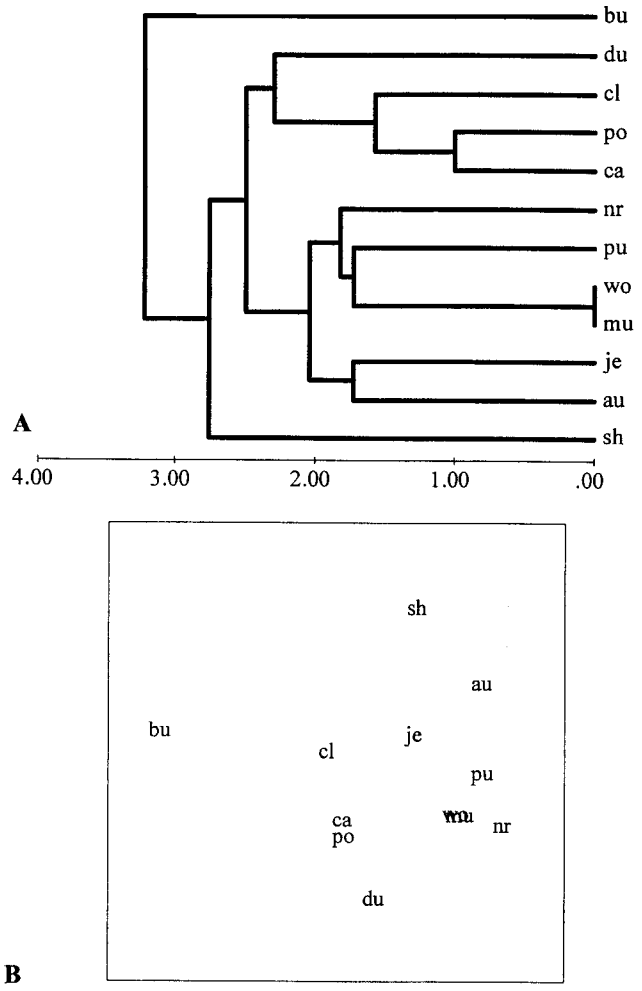

Fig. 2. Dendrogram (**A**) for hierarchical clustering of the nuclear reorganization similarity for 12 *Paramecium* species (UPGMA linking of Euclidean distance similarity) and topogram of non-metric MDS ordination of the features (**B**). au - P. aurelia complex; bu - *P. bursaria*; ca - *P. caudatum*; cl - *P. calkinsi*; du - *P. duboscqui*; je - *P. jenningsi*; mu - *P. multimicronucleatum*; nr - *P. nephridiatum*; po - *P. polycaryum*; pu - *P. putrinum*; sh - *P. schewiakoffi*; wo - *P. woodruffi*

without Ma fragments. Comparison of number of Ma anlagen differentiating from the front group of nuclei and number of Ma anlagen developing from the back group of nuclei (20 cells were investigated) showed slight deviation from the proportion of 4 : 4. Formation of nuclear apparatus, typical for vegetative stage of cell and composed of 1 Ma and 2-5 Mi takes place as a result of two cellular fissions of exconjugants. Ma anlagen are split into daughter cells without their previous division, and Mi anlagen by their mitotic divisions (Fig. 1 C).

Paramecium schewiakoffi. The species revealed in samples collected in November 1999 in China (Fokin *et al.* 2001b). Morphologically it reminds the other species of the "*aurelia*" subgroup, i.e. *P. caudatum*, *P. multimicronucleatum*, *P. jenningsi*, P. aurelia spp. complex. However, the peculiar course of NR of *P. schewiakoffi*, allows easily separating the species from the above-mentioned ones (Fokin *et al.* 2001a). The NR was observed in clones in selfing Con and during autogamy. The conjugating pairs were also regularly obtained by mixing clones representing the two complimentary MT, mature for mating reaction. The course of NR in autogamy occurs similarly like in Con, besides capacity of pronuclei. Autogamy appears in this species regularly in intervals of 8-10 days (16-24 fissions).

Single, relatively large Mi (7-8 μm) of chromosomal type is typical for the species. In prophase of I meiotic division appears „parachute" stage, not „crescent" typical for the majority of *Paramecium* species. Both products of the I-st Mi division enter the II progamic division, and III division enters only one (of 4 Mi) situated near oral zone of the cell. At that time, Ma begins formations of ribbons; the process is finished when exchange of pronuclei takes place. At I metagamic division, the Ma preserves the ribbon form. After that division, the partners of conjugation separate and the old Ma is fragmented. Many round or slightly prolonged fragments ($\overline{x}$ = 25.5 ± 4.7, n=30) of diverse dimensions appear. Both products of I synkarion division start II metagamic division, as a result of it two small morphologically similar nuclei appear on each pole of the cells. The Ma and Mi anlagen were counted in exconjugants (n=40) and some slight deviations from 2 : 2 proportion were found, sometimes Excon showed 3 Ma anlagen and 1 Mi. In Excon (before cell fission) two nuclei develop into Ma anlagen, one nucleus develop into Mi, and one degenerate. Ma anlagen are distributed into daughter cells at the first Excon fission without previous division of nuclei, and single Mi divides mitotically (Fig. 1 A).

Paramecium jenningsi. Con in the species was known since description of the species (Diller and Earl 1958). The whole process of NR in the species was not fully described (Mitchell 1962, 1963), in spite of many investigations carried out on different stages of Con (Przyboś 1975, 1978, 1980, 1986a).

In vegetative stage, two Mi of chromosomal type (Fokin 1997) with diameter of about 5 μm appear. Both Mi enter I progamic division, showing „crescent" stage in prophase. Only one (situated near oral zone of cell) of products of II progamic division do not degenerate. The

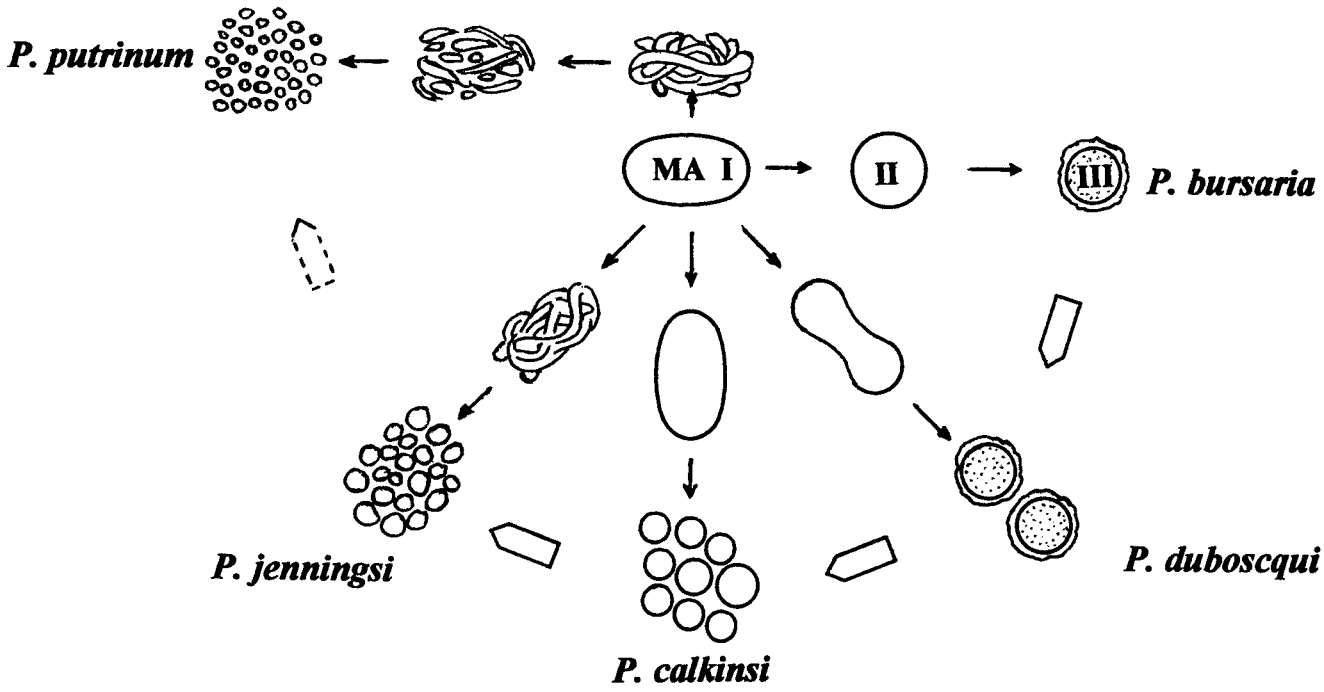

Fig. 3. Scheme of evolutionary changes of the old macronucleus during its nuclear reorganization in the species of *Paramecium* genus. MA - macronucleus; I- progamic phase; II - metagamic phase; III - exconjugant phase

remaining nucleus divides mitotically giving two pronuclei. The process occurs in both partners synchronously. At that time, the Ma loses its round shape and begins formation of ribbons. During synkarion division, the Ma appears as numerous, round or oval fragments, differing in dimensions ($\overline{x}$ = 32.3 ± 4.1, n=16). One of the products of the I synkarion division degenerates, second one enters into II division. The polar pairs of nuclei appear in III division, the Ma and Mi anlagen. Similarly as in the other *Paramecium* species, exconjugants at the last metagamic division are characterized by smaller dimensions and typical form of the cells (it helps to find easily paramecia in that stage of NR between other Excon). At the first fission of Excon, the vegetative form of nuclear apparatus is reconstructed. Both Mi anlagen divide mitotically, Ma anlagen are separated into daughter cells without division (Fig. 1 B).

Similarly, excluding exchange of pronuclei, the process of NR occurs in autogamic individuals. Autogamy is typical for the species, occurs each 7 to 8 days (20-24 fissions).

Other *Paramecium* species. As the peculiarities of NR in the studied *Paramecium* species are presented in Table 2, the basic stages of the process in the remaining species will be analyzed only in comparative aspect. In *P. wichtermani* the process of NR was only shortly described by Nashid (Wichterman 1986), thus there are no information at all concerning some stages of the process. That is the reason for not taking the data concerning the species for the NR comparison.

Comparison of the basic stages of NR in the studied *Paramecium* species allows defining the range of diversity of the process in all morphological species of the genus, existing at present as laboratory cultures (Table 2). This restriction is caused by the fact that some of the undoubtedly valid species, e.g. *P. wichtermani* do not exist as alive cultures in any laboratory in the world, and there is total lack of data concerning Con in *P. africanum*, *P. ugandae*, *P. pseudotrichium*, and *P. jankowski* (Przyboś 1986b, Wichterman 1986). At the same time, the P. aurelia complex composed of 15 biological species, i.e. 14 species (former syngens) named by Sonneborn (1975) and *P. sonneborni* (Aufderheide *et al.* 1983) do not show any differences in the course of NR.

The simplest and sure moment marking the beginning of NR, which we can test, seems characteristic form of prophase of I progamic (meiotic) division of Mi. Among

the investigated species only in three of them, i.e. *P. putrinum*, *P. wichtermani*, and *P. schewiakoffi* the Mi prophase appears as „parachute", in the other 9 species, it appears as „crescent" in different forms (Table 2). Both types of meiotic prophase are widely distributed in ciliates (Raikov 1982, Przyboś 1986c). The „parachute" stage, homologous with zygotene of classical meiosis (Raikov 1982) appears in Karyorelictea, Prostomatea, Nassophorea, Spirotrichea, and Colpodea. In other ciliate groups, mainly in Oligohymenophorea, appears „crescent" instead of „parachute" stage. However, in two species (not free living) of the class, one belonging to Astomatida and second to Apostomatida, the „parachute" was described (Poljansky 1926, Summers and Kidder 1936). Later (Serrano *et al.* 1987) the parachute was found in very common free living peniculine *Urocentrum turbo* as well.

Thus, within *Paramecium* genus stages typical for different subclasses of class Oligohemenophorea can be found what seems very intriguing. On the other hand, relatively few species of Oligohymenophorea were investigated in details karyologically. The situation illustrates state of our present knowledge. In *Frontonia* sp. there are species showing „parachute", and others „crescent" stage (Devi 1961, Perez-Silva 1965, Fokin unpublished), such diversity seems very fundamental.

The other stages of progamic cycle of Mi divisions following prophase of I division, go similarly in majority of *Paramecium* species (Table 2). It is worth to notice, however, some events: in *P. bursaria* one of products of I progamic division always degenerates; in *P. nephridiatum* sometime extra pronuclei appear, later degenerating (Jankowski 1961); in *P. putrinum* great diversity observed in Con is characteristic for the species, there are variants of NR showing behavior of pronuclei and synkarion differing from the most common "amphimixis" type (Jankowski 1972).

According course of the old Ma fragmentation, two groups of *Paramecium* species can be formed (Table 2). One group includes *P. bursaria* and *P. duboscqui,* species without fragmentation, the second group includes species in which fragmentation begins before separation of conjugants (*P. putrinum*, *P. woodruffi*, *P. nephridiatum*, *P. multimicronucleatum*, *P. jenningsi*, the P. aurelia species complex, and *P. schewiakoffi*) or later in Excon (*P. calkinsi*, *P. polycaryum*, *P. caudatum*). Number of the old Ma fragments seems to be specific for the species (Jankowski 1972), e.g. 12 fragments in *P. calkinsi*, in the other species from 19 fragments in *P. polycaryum* to 85 in *P. putrinum* (Table 2). In *P. duboscqui* changes of old Ma in NR have unusual character, Ma do not degenerate like in *P. bursaria* but its extra division takes place during III metagamic cycle (Table 2, Fig. 3). Similar alteration of the old Ma was observed in *Urocentrum turbo* (Serrano *et al.* 1987), which is not a close relative of *Paramecium* (Strüder-Kypke *et al.* 2000b).

It should be stressed that the process of NR was studied, besides *Paramecium*, only in two others Peniculina, i.e. *Frontonia leucas* (Devi 1961) and *F. acuminata* (Perez-Silva 1965). Some details of the cited above descriptions showed that in *Frontonia* spp. appear some variants of the old Ma behavior, similar like in *Paramecium*, e.g. absence of fragmentation in *F. acuminata* (Perez-Silva 1965), extra Ma division (?) before its fragmentation in autogamous *F. leucas* (Devi 1961). Contemporary studies of NR in Con in two *Frontonia* species (Fokin, unpublished) proved existence of variants of old Ma behavior as well.

As a result of fusion of two haploid pronuclei, derivatives of III progamic division, usually in *Paramecium* species the diploid synkarion appears. In some species (*P. bursaria*, *P. putrinum*, *P. caudatum*) several deviations from the statement scheme may be observed, causing polyploidy (heteroploidy) (Chen 1940b, Cheissin *et al.* 1964, Borchsenius and Ossipov 1971, Jankowski 1972). For instance, pronuclei in such cases may be not haploid, so synkarion might be triploid or higher ploidy (Raikov 1972, 1982; Ossipov 1981), more than two pronuclei may be fused or numerous synkarions may be made, as in *P. caudatum* and *P. putrinum* (Jankowski 1972; Raikov 1972, 1982; Ossipov 1981) with further their fusion. Such cases might be fixed in evolution because poliploid Mi could show functional advantage in vegetative stage over diploid one (Fokin and Ossipov 1981). In *Paramecium*, excluding *P. bursaria* (Chen 1940b, Ovchinnikova 1970) such variants are not often cytologically observed.

Differences of NR course during metagamic cycle agree with it's lasting, could be 2, 3, or 4 divisions of synkarion and its derivatives and degeneration of different anlagen in several stages of the process. Partly, such changes appear in exconjugants (Table 2). Majority of *Paramecium* species (11) show 3 synkarion divisions, though as a result of pycnosis (*P. bursaria*, *P. calkinsi*, *P. jenningsi*) of one of two products of first synkarion division, the final number of nuclei is 4. Such number of nuclei also appears in species of the P. aurelia complex and *P. schewiakoffi*, species within two metagamic divisions. In *P. nephridiatum*, according to Jankowski

(1961) (presently, our scanty data do not prove it) pycnosis of one product of I synkarion division takes place causing that the final number of nuclei equal 8 is obtained after 4-th division. That distinguishes *P. nephridiatum* from relative *P. woodruffi* and the other *Paramecium* species (Table 2). Four metagamic divisions of synkarion were described (beside *P. nephridiatum*) only in autogamous NR of *F. leucas* (Devi 1961). In *F. acuminata* (Perez-Silva 1965, Fokin unpublished) only two metagamic divisions appear.

Sometime in a species, the course of Con may be variable depending on individual features of cells (Skoblo and Ossipov 1968, Jankowski 1972). In *P. putrinum* being characterized by composed structure of species (subspecies, syngens) a great variability of NR appears. At present work, the most typical amphimixis type (Jankowski 1972) is discussed only.

In *Paramecium* species, as result of metagamic divisions, 2 or 4 Ma anlagen and similar number of Mi anlagen are formed. Reduction of Ma anlagen number does not appear usually, however sometimes the number may differ. Number of Mi anlagen in some species (*P. putrinum*, *P. caudatum, P. schewiakoffi*) is reduced, by pycnosis of 3 from 4 nuclei (*P. putrinum*, *P. caudatum*) or 1 from 2 nuclei (*P. schewiakoffi*). The reason of degeneration of some morphologically and topologically identical nuclei that looks like apoptosis (Davis *et al.* 1992) is unclear till now (Raikov 1972, 1982; Ossipov 1981; Hiwatashi and Mikami 1989).

Fragmentation of the old Ma has functional character as its fragments do not undergo pycnosis and in some species under suitable conditions, process of Ma regeneration takes place (Jankowski 1961, 1972; Raikov 1982; Ossipov 1981; Fokin 1998). In many of *Paramecium* species (5), the fragmentation starts in progamic part of Con (Table 2), sometime (*P. putrinum*) even during I meiotic division (Jankowski 1972). In *P. calkinsi*, *P. polycaryum*, and *P. caudatum* fragmentation of Ma appears during II or III divisions of metagamic cycle, sometime in exconjugants. Number of Ma fragments is typical for species (Jankowski 1972), though our calculations in *P. nephridiatum*, *P. caudatum*, and *P. multimicronucleatum* showed 35, 46, 48 in sequence, less than cited by Jankowski (Table 2).

Analysis of NR course in *Paramecium* species (Table 2) allows to make dendrogram and MDS topogram of nuclear reorganization similarity for 12 species (Figs 2 A, B). Large number of features taken for analysis makes the obtained figures credible. *Paramecium bursaria* branches basally to all other *Paramecium* species showing definitely a very different features of NR (Fig. 2 A). The other species branching of the tree is *P. schewiakoffi*. It has not so different features of NR in comparison with the other species but its combination looks quite unusual. The position of the two species on the MDS topogram (Fig. 2 B) confirms that the species are located quite far away from the other concerning NR. The next clade includes *P. duboscqui*, *P. calkinsi*, *P. polycaryum*, and *P. caudatum* (Fig. 2 A). Only *P. caudatum* and *P. polycaryum* have quite similar NR since *P. duboscqui* and *P. calkinsi* are located on the border of the group (Fig. 2 B). Two other groups of species apparently have more NR similarity. There are *P. jenningsi* and the P. aurelia complex and, from the other side *P. nephridiatum*, *P. putrinum*, *P. woodruffi*, and *P. multimicronucleatum* (Fig. 2 A). The position of *P. nephridiatum* in the cluster is caused by extra, 4-th metagamic cycle. In other respects it is really similar with the NR of *P. woodruffi*. It seems surprising that NR of *P. woodruffi* and *P. multimicronucleatum* are almost identical (Figs 2 A, B). According to NR, the position of *P. putrinum* which should be considered as an ancient species is astonishing.

As a result of SSrRNA gene sequences comparison in 12 *Paramecium* species the phylogenetic relationships of species was constructed (Strüder-Kypke *et al.* 2000a, b). The genus *Paramecium* seems to be monophyletic cluster of species *P. bursaria* branches basally. The next clade includes *P. putrinum* and *P. duboscqui*, evolutionary very remote from the other species of *"woodruffi"* subgroup, i.e. *P. woodruffi*, *P. nephridiatum*, and *P. calkinsi* which appear as relative species composing a distinct cluster. The position of *P. polycaryum* is not so clear; it may belong to subgroup "*woodruffi"* (more likely) or to "aurelia". The members of "aurelia" subgroup compose monophyletic cluster in which the most related are species of the P. aurelia complex; *P. jenningsi* is very closely related to them; *P. caudatum* and *P. multimicronucleatum* seem more distantly related each other and with the other species of the subgroup.

Using comparative data on diversity of NR course in particular *Paramecium* species correlated with phylogenetic position of the species in the cluster, it seems possible to estimate the evolutionary direction of variation of the NR process in *Paramecium*.

It should be noted that evolutionary specialization proceeds independently in different organelles or processes in the same animal (Jankowski 1972, Corliss

1975, Raikov 1982) and it is called mosaic evolution or evolutionary heterochrony (Jankowski 1972, Raikov 1982). It might be the reason that NR tree did not coincide in several points with the results of analysis on molecular level. However, the position of *P. bursaria* arising from its NR is completely conformable with its phylogenetic one, and this ancient species of *Paramecium* in some traits is similar to *Frontonia*. The other features of *P. bursaria* antiquity (besides the behavior of the old Ma) are prominent symbiosis with *Chlorella* algae and peculiar structure in the Mi mitotic apparatus called by Schwartz (1978) "kinetosome". The typical kinetochores were not found in *P. bursaria* (Lewis 1975, Raikov 1982).

Paramecium putrinum was regarded by Jankowski (1972) as the most primitive *Paramecium* species, very close to *P. bursaria*. However, concerning the NR of *P. putrinum*, the mentioned author proposed, "the nuclear reorganization scheme has been secondary modified in this primitive paramecium ". The morphometric, biological and molecular analyses (Fokin and Chivilev 1999, 2000; Fokin 2000; Fokin *et al.* 1999b; Strüder-Kypke *et al.* 2000b) indicated that this species had separated from the rest of the *Paramecium* species after *P. bursaria*, but not as a sister species. It also shows considerable evolutionary distance from all other species of *Paramecium* except *P. duboscqui* (Strüder-Kypke *et al.* 2000b). The appearance of the „parachute" stage also separates *P. putrinum* from the majority of *Paramecium* species.

Only *P. bursaria* and *P. putrinum* among of the genus have a multiple MT system, the most common in Ciliophora. According to Jankowski (1972) those species inherited the multiple MT system from the ancestral form or forms. Unfortunately, up to present, we have no data on the MT system of the nearest relatives of *Paramecium*, i.e. *Frontonia, Disematostoma, Lembadion*. Miyake (1996) suggested that "the most primitive of the mating type systems is the binary one and ... one of possible general tendencies in evolution of MT is the increase of the number of MT". Following this idea, it should be admitted that in two most primitive species, i.e. *P. bursaria* and *P. putrinum*, the system of MT has been secondary modified.

The idea of secondary modification of NR process in *P. putrinum* (Jankowski 1972) seems true. Only *P. bursaria* and *P. putrinum* are the real outbreeders within the genus *Paramecium* and *P. putrinum* has a very short immaturity period. According to Dini and Nyberg (1993), the species with short immaturity period and outbreeding strategy could show faster evolutionary rate. *Paramecium putrinum* has five different patterns of NR, which mainly correspond, with the different syngens of this species and three morphological subspecies were mentioned for the paramecium (Jankowski 1972). It is likely that *P. putrinum* developed its current NR pattern during evolution of the species.

Morphologically *P. duboscqui* resembles the "*woodruffi*" subgroup of species (Fokin and Chivilev 1999) but its some biological features and results of molecular analysis indicate its position as situated closer to the base of the genus tree (Fokin and Chivilev, 2000; Strüder-Kypke *et al.* 2000a, b). In our both constructions, NR tree and MDS topogram (Figs 2 A, B), the species is located far away from the rest of the "*woodruffi*" subgroup (mainly caused by the behavior of the old Ma, as the other events in NR remind those of the "*woodruffi*" representatives).

Within the "*woodruffi*" subgroup, rather weak similarity can be find, as concerns the NR, between *P. calkinsi* and *P. polycaryum* (Figs 2 A, B). It is supported also by other analyses (Fokin 2000, Fokin and Chivilev 2000, Strüder-Kypke *et al.* 2000b). *Paramecium nephridiatum* and *P. woodruffi* have similar morphology and evolutionary distance between them is very short according to SSrRNA gene sequences (Fokin and Chivilev 1999, Strüder-Kypke *et al.* 2000b). Apparently, the NR process of *P. nephridiatum* (Jankowski 1961) should be reinvestigated, as the data on the fourth metagamic cycle seem not true. The position of *P. polycaryum* within the genus is a bit unstable as concerns morphometric and biological analysis from one side and phylogenetic investigation from another (Fokin and Chivilev 1999, 2000; Fokin 2000; Strüder-Kypke 2000a, b). The species is similar to *P. caudatum* (from the "aurelia" subgroup) according its NR peculiarities but according to SS rRNA gene sequence it cluster consistently with the "*woodruffi*" subgroup.

Paramecium calkinsi has only 2 Ma anlagen, 3 metagamic cycles (caused by degeneration of one of its synkarion products), and a special way of the old Ma fragmentation (as concerns time and number of fragments). The last feature appears also in *P. polycaryum*.

The higher *Paramecium* subgroup, the "aurelia", also does not manifest one type of NR (Figs 2 A, B). The process of NR is similar in *P. jenningsi* and the P. aurelia complex, it agrees with our phylogenetic results (Strüder-Kypke *et al.* 2000b). The different features of NR manifested by *P. caudatum* and *P. multimicronucleatum* correspond to more distant

relationship between the species in comparison with the aurelia and *jenningsi* relationship. Interesting enough that *P. multimicronucleatum* and *P. woodruffi,* which belong to different subgroups but both are rather large in size and have plural Mi, also manifest very similar pathway of the NR.

Paramecium schewiakoffi, apparently, should be placed in the "aurelia" subgroup but its phylogenetic position is not yet settled. The species reminds morphologically *P. jenningsi*, *P. caudatum*, and *P. wichtermani* (at least as the parachute stage is concerned for the last species). Nevertheless, its NR pattern is completely different from all other *Paramecium* species (Fig. 2 A). The key points for its discrimination are: the "parachute" stage in prophase of I-st progamic division of Mi and existence of 2 Ma anlagen, which develop in two metagamic cycles. Its life strategy seems to lead to the high rate of evolution as in the case of P. aurelia complex and *P. jenningsi. Paramecium schewiakoffi* might appeared not long ago. The species was found only in one locality in China but still the huge area of subtropical Eurasia is almost not investigated as ciliate fauna is concerned (Przyboś and Fokin 2000a, b).

As was shown previously, the *Paramecium* species maintain morphological stability being molecularly differentiated, at least as measured by the SS rRNA sequence divergence (Strüder-Kypke *et al.* 2000b). The genus is showing also a variety of karyological characteristics but it is possible to find out in their NR pattern some evolutionary tendency. Behavior of the old Ma could be the example. There are two main patterns of macronuclear degeneration in ciliates, with its fragmentation, which is more frequent (Raikov 1969), and without it. The ability of Ma fragments to regenerate means that they do not undergo the irreversible degenerative changes for a long time (Raikov 1972, 1982). Their functional interactions with the Ma anlagen, i.e. inhibition of the old Ma fragments or suppression of development of the Ma anlagen, indicate that the process is dramatically important for ciliate's cell (Sonneborn 1947, Jankowski 1961, Ossipov and Skoblo 1968, Berger 1973, Raikov 1982, Fokin 1998).

The absence of the old Ma fragmentation is, apparently the primitive feature in the evolution of nuclear dualism (Raikov 1972, 1982; Orias 1986). It seems that the species manifesting the old Ma fragmentation in different stages of NR, developed it in different time during evolution. Summing up our data and literature ones, it is possible to prepare the scheme of evolution of the old Ma behavior in ciliates, using as a model *Paramecium* genus (Fig. 3). Ancient pattern of the old Ma resorption without nuclear fragmentation is demonstrated by *P. bursaria*, that type can be often found in Ciliophora (Jankowski 1972; Raikov 1969, 1972, 1982). In *P. duboscqui* the process is going on with one additional macronuclear division, which could be homologous with the first step of fragmentation as in *F. leucas*. In *P. caudatum, P. polycaryum*, and *P. calkinsi* the fragmentation takes place in exconjugants only, and the number of fragments in two last species is rather small. In the next group of *Paramecium* species, i.e. *P. schewiakoffi, P. jenningsi*, the P. aurelia complex, *P. multimicronucleatum*, and probably *P. wichtermani*, the fragmentation occurs a little before or during separation of the conjugation partners, in the middle of the NR. Evolutionary these species belong to the "aurelia" subgroup. Only three species *P. nephridiatum, P. woodruffi* and *P. putrinum* manifest the old Ma fragmentation at the beginning of NR or in the first part of it. According our analysis, *P. nephridiatum* and *P. woodruffi* are very close related species, which diverged quite recently. A number of syngens of *P. putrinum* with different pattern of the NR and even morphological divergence within this taxonomic species (Jankowski 1972) indicates that we are dealing with a series of quite recent secondary modifications. Thus, general evolutionary direction of the old Ma changes during the NR is from the absence of fragmentation to the appearance of it at the early NR stages (Fig. 3).

Type of Mi I-st progamic prophase, the „crescent" or the „parachute" stage, appear in different ciliates. Further investigations of Oligohymenophorea may bring more examples of species showing parachute stage.

It is likely, that the ciliate divergence occurred after evolution of the functional features of meiosis and fertilization of the nuclear cycle, which enabled a life cycle with haploid and diploid phases (Orias 1986). Short haploid phase and very important beginning of diploid one occur during the NR process in ciliates. As a basic, progamic phase of the sexual process is more stable. Part of the NR stages (mainly during metagamic phase of Con) has a wide diversity in *Paramecium* species. Several of the variations probably reflect some evolutionary stages of the NR development. May be the NR process in *Paramecium* generally has a tendency for shortening (see Fig. 1).

However, taking into consideration the existence of mosaic evolution or evolutionary heterochrony of some features in *Paramecium*, it seems better to use for the

phylogenetic schemes a combination of data obtained from several different traits and by different approaches.

Acknowledgements. We are grateful to Dr M Fujishima and Dr S. V. Dobretzov for help in getting some of the samples. The writing of this article partly was supported by a grant from DAAD: 325/tr-lin, Germany in which the senior author was participating.

REFERENCES

Aufderheide K., Daggett J., Nerad T. A. (1983) *Paramecium sonneborni* n. sp., a new member of the *Paramecium aurelia* species-complex. *J. Protozool.* **30:** 128-130

Barnett A. (1964) Cytology of conjugation in *Paramecium multimicronucleatum*, syngen 2, stock 11. *J. Protozool.* **11:** 147-153

Berger J. D. (1973) Selective inhibition of DNA synthesis in macronuclear fragments in *Paramecium aurelia* exconjugants and it reversal during macronuclear regeneration. *Chromosoma* **44:** 33-48

Borchsenius O. N., Ossipov D. V. (1971) Polymorphism of micronuclei in *Paramecium caudatum*. III. Cytofluometric investigation of the quontaty of DNA. *Cytologia* **13:** 1041-1043 (in Russian with English summary)

Braverman E. M. (1965) On potential function procedure. *Autom.Telemech.* **21:** 21-26

Calkins G. N., Cull S. W. (1907) The conjugation of *Paramecium aurelia* (*caudatum*). *Arch. Protistenkd.* **10:** 375-415

Cheissin E. M., Ovchinnikova L.P., Kudrjavtcev B. N. (1964) A photometric study of DNA content in macronuclei and micronuclei of different strains of *Paramecium caudatum*. *Acta Protozool.* **1:** 63-69

Chen T. T. (1940a) Conjugation in *Paramecium bursaria* between animals with diverse nuclear constitution. *J. Hered.* **31:** 185-196

Chen T. T. (1940b) Polyploidy and its origin in *Paramecium*. *J. Hered*. **31:** 175-184

Corliss J. O. (1975) Nuclear characteristics and phylogeny in the protistan phylum Ciliophora. *Biosystems* **7:** 338-349

Davis M. C., Ward J. G., Herrick C., Allis C. D. (1992) Programmed nuclear death: apoptotic-like degradation of specific nuclei in conjugating *Tetrahymena. Dev. Biol.* **154:** 419-432

Devi R. V. (1961) Autogamy in *Frontonia leucas* (Ehrbg.). *J. Protozool*. **8:** 277-283

Diller W. F. (1948) Nuclear behavior of *Paramecium trichium* during conjugation. *J. Morphol.* 82: 1-52

Diller W. F. (1954) Autogamy in *Paramecium polycaryum*. *J. Protozool.* **1:** 60-70

Diller W. F. (1958) Studies of conjugation in *Paramecium polycaryum*. *J. Protozool.* **5:** 282-292

Diller W. F., Earl P. R. (1958) *Paramecium jenningsi* n. sp. *J. Protozool*. **5:** 155-158

Dini F., Nyberg D. (1993) Sex in Ciliates. In: Advances in Microbial Ecology (Ed. J. G. Jones). Plenum Press, New York. **13:** 85-153

Fokin S. I. (1986) Morphology of the contractile vacuoles in *Paramecium* genus (Hymenostomatida, Peniculina) as a species-specific trait. *Zool. Zh.* **65:** 5-16 (in Russian with English summary)

Fokin S. I. (1997) Morphological diversity of the micronuclei in *Paramecium*. *Arch. Protistenkd.* **148:** 375-387

Fokin S. I. (1998) Strategies of the macronuclear endocytobionts of *Paramecium* during the sexual process of the host. *Symbiosis* **25:** 323-342

Fokin S. I. (2000) Host specificity of *Holospora* and its relationships with *Paramecium* phylogeny. *Japan. J. Protozool.* **33:** 94

Fokin S. I., Chivilev S. M. (1999) Brackish water *Paramecium* species and *Paramecium polycaryum.* Morphometric analysis and some biological peculiarities. *Acta Protozool.* **38:** 105-117

Fokin S. I., Chivilev S. M. (2000) *Paramecium.* Morphometric analysis and taxonomy. *Acta Protozool.* **39:** 1-14

Fokin S. I., Ossipov D. V. (1981) Generative nucleus control over cell vegetative functions in *Paramecium*. *Acta Protozool*. **20:** 51-73

Fokin S. I., Stoeck T., Schmidt H. J. (1999a) Rediscovery of *Paramecium nephridiatum* Gelei, 1925 and its characteristics. *J. Euk. Microbiol.* **46:** 416-426

Fokin S. I., Strüder-Kypke M. C., Chivilev S. M., Wright A.-D.G., Lynn D. H., (1999b) Relationships in the genus *Paramecium*. Biological, morphometric and sequencing analysis. Abstr. 3-rd Europ.Congr.Protistol. Helsingor, Denmark, 31

Fokin S. I., Przyboś E., Chivilev S. M. (2001a) Nuclear reorganization variety in *Paramecium* genus and it's possible evolution. Abstr. XI Intern. Congress of Protozoology. Salzburg, Austria, 37

Fokin S. I., Przyboś E., Chivilev S. M., Fujishima M. (2001b) *Paramecium schewiakoffi* n. sp. (Peniculida, Ciliophora), a new member of the genus. Abstr. XI Intern.Congress of Protozoology. Salzburg, Austria, 66

Hamburger C. (1904) Die Konjugation von *Paramecium bursaria* Focke. *Arch. Protistenkd.* **4:** 199-239

Hiwatashi K., Mikami K. (1989) Fertilization in *Paramecium*: processes of the nuclear reorganozation. *Rev. Cytol.* **114:** 1-20

Jankowski A. V. (1961) Conjugation process of the rare brackishwater ciliate *Paramecium woodruffi*. *Dok. AS USSR*. **137:** 989-992 (in Russian)

Jankowski A.V. (1972) Cytogenetic of *Paramecium putrinum* C. et L., 1858. *Acta Protozool.* **10:** 285-394

Jurand A., Selman G. G. (1969) The Anatomy of *Paramecium aurelia*. Macmillan, St. Martin's Press, London, New York

Kruskal J. B., Wish M. (1978) Multidimensional Scaling. Sage Populations. Beverly Hills, California

Lewis L. W. (1975) The evolutionary significance of ultrastructural variations in the micronuclear spindle apparatus in the genus *Paramecium*. *Biosystems* **7:** 380-385

Mitchell J. B. (1962) Nuclear reorganization in *Paramecium jenningsi*. *J. Protozool.* **9 (Suppl.):** 26

Mitchell J. B. (1963) Nuclear activity in *Paramecium jenningsi* with reference to other members of the aurelia group. *J. Protozool.* **10 (Suppl.):** 11

Miyake A. (1996) Fertilization and sexuality in Ciliates. In: Ciliates. Cells as a Organisms (Eds. K. Hausmann and Ph. C. Bradbury). G. Fischer, Stuttgart, 243-290

Nakata A. (1958) Mating types, *Paramecium calkinsi*. *Zool. Mag.* (Tokyo) **67:** 210-213

Orias E. (1986) Ciliate conjugation. In: The Molecular Biology of Ciliated Protozoa (Ed. J. G. Gall). Academic Press, Orlando, Florida, 45-84

Ossipov D. V. (1981) Problems of Nuclear Heteromorphism in the Unicellular Organisms. Nauka, Leningrad (in Russian)

Ossipov D. V., Skoblo I. I. (1968) Autogamy during conjugation in *Paramecium caudatum* Ehrbg. II. The ex-autogamont stages of nuclear reorganization. *Acta Protozool.* **6:** 33-48

Ovchinnikova L. P. (1970) Variability of DNA content in micronuclei of *Paramecium bursaria. Acta Protozool.* **7:** 211-220

Perez-Silva J. (1965) Conjugation in *Frontonia acuminata,* Ehrenberg. In: Progress in Protozoology. Excerpta Medica Foundation, Amsterdam, London, 216-217

Poljansky G. I. (1926) Die Conjugation von *Dogielella shaerii* (Infusoria, Holotricha, Astomata). *Archiv Protistenkd.* **53:** 407-434

Przyboś E. (1975) Genetic studies of *Paramecium jenningsi* strains (Diller, Earl, 1958). *Folia biol*. (Kraków) **23:** 425-471

Przyboś E. (1978) Cytological and karyological studies of *Paramecium jenningsi*. *Folia biol.* (Kraków) **26:** 25-29

Przyboś E. (1980) The African strain of *Paramecium jenningsi*. Cytological and karyological investigations. *Folia biol*. (Kraków) **28:** 391-397

Przyboś E. (1986a) Chromosomes in *Paramecium jenningsi* (Diller and Earl, 1958): A serial section study. *Folia biol*. (Kraków) **34:** 133-160

Przyboś E. (1986b) Species structure in Ciliates. *Folia biol*. (Kraków) **34:** 103-132

Przyboś E. (1986c): Cytological and karyological studies on Ciliates. *Folia biol.* (Kraków) **34:** 241-262

Przyboś E., Fokin S. (2000a) Data on the occurrence of species of the Paramecium aurelia complex world-wide. *Protistology* **1:** 179-184

Przyboś E., Fokin S. (2000b) Occurrence of *Paramecium* spp. (Protista, Ciliophora) in the world fauna. Abstr. 18-th Intern. Zool. Congr. Athens, Greece, 202

Przyboś E., Kościuszko H., Komala Z. (1979) Karyological studies of strain 324 of *Paramecium triaurelia*. *Folia biol.* (Kraków) **27:** 355-359

Raikov I. B. (1969) The macronucleus of ciliates. In: Research in Protozoology (Ed. Chen T. T.). Pergamon Press, Oxford **3:** 1-128

Raikov I. B. (1972): Nuclear phenomena during conjugation and autogamy in Ciliates. In: Research in Protozoology (Ed. Chen T. T.). Pergamon Press, Oxford, **4:** 147- 291

Raikov I. B. (1982) The Protozoan Nucleus. Morphology and Evolution. Springer-Verlag. Wien, New York

Schwartz V. (1978) Structur und Enwicklung des Macronucleus von *Paramecium bursaria. Archiv Protistenkd.* **120:** 255-277

Serrano S., Martin-Gonzalez A., Fernandez-Galiano D. (1987) Nuclear phenomena and oral reorganization during the conjugation of *Urocentrum turbo* O.F.M. (Ciliata). *Archiv Protistenkd.* **133:** 257-268

Shimomura F., Takagi Y. (1984) Chemical induction of autogamy in *Paramecium multimicronucleatum*, syngen 2. *J. Protozool*. **31:** 360-362

Skoblo I. I., Ossipov D. V. (1968) The autogamy during conjugation in *Paramecium caudatum* Ehrenb. I. Study on the nuclear reorganization up to stage of the third synkaryon division. *Acta Protozool*. **5:** 273-290

Skovorodkin I. N. (1990) A device for immobilization of small biological objects during it light microscopical observation. *Cytologia* (St. Petersburg) **32:** 87-91 (in Russian with English summary)

Sneath P. H. A., Sokal R. R. (1973) Numerical Taxonomy. W. H. Freeman & Co, San Francisco

Sonneborn T. M. (1947) Recent advances in the genetics of *Paramecium* and *Euplotes*. *Adv. Genet.* **1:** 263-358

Sonneborn T. M. (1970) Methods of *Paramecium* research. In: Methods in Cell Physiology. Acad. Press, New York. **4:** 241-339

Sonneborn T. M. (1975) The *Paramecium aurelia* complex of fourteen sibling species. *Trans. Am. Microsc. Soc.* **94:** 155-178

Strüder-Kypke M. C., Wright A.-D. G., Fokin S., Lynn D. H. (2000a) Phylogenetic relationships of the genus *Paramecium* inferred from small subunit rRNA gene sequences. *Mol. Phylogen. Evol.* **14:** 122-130

Strüder-Kypke M. C., Wright A.-D. G., Fokin S., Lynn D. H. (2000b) Phylogenetic relationships of the subclass Peniculia (Oligohymenophorea, Ciliophora) inferred from small subunit rRNA gene sequences. *J. Eukaryot. Microbiol.* **47:** 419-429

Summers F. M., Kidder G. W. (1936) Taxonomic and cytological studies on the ciliates associated with the amphipod family Orchestiidae from the woodshole district. II The coeloric astomatous parasites. *Archiv Protistenkd.* **86:** 379-402

Viver E. (1974) Morphology, taxonomy and general biology of the genus *Paramecium.* In: *Paramecium*. A Current Survey (Ed. W. J. Van Wagtendonk). Elsevier Scientific Publishing, Company, 1-90

Watanabe T., Shi X., Lin G., Jin M. (1996) Cytological studies of conjugation and nuclear processes in *Paramecium duboscqui* Chatton&Brachon 1933. *Europ. J. Protistol.* **32(suppl. 1):** 175-182

Wichterman R. (1948) The time schedule of mating and nuclear events in the conjugation of *Paramecium bursaria. Turt. News* **26:** 1-7

Wichterman R. (1953) The Biology of *Paramecium*. Blakiston, Toronto

Wichterman R. (1986) The Biology of *Paramecium,* 2 ed. Plenum Press, New York, London

Woodruff L. L. (1945) The early history of the genus *Paramecium* with secial reference to *P. aurelia* and *P. caudatum. Trans. Conn. Acad. Art. Sci.* **36:** 517-531

Yanagi A., Haga N. (1996) A simple method of induction of autogamy by methylcellulose in *Paramecium caudatum*. *Europ. J. Protistol.* **32(Suppl. 1):** 183-186

Received on 25th June, 2001; accepted on 14th September, 2001

Acta Protozool. (2001) 40: 263 - 272

ACTA
PROTOZOOLOGICA

Confocal and Light Microscope Examination of Protozoa and Other Microorganisms in the Biofilms from a Rotating Biological Contactor Wastewater Treatment Plant

Mercedes MARTÍN-CERECEDA[1], Alberto M. ÁLVAREZ[2], Susana SERRANO[1] and Almudena GUINEA[1]

[1]Departamento de Microbiología III, Facultad de Biología, Ciudad Universitaria s/n, Madrid; [2]Centro de Citometría de Flujo y Microscopía Confocal, Facultad de Farmacia,Ciudad Universitaria s/n, Madrid, Spain

Summary. Wastewater biofilms from a full-scale treatment plant by rotating biological contactor (RBC) system are described using confocal scanning laser microscopy (CSLM) and light microscopy (LM). The main objective was to determine the internal architecture of biofilms, with a particular emphasis on the spatial distribution of protozoa and their relation to other microorganisms and non-cellular components. Biofilms were composed of a wide variety of microorganisms: i.e. filamentous bacteria, green algae, ciliated protozoa, nematodes and rotifers. Peritrich ciliates constituted the most abundant group within protozoan and metazoan biofilm communities, and they played an important role in maintaining the multilayer biofilm organisation owing to the intricate entanglement formed by their peduncles together with the filamentous bacteria. Identification of ciliates to species level was approached by light microscopy, *Vorticella convallaria, Epistylis entzii, Carchesium polypinum, Vorticella infusionum* and *Opercularia articulata* being the most abundant species. It was shown by confocal microscopy that microbial distribution changed with biofilm depth, outer layers having the highest heterogeneity. Architectural biofilm organisation consisted of bioaggregates surrounded by an extensive exopolymeric matrix whose porosity decreased from outer to inner layers. The role of exopolymers as a structural component of RBC biofilms is also revealed by confocal microscopy. This study demonstrates the utility of confocal microscopy for the analysis of protozoan distribution within thick living wastewater biofilms.

Key words: biofilm architecture, ciliates, confocal scanning laser microscopy, full-scale wastewater treatment plant, metazoa, protozoa, rotating biological contactors.

INTRODUCTION

Rotating biological contactor (RBC) system is one of the biological methods used for the sewage treatment. This system consists of a series of closely spaced discs partially immersed in a tank through which wastewater flows. Its biological principle is based on the metabolic activities of complex microbial communities that grow on the disc surface forming a biofilm (Bishop and Kinner 1986). Protozoa play a key role within biofilm microbiota; they are responsible of decreasing bacterial numbers contained in wastewater, and some of them have the capability to consume dissolved and flocculated organic matter (Bishop and Kinner 1986). Moreover, ciliates have been showed as bioindicators of biological process

Address for correspondence: Mercedes Martín-Cereceda, Departamento de Microbiología III, Facultad de Biología, Ciudad Universitaria s/n, Madrid 28040, Spain; Fax: +34 (91) 3944964; E-mail: cereceda@eucmax.sim.ucm.es

efficiency (Kinner and Curds 1987, Kinner *et al.* 1989, Luna-Pabello *et al.* 1990).

The spatial distribution of these microorganisms and their interactions within biofilm structure has been scarcely studied. To date, architecture of RBC biofilms has been only addressed by scanning and transmission electron microscopy (Alleman *et al.* 1982, Kinner *et al.* 1983); however, as these techniques require a previous sample dehydration and fixation, they do not allow for a non-disturbing architectural observation. Confocal scanning laser microscopy (CSLM), due to its optical sectioning features, high spatial resolution and minimal sample manipulation, is a very powerful tool for the non-destructive examination of thick biological samples (Caldwell *et al.* 1992, Laurent *et al.* 1994). Recently, confocal microscopy has been successfully applied to different aspects of microbial ecology. Bacterial dynamics in soil smears (Bloem *et al.* 1995), structure of suspended flocs from freshwater (Droppo *et al.* 1996, 1997; Liss *et al.* 1996; Neu 2000) and from activated sludge wastewater treatment system (Wagner *et al.* 1994a, b; Droppo *et al.* 1996; Liss *et al.* 1996; Wagner *et al.* 1996; Olofsson *et al.* 1998), have been described using CSLM. Spatial arrangement, composition and properties of different types of microbial biofilms have also been approached by confocal microscopy: studies of bacterial monoculture biofilms (Korber *et al.* 1994, Kuehn *et al.* 1998), laboratory-grown mixed biofilms (Lawrence *et al.* 1991, Stoodley *et al.* 1994, Wolfaardt *et al.* 1994, Massol-Deyá *et al.* 1995, Hausner and Wuertz 1999), and natural biofilms colonising plant leaf surfaces (Morris *et al.* 1997), or reactors treating river waters (Neu and Lawrence 1997) and petroleum-contaminated groundwaters (Massol-Deyá *et al.* 1995), have revealed the heterogeneous biofilm organisation.

However, there are hitherto no studies on the application of CSLM to reveal the occurrence *in situ* of protozoa within mature biofilms of full-scale wastewater treatment plants. Therefore, the main aim of this work was to provide a first descriptive report on the spatial distribution of protozoa (and other) microorganisms within RBC biofilms using confocal microscopy. Arrangement of non-cellular components (i.e. exopolymers and debris) and their relation to biofilm microbial community was also outlined through this microscopical technique. Confocal microscopy approach was complemented with light microscopy (LM) to get further information concerning abundance and identification of protozoan species in the biofilms.

MATERIALS AND METHODS

Sampling

Biofilm samples (6 individual samples) were taken from the external discs of a four series RBC system (surface area 9290 m^2 each; organic loading 0.006-0.01 Kg BOD_5 m^2 d^{-1}) at a full-scale wastewater treatment facility ("Las Matas", North of Madrid, Spain) treating domestic sewage derived from a population of 10,000 people. Biofilm thickness ranged between 0.4-0.5 cm, but sometimes biofilms could reach up to 1 cm thick. Sampling of biofilm was done by pressing a spatula against the disc surface and scrapping carefully biofilm strips preserving biofilm architecture. These were placed on microscopical slides, kept in humid chambers to maintain hydration, and transported to the laboratory in a refrigerated container.

Biofilm processing

Samples were maintained in humid chambers to preserve hydration during study and examined within 2-3 h of collection. Biofilm segments of 5 by 5 mm were carefully sliced avoiding disruption using a razor blade, and stained with DTAF (5-(4,b-dichlorotriazin-2-yl) aminofluorescein, Sigma-Aldrich Co.; 2 µg/ml PBS) and PI (propidium iodide, Sigma-Aldrich Co.; 10 µg/ml PBS). DTAF labels proteins with green fluorescence, while membrane-impermeable PI labels nucleic acids of damaged (dead) cells with red fluorescence. Thus, PI dye was used to assess cell viability. To detect the exopolysaccharide matrix, some biofilm samples were only stained with a sugar non-specific fluorescent marker (CR, Congo Red, Sigma-Aldrich Co.; 10 µg/ml PBS) (based on Allison and Sutherland, 1984). After 40 min at room temperature all stained samples were rinsed with PBS to remove excess of fluorochromes, deposited on coverslips and imaged by confocal microscope. Outer biofilm layers were those oriented to the liquid phase flow and inner biofilm layers were those in contact to the RBC support.

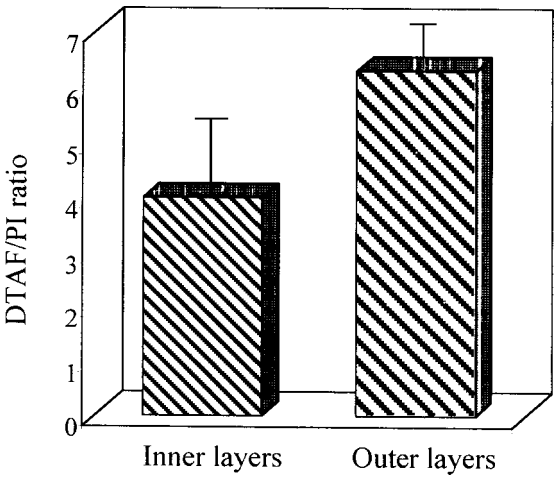

Fig. 1. DTAF/PI ratio (determined as the average DTAF value to the average PI value of images from each depth) in both inner and outer layers of the RBC biofilms studied

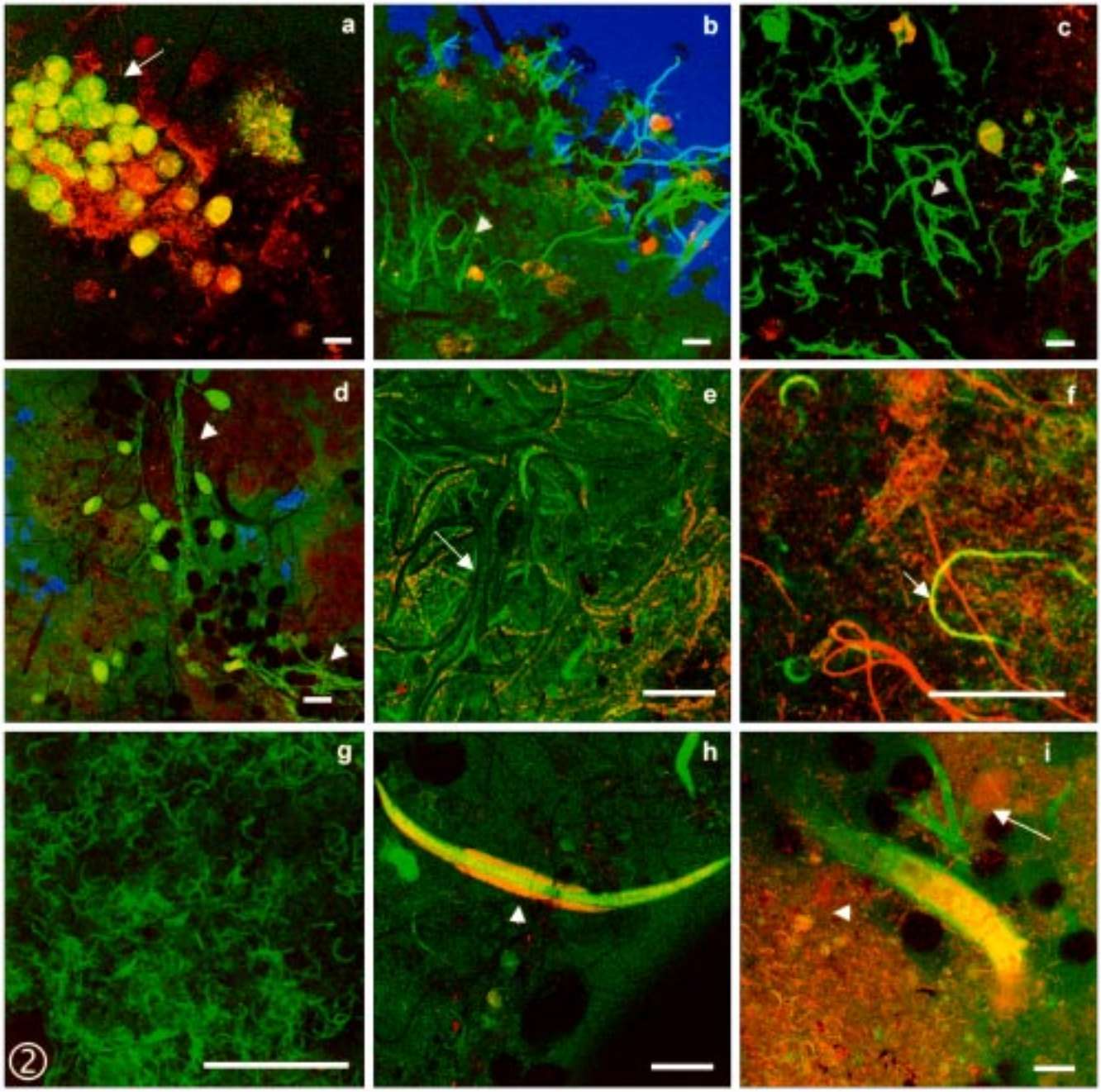

Figs 2 a-i. Single horizontal CSLM sections stained jointly with DTAF and PI dyes illustrating the microbial diversity in the outer RBC biofilm layers. **a**- peritrich ciliated protozoa colonies (arrow) like *Carchesium polypinum* were usually observed. **b-d** - entanglement of peritrich peduncles (arrow head) maintained multilayer biofilm arrangement. **e-f** - extensive filamentous bacterial mats (*Beggiatoa* spp.) provided consistence to the biofilm (arrow). **g** - green algae of genus *Selenastrum* occupied wide areas of the outer biofilm. **h-i** - aerobic nematodes (arrow head in h) were common inhabitants of these regions. Note the presence of peritrich ciliates (arrow in i) and *Selenastrum* cells (arrow head in i). Scale bar - 50 µm, except **b** and **d** - 100 µm. Colour coding: green - DTAF; red - Congo Red; blue - transmission signal (phase contrast)

Confocal microscopy examination

A MRC-1024 confocal scanning laser microscope (Bio-Rad, Hemel Hempstead, UK) coupled to an inverted microscope (Eclipse TE300 Nikon) was used to analyse biofilm architecture. DTAF and PI were excited at 488 nm and fluorescence emission was collected through BP 515/15 nm and BP 605/20 nm respectively. Congo Red stained samples were examined at the same wavelength as set for PI. Observations were made with the following fluorite lenses (Nikon): x20 (0.45 Numerical Aperture, NA), x40 (0.60 NA) and x63 -oil immers-

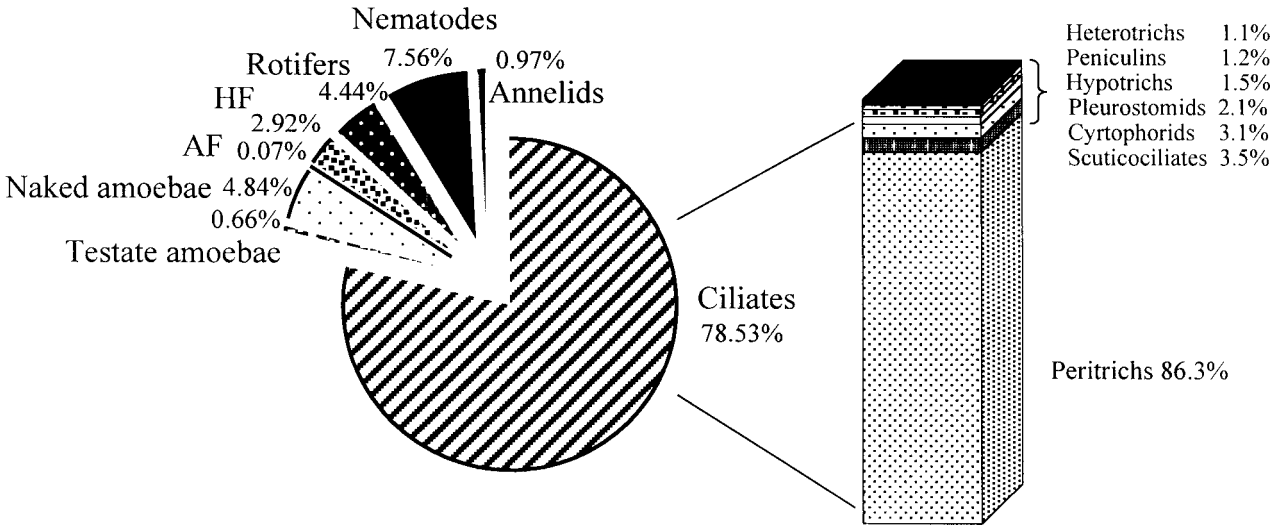

Fig. 3. Relative abundances (%) of protozoan and metazoan communities in the RBC biofilms studied, and distribution of ciliate abundances into taxonomic groups (Order). HF - heterotrophic flagellates; AF - autotrophic flagellates

ible (1.4 NA). Twenty five single images were recorded for each of the 6 individual samples collected. In some cases, sequences of images were taken along the optical Z axis using the confocal optical sectioning facility. Image acquisition was performed with the software package delivered with the instrument (Lasersharp v.3.2.). A minimum processing of samples was done with the program Confocal Assistant (v.4.02).

Identification of microorganisms

Replicate samples of biofilm were collected to determine abundances of protozoan and metazoan groups, and to conduct microorganism identifications. These samples were mixed with 0.45 µm filtered bulk wastewater liquor, and the biofilm suspensions obtained were then analysed through light microscopy (bright field and phase contrast). Counts were made as described Madoni (1988) for activated sludge system. To characterise ciliates to species level, pyridinated carbonate (Fernández-Galiano 1994) and protargol (Wilbert 1975) methods were applied. Several taxonomical works were used to help in the identifications (Kahl 1930-35; Foissner *et al.* 1991, 1992, 1994, 1995 and references therein). Specialised literature on metazoa and algae were also checked (Edmondson 1959, Pentecost 1984 and references therein).

RESULTS AND DISCUSSION

Examination by confocal microscope was made in the outer layers (up to 200 µm from external surface) and the inner layers (up to 200 µm from the disc support) of the removed RBC biofilms. A different distribution of fluorescence intensity was observed with depth; DTAF/PI ratio was higher in outer layers (Fig. 1), owing to the higher DTAF signal and the lower PI signal obtained in these layers. These results indicate that microbial biomass and architecture of biofilm matrix changed with depth.

In outer layers, microbial biocenosis was very heterogeneous (Fig. 2). Complex communities mainly constituted by filamentous bacteria, protozoa, green eukaryotic algae and small metazoa were observed. Filamentous bacteria in the RBC plant studied (Figs 2 e, f), which were mainly represented by *Beggiatoa* spp. (Galván *et al.* 2000), were entangled and forming a wide coverage

Figs 4 a-u. Light microscope (phase contrast) microphotographs of the most representative species of ciliates in the RBC biofilms studied. **Peritrichs: a** - *Vorticella convallaria* (x270); **b** - *Epistylis entzii* (x180); **c** - *Carchesium polypinum* (x60); **d** - *Vorticella infusionum* (x225); **e** - *Opercularia articulata* (x255). **Scuticociliates: f** - *Dexiotricha tranquilla* (x640); **g** - *Cinetochilum margaritaceum* (x880); **h** - *Uronema nigricans* (x990); **i** - *Cyclidium glaucoma* (x530). **Cyrtophorids: j** - *Trochilia minuta* (x900); **k** - *Trithigmostoma cucullulus*(x245). **Pleurostomatids: l** - *Litonotus lamella* (x320); **m** - *Amphileptus pleurosigma* (x230); **n** - *Acineria incurvata* (x350); **o** - *Litonotus cygnus* (x230). **Hypotrichs: p** - *Aspidisca cicada* (x1000*)*; **q** - *Euplotes affinis* (x460). **Peniculins: r** - Paramecium aurelia complex (x400); **s** - *Paramecium caudatum* (x250). **Heterotrichs: t** - *Metopuses* (x430*)*; **u** - *Stentor roeselii* (x90)

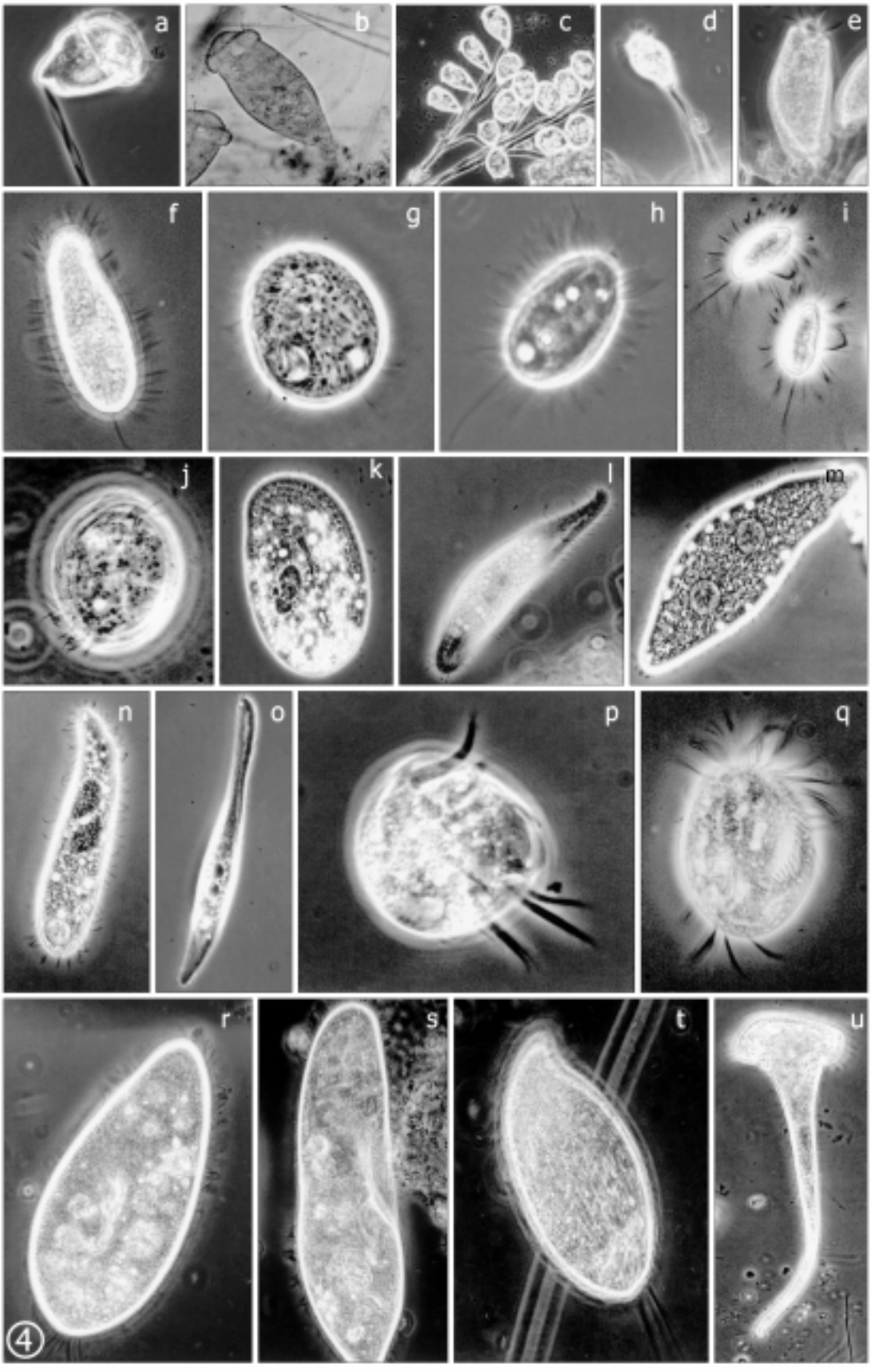
a
b
c
d
e
f
g
h
i
j
k
l
m
n
o
p
q
r
s
t
u
④

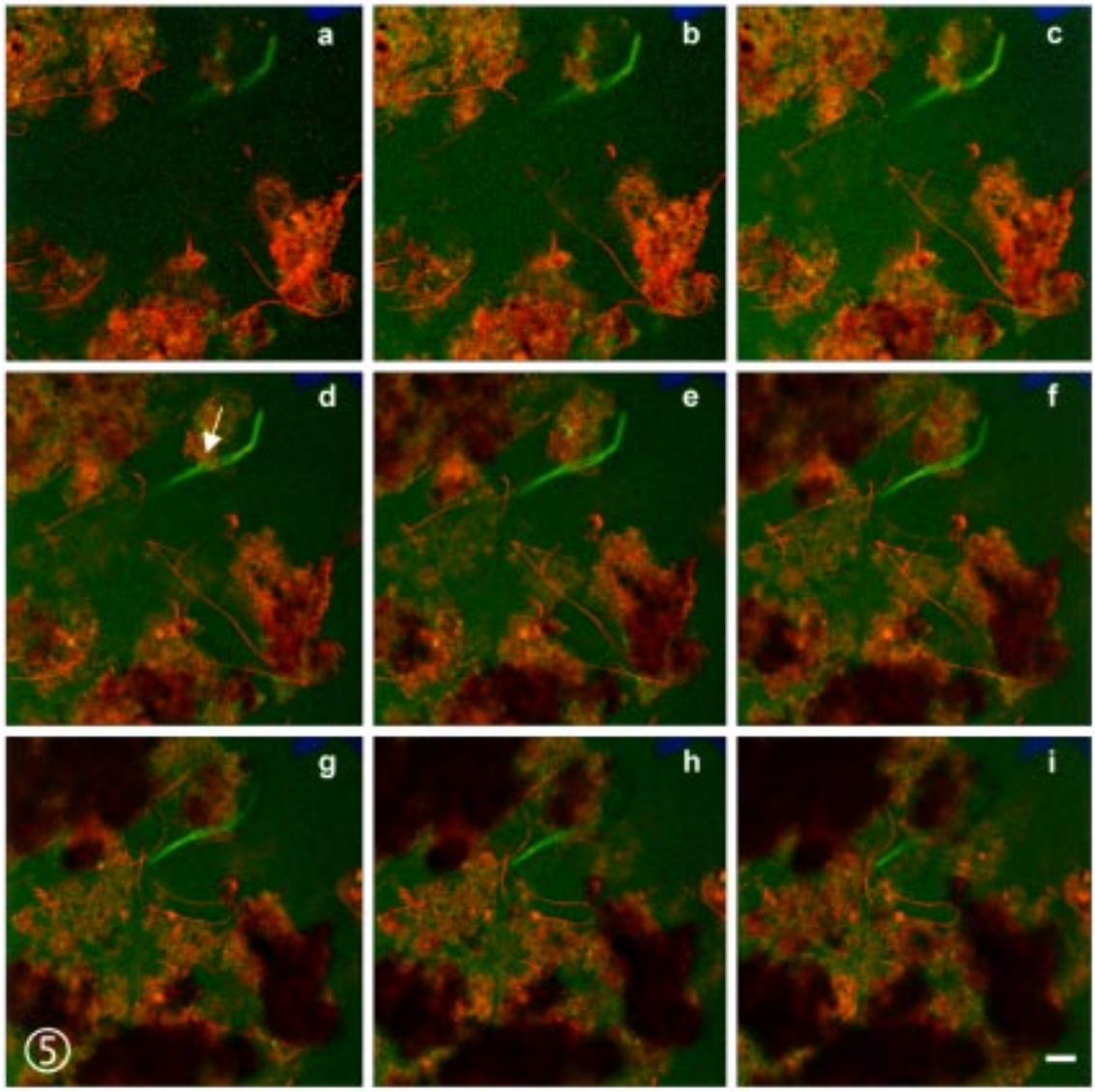

Figs 5 a-i. Series of horizontal CSLM sections of the outer RBC biofilm layers stained jointly with DTAF and PI dyes. Images are arranged towards the outermost surface of biofilm. Sections were taken at 10 µm intervals. Note the organisation in bioaggregates scattered on the proteic sheet (green fluorescence of DTAF), and the organic or inorganic material incorporated to biofilm surface (see g, h, i, sections). Arrow points a live nematode individual. Scale bar - 100 µm

within the biofilm. Confocal microscope observations denoted that peritrich ciliates were the most abundant group of protozoan and metazoan communities in these RBC biofilm layers. Peduncles of these ciliates appeared connected between and together with the filamentous bacteria, resulting in a complicate network that supports the multilayer biofilm organisation (Figs 2 a-d). Abundances of protozoan and metazoan communities in biofilm suspensions were obtained through light microscope counts, confirming that the peritrich ciliates hold around 90 % of total abundance (Fig. 3). Other ciliate groups (Order) represented in the biofilms were scuticociliates, cyrtophorids, pleurostomatids, hypotrichs, peniculins and heterotrichs, but their abundances were extremely lower than that of the peritrich group (Fig. 3). Representatives of tetrahymenids, suctorians gymnostomids, nassulids and prostomids were also occasionally found in RBC biofilms, and they accounted together for less than 1% of total ciliate abundance. Using light microscopy in conjunction with silver nitrate methods, the biofilm ciliate species were characterised to species level. The peritrich ciliates were mainly

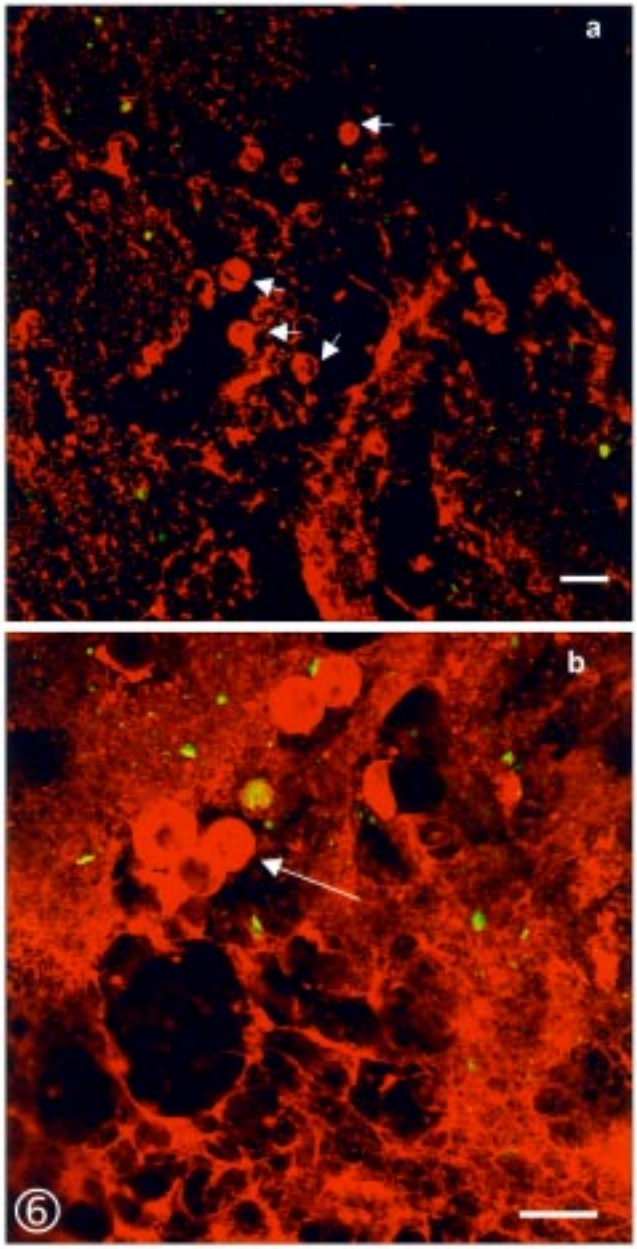

Figs 6 a, b. Exopolysaccharide matrix, stained with Congo Red dye and visualised by CSLM, in the outer RBC biofilm layers. Macropored organisation made of intersticies, voids and interconnecting fibrils. Spherical structures (arrow) are peritrich zooids having cell-wall mucopolysaccharides revealed by Congo Red staining. Scale bars - 100 μm

represented by *Vorticella convallaria, Epistylis entzii, Carchesium polypinum, Vorticella infusionum* and *Opercularia articulata* (Figs 4 a-e). Other representative species of ciliates in the RBC biofilms studied are shown in Fig. 4. These species were rarely seen when using confocal microscope, owing to their lower abundance and their fast movement.

The architecture of outer layers was depicted by a patchy distribution of microbial aggregates dispersed in a smooth organic layer with high protein content, as showed the green staining with DTAF (Fig. 5). The outermost regions had material not labelled with the fluorochromes used (see Figs 5 g-i - brownish areas in sections). This material seems to be suspended or colloidal organic debris and mineral particles, which provide additional surfaces for microbial colonisation rendering in a heterogeneous biofilm development (Neu and Lawrence 1997). A widespread network of carbohydrate extracellular material was revealed by Congo Red staining (Fig. 6). This network had a very porous organisation, with numerous interstices and channels interconnected by fibres that represent a backbone matrix binding together biofilm components. Zooids of peritrichs were usually surrounded by this carbohydrate component as it can be seen in Fig. 6. These results are consistent with those observed by Droppo *et al.* (1996) in activated sludge flocs, in which the exopolysaccharide matrix is described as a fibrous-textured net with sorption properties. Channels appear as stable components of biofilm architecture, and they could be due to the high presence of protozoa and metazoa in the RBC biofilms studied. These microorganisms, by their continuous movements and the predation on bacteria, may contribute to restore the voids and maintain the porosity (Massol-Deyá *et al.* 1995). According to some authors (de Beer *et al.* 1994, Lawrence *et al.* 1994), the formation of channels in thick biofilms seems to be a microbial strategy to solve the problem of nutrient and gases transport towards inner layers.

Inner layers of RBC biofilms had a more uniform and compact aspect. DTAF staining of bacteria was reduced in the most internal zones (Figs 7 d-f sections), revealing the decrease of bacterial biomass with depth. This vertical stratification of biomass in wastewater biofilms agrees with that previously reported in other biofilms, since using microslicing techniques (Okabe *et al.* 1996, Zhang and Bishop 1997) or CSLM (Massol-Deyá *et al.* 1995, Neu and Lawrence 1997), it was also revealed that microbial density was reduced in the innermost biofilm layers. Generally, inner layers had a larger percentage of non-viable bacteria than the outer layers, as it was revealed by their higher PI signal (Fig. 8 a), and the lower proportion of protozoa and metazoa. Peritrich ciliates were very rarely seen in these layers, and concerning metazoa, only nematodes were sporadically present. This fact is explained because the majority of protozoa and metazoa identified in these

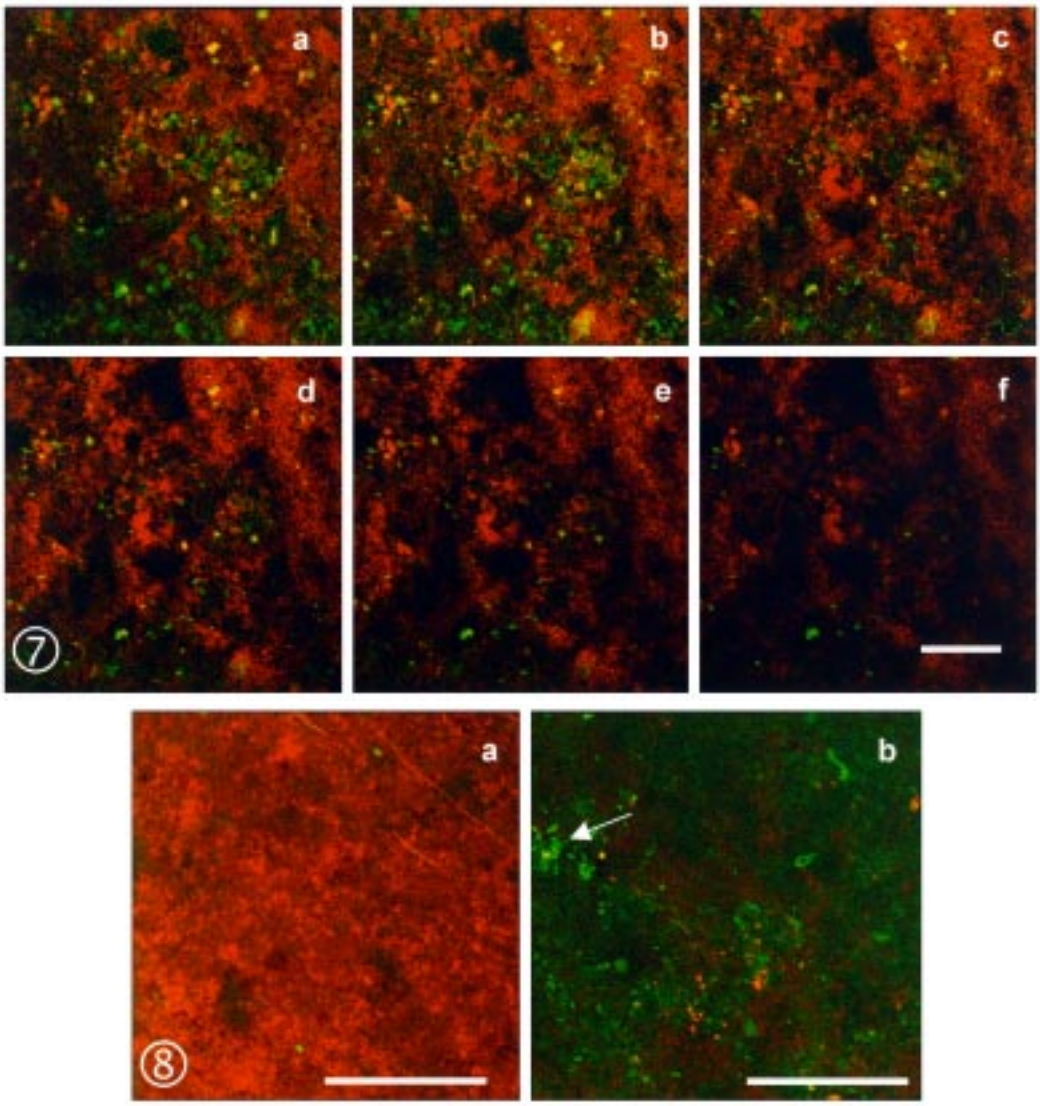

Figs 7, 8. Spatial organisation of the inner RBC biofilm layers. Biofilms were stained with both DTAF and PI dyes. **7** - series of horizontal CSLM sections arranged towards the innermost layers. Sections were taken at 10 µm intervals. Live biomass (green fluorescent staining) appeared to be decreased in the deepest layers (last sections). Scale bar 50 µm. **8 a** - putative dead cells stained with PI (red fluorescence) were viewed in higher proportion in inner layers. **8 b** - putative live bacterial clusters (arrow) stained with DTAF (green fluorescence) were also noticed in inner layers. Scale bars - 50 µm

RBC biofilms hold an aerobic metabolism (Martín-Cereceda *et al.* 2001a, b), and oxygen availability is recognised to be very low in the deep layers of wastewater biofilms (Bishop and Kinner 1986). In this sense, only the anaerobic ciliate M*etopus es* was at times observed in the inner biofilm layers. Presence of viable bacteria clumps in the internal zones (Fig. 8 b) was observed, and these could be involved in the attachment of the basal layer to the disc support (Massol-Deyá *et al.* 1995).

Polysaccharide exopolymeric matrix (Congo Red staining) of inner layers presented low porosity. The less macro-pored organisation is probably due to the higher biofilm compacting with age, the inner being the oldest layers (Bishop *et al.* 1995). Exopolysaccharide inner material is characterised by enlarged and amorphous structures, and by a laminate matrix with diffuse appearance addressed towards outer layers (Fig. 9). Presence of extracellular polymeric material proposes that at least a part of the biomass existing in inner layers is active (Eighmy *et al.* 1983).

Extracellular polymeric substances (EPS) are an important component in biological aggregates since they create a highly hydrated 3-D network which embraces

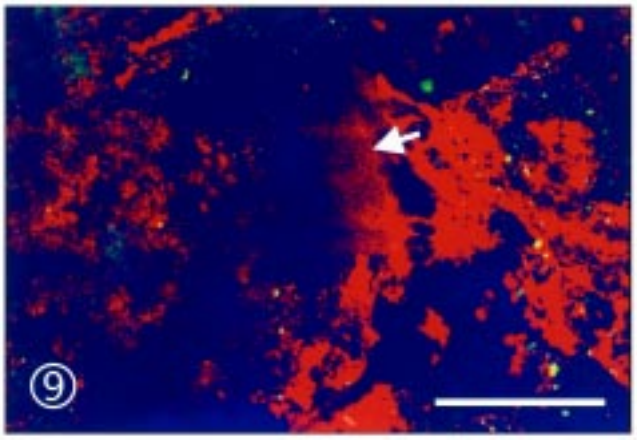

Fig. 9. Exopolysaccharide matrix, stained with Congo Red dye and visualised by CSLM, in the inner RBC biofilm layers. Note the mucoid-like appearance of matrix (arrow head). Scale bar - 100 μm

together microorganisms, organic and inorganic particles (Characklis and Marshall 1990, Neu 1994). Exopolymers represent approximately 28% of volatile solids content (VS) in the RBC biofilms studied, proteins (17% of VS) and polysaccharides (4% of VS) being the most abundant components (Martín-Cereceda *et al.* 2001c). Microbial excretion is believed one of the main origins of extracellular substances, so the conspicuous presence of exopolymeric materials in the RBC biofilms studied seems to be an indicator of active metabolism inside these biofilms. Exopolymers would be involved in different aspects of biofilm dynamic (Lappin-Scott *et al.* 1992, Neu 1994, Neu and Lawrence 1997): (i) representing a structural component; (ii) permitting attachment to the disc; (iii) supplying an extensive surface area for colonisation of bacteria, protozoa and metazoa; (iv) contributing to assemble the bioaggregates serving as a glue among microorganisms, and (v) providing a site for the sorption of soluble nutrients and suspended or colloidal material to be integrated inside biofilm structure.

The high nutrient content and the variety of products coming in raw sewage determine a large structural complexity and developing of wastewater mature biofilms. Adequate techniques are needed to the undamaged revealing of biofilm organisation. This study has demonstrated that confocal microscopy is perfectly suited for the easy, direct, and non-destructive analysis of such a thick biofilm. Our results indicate that microbial communities of wastewater biofilms grow up along discrete aggregates surrounded by an exopolymeric matrix rich in interstitial voids. These results are consistent with the modern concept of biofilm architecture describing biofilms as cluster of cells embedded in a complex EPS matrix with abundant water-permeable channels (Lawrence *et al.* 1991, Caldwell *et al.* 1992, Massol-Deyá *et al.* 1995), rather than with the traditional view of a homogeneous biofilm (Lock *et al.* 1984).

In this study, confocal microscopy has been applied for the first time to obtain undisrupted images of the protozoan distribution within wastewater biofilms, revealing how is the microenvironment around the protozoa and the *in situ* interactions with other microbial and non-cellular components. It is suggested that protozoa play a fundamental role in the structure of RBC biofilms since they are involved in the spatial biofilm organisation by maintaining the stability of multilayer arrangement and by contributing to the biofilm porosity.

Acknowledgements. This work was financially supported by a fellowship from Universidad Complutense de Madrid to M.M-C, and the projects I+D nº 0125/94 from the Comunidad Autónoma de Madrid (Spain) and DGES-PB97-0710-C02-02 from Ministerio de Educación y Ciencia (Spain).

REFERENCES

Alleman J. E., Veil J. A., Canaday T. J. (1982) Scanning electron microscope evaluation of rotating biological contactor biofilm. *Wat. Res.* **16:** 543-560

Allison D. G., Sutherland I. W. (1984) A staining technique for attached bacteria and its correlaton to extracellular carbohydrate production. *J. Microbiol. Methods* **2:** 93-99

Bishop P. L., Kinner N. E. (1986) Aerobic Fixed-Film Processes. In: Biotechnology, (Ed. W. Schönborn) 1 ed., VCH Verlagsgesellschaft, Weinheim, **8:** 113-176

Bishop P. L., Zhang T. C., Fu Y. C. (1995) Effects of biofilm structure, microbial distributions and mass transport on biodegradation processes. *Wat. Sci. Technol.* **31:** 43-53

Bloem J., Veninga M., Shepherd J. (1995) Fully automated determination of soil bacterium numbers, cell volumes and frequencies of dividing cells by confocal laser scanning microscopy and image analysis. *Appl. Environ. Microbiol.* **61:** 926-936

Caldwell D. E., Korber D. R., Lawrence J. R. (1992) Confocal laser microscopy and digital image analysis in microbial ecology. *Adv. Microbiol. Ecol.* **12:** 1-67

Characklis W. G., Marshall K. C. (1990) Biofilms: a basis for an interdisciplinary approach. In: Biofilms, Eds. W. G. Characklis and K. C. Marshall), John Wiley and Sons, New York, 3-52

de Beer D., Stoodley P., Roe F., Lewandowski Z. (1994) Effects of biofilm structures on oxygen distribution and mass transfer. *Biotechnol. Bioeng.* **43:** 1131-1138

Droppo I. G., Flannigan D. T., Leppard G. C., Jaskot C., Liss S. N. (1996) Floc stabilization for multiple microscopic techniques. *Appl. Environ. Microbiol.* **62:** 3508-3515

Droppo I. G., Leppard G. G., Flannigan D. T., Liss S. N. (1997) The freshwater floc: a functional relationship of water and organic and inorganic floc constituents affecting suspended sediment properties. *Wat. Air Soil Pollut.* **99:** 43-54

Edmondson W. T. (1959) Rotifera. In: Freshwater Biology, (Ed. W. T. Edmondson) 2 ed., J. Wiley and Sons, New York

Eighmy T. T., Maratea D., Bishop P. L. (1983) Electron microscopy examination of wastewater biofilm formation and structural components. *Appl. Environ. Microbiol.* **45:** 1921-1931

Fernández-Galiano D. (1994) The ammoniacal silver carbonate method as a general procedure in the study of protozoa from sewage (and other) waters. *Wat. Res.* **28:** 495-496

Foissner W., Blatterer H., Berger H., Kohmann F. (1991) Taxonomische und Ökologische Revision der Ciliaten des Saprobiensystems. Band I: Cyrtophorida, Oligotrichida, Hypotrichida, Colpodea. Bayer, Munich. Landesamtes für Wasserwirtschaft

Foissner W., Berger H., Kohmann F. (1992) Taxonomische und Ökologische Revision der Ciliaten des Saprobiensystems. Band II: Peritrichia, Heterotrichida, Odontostomatida. Bayer, Munich. Landesamtes für Wasserwirtschaf

Foissner W., Berger H., Kohmann F. (1994) Taxonomische und Ökologische Revision der Ciliaten des Saprobiensystems. Band III: Hymenostomata, Prostomatida, Nassulida. Bayer, Munich. Landesamtes für Wasserwirtschaft

Foissner W., Berger H., Blatterer H., Kohmann F. (1995) Taxonomische und Ökologische Revision der Ciliaten des Saprobiensystems. Band IV: Gymnostomatea, *Loxodes,* Suctoria. Bayer Munich. Landesamtes für Wasserwirtschaft

Galván A., Urbina P., de Castro F. (2000) Characterization of filamentous microorganisms in rotating biological contactor biofilms of wastewater treatment plants. *Biopr. Eng.* **22:** 257-260

Hausner M., Wuertz S. (1999) High rates of conjugation in bacterial biofilms as determined by quantitative in situ analysis. *Appl. Environ. Microbiol.* **65:** 3710-3713

Kahl A. (1930-1935) *Urtiere oder Protozoa. I. Wimpertiere oder Ciliata (Infusoria).* I: Die Tierwelt Deutschlands. (Ed. F. Dahl), G. Fischer, Jena

Kinner N. E., Balkwill D. L., Bishop P. L. (1983) Light and electron microscopic studies of microorganisms growing in RBC biofilms. *Appl. Environ. Microbiol.* **45:** 1659-1669

Kinner N. E., Curds C. R. (1987) Development of protozoan and metazoan communities in rotating biological contactor biofilms. *Wat. Res.* **21:** 481-490

Kinner N. E., Curds C. R., Meeker L. D. (1989) Protozoa and metazoa as indicators of treatment efficiency in rotating biological contactors. *Wat. Sci. Tech.* **20:** 199-204

Korber D. R., James G. A., Costerton J. W. (1994) Evaluation of fleroxacin activity against establised *Pseudomonas fluorescens* biofilms. *Appl. Environ. Microbiol.* **61:** 1013-1019

Kuehn M., Hausner M., Bungartz H-J., Wagner M., Wilderer P. A., Wuertz S. (1998) Automated confocal laser scanning microscopy and semiautomated image processing for analysis of biofilms. *Appl. Environ. Microbiol.* **64:** 4115-4127

Lappin-Scott H. M., Costerton J. W., Marrie T. J. (1992) Biofilms and Biofouling. *Encyclop. Microbiol.* **1:** 277-284

Laurent M., Johannin G., Gilbert N., Lucas L., Cassio D., Petit P., Fleury A. (1994) Power and limits of laser scanning confocal microscopy. *Biol. Cell.* **80:** 229-240

Lawrence J. R., Korber D. R., Hoyle B. D., Costerton J. W., Caldwell D. E. (1991) Optical sectioning of microbial biofilms. *J. Bacteriol.* **173:** 6558-6567

Lawrence J. R., Wolfaardt G. M., Korber D. R. (1994) Determination of diffusion coefficients in biofilm by confocal laser microscopy. *Appl. Environ. Microbiol.* **60:** 1166-1173

Liss S. N., Droppo I. G., Flannigan D. T., Leppard G. C. (1996) Floc architecture in wastewater and natural riverine systems. *Environ. Sci. Technol.* **30:** 680-686

Lock M., Wallace R. R., Costerton J. W., Ventullo R. M., Charlton S. E. (1984). River epilithon (biofilm): toward a structural functional model. *Oikos* **42:** 10-22

Luna-Pabello V. M., Mayén R., Olvera-Viascan V., Saavedra J., Durán de Bazúa C. (1990) Ciliated protozoa as indicators of a wastewater treatment system performance. *Biol. Wastes* **32:** 81-90

Madoni P. (1988) I protozoi ciliati nel controllo di efficienza dei fanghi attivi. Centro Italiano Studi di Biologia Ambientale, Reggio Emilia (in Italian)

Martín-Cereceda M., Serrano S., Guinea A. (2001a) Biofilm communities and operational monitoring of a rotating biological contactor system. *Wat., Air Soil Pollut.* **126:** 193-206

Martín-Cereceda M., Pérez-Uz B., Serrano S., Guinea A. (2001b) Dynamics of protozoan and metazoan communities in a full-scale wastewater treatment plant by rotating biological contactors. *Microbiol. Res.* **156:** 225-238

Martín-Cereceda M., Jorand F., Guinea A., Block J. C. (2001c) Characterization of extracelullar polymeric substances in rotating biological contactor biofilms and activated sludge flocs. *Environ. Technol.* **22:** 951-959

Massol-Deyá M. M., Whallon J., Hickey R. F., Tiedje J. M. (1995) Channel structures in aerobic biofilms of fixed-film reactors treating contaminated groundwater. *Appl. Environ. Microbiol.* **61:** 769-777

Morris C. E., Monier J. M., Jacques M. A. (1997) Methods for observing microbial biofilms directly on leaf surfaces and recovering them for isolation of culturable microorganisms. *Appl. Environ. Microbiol.* **63:** 1570-1577

Neu T. R. (1994) The challenge to analyse extracellular polymers in biofilms. In: Microbial Mats, Structure, Development and Environmental Significance (Eds. L. J. Stal and P. Caumette), NATO ASI Series, Springer, Berlin, **G35:** 221-227

Neu T. R. (2000) In situ cell and glycoconjugate distribution of river snow as studied by confocal laser scanning microscopy. *Aquatic Microb. Ecol.* **21:** 85-95

Neu T. R., Lawrence J. R. (1997) Development and structure of microbial biofilms in river water studied by confocal laser scanning microscopy. *FEMS Microbiol. Ecol.* **24:** 11-25

Olofsson A-C., Zita A., Hermansson M. (1998) Floc stability and adhesion of gree-fluorescent-protein-marked bacteria to flocs in activated sludge. *Microbiology* **144:** 519-528

Okabe S., Hiratia K., Ozawa Y., Watanabe Y. (1996) Spatial microbial distributions of nitrifiers and heterotrophs in mixed-population biofilms. *Biotechnol. Bioeng.* **50:** 24-35

Pentecost A. (1984) Introduction to Freshwater Algae. The Richmond Publishing Co. Ltd. Surrey, Great Britain

Stoodley P., de Beer D., Lewandowsky Z. (1994) Liquid flow in biofilms. *Appl. Environ. Microbiol.* **60:** 2711-2716

Wagner M., Amann R., Kämpfer P., Abmus B., Hartmann A., Hutzler P., Springer N., Schleifer K.H. (1994a) Identification and in situ detection of gram negative filamentous bacteria in activated sludge. *Syst. Appl. Microbiol.* **17:** 405-407

Wagner M., Abmus B., Hartmann A., Hutzler P., Amann R. (1994b) In situ analysis of microbial consortia in activated sludge using fluorescently labelled, rRNA-targeted oligonucleotide probes and confocal scanning laser microscopy. *J. Microsc.* **176:**181-187

Wagner M., Rath G., Koops H-P., Flood J., Amann R. (1996) In situ analysis of nitrifying bacteria in sewage treatment plants. *Wat. Sci. Technol.* **34:** 237-244

Wilbert P. N. (1975). Eine verbessertet technik der protargolimprägnation für ciliaten. *Mikrokosmos* **64:** 171-179

Wolfaardt G. M., Lawrence J. R., Robarts R. D., Caldwell D. E. (1994) The role of interactions, sessile growth and nutrient amendment on the degradative efficiency of a bacterial consortium. *Can. J. Microbiol.* **40:** 331-340

Zhang T. C., Bishop L. (1994) Density, porosity and pore structure of biofilms. *Wat. Res.* **28:** 2267-2277

Received on 22nd January, 2001; accepted on 30th July, 2001

Acta Protozool. (2001) 40: 273 - 279

ACTA
PROTOZOOLOGICA

Alteration of *Cryptosporidium parvum* (Apicomplexa: Eucoccidiorida) Oocyst Antigens Following Bleach Treatment

Sheng-Fa LIAO, Chunwei DU, Shiguang YANG, and Mark C. HEALEY

Department of Animal, Dairy, and Veterinary Sciences, College of Agriculture, Utah State University, Logan, USA

Summary. Oocysts of the protozoan parasite *Cryptosporidium parvum* are passed in infected feces and subsequently ingested by susceptible hosts, thus perpetuating transmission of the infection in the natural environment. Detection of oocysts is important to the water industry, especially in treatment plants using sanitizing and disinfecting chemicals. Commercial bleach containing sodium hypochlorite is frequently used by researchers to decontaminate the surface of oocysts prior to inoculating cell cultures. The present study analyzed oocyst protein patterns and antigen profiles before and after bleach treatment. Oocysts isolated from mouse feces were treated with a 20% bleach solution at 4°C for 30 min. Treated and non-treated oocysts were frozen, thawed, and sonicated to produce a *C. parvum*-oocyst homogenate (CPOH), which was subjected to gel electrophoresis and immunoblotting. Coomassie blue-stained electrophoretic gels revealed 33 and 15 protein bands from non-treated and treated CPOH, respectively. On Western blotting, 15 protein bands from non-treated CPOH were identified by polyclonal antibodies (hyperimmune mouse serum), but only 10 bands could be observed following bleach treatment. Monoclonal antibodies (Mabs) 6B4 and 9D10, specific for epitopes on the intact oocyst wall, revealed different immunoblotting patterns before and after bleach treatment. Prior to treatment, Mab 6B4 reacted with 2 protein bands with molecular weights of 55 and 246 kD, while Mab 9D10 reacted with 2 bands with molecular weights of 168 and 230 kD. Following bleach treatment, both the 55 and 246 kD bands (Mab 6B4) were still visible, but bands at 168 and 230 kD (Mab 9D10) were not. The utility of polyclonal and monoclonal antibodies in detecting oocysts from different sources will depend upon the chemical sensitivities of their target epitopes.

Key words: antigens, bleach, cryptosporidiosis, *Cryptosporidium parvum*, epitopes, monoclonal antibodies, oocysts.

Abbreviations: CPOH - *C. parvum*-oocyst homogenate, FITC - fluroecsein isothiocyanate, HMS - hyperimmune mouse sera, IFA - indirect immunofluorescent assay, Mab(s) - monoclonal antibody(ies), PBS - phosphate buffered saline, PVDF - polyvinylidene difluoride, SDS-PAGE - sodium dodecyl sulfate-polyacrylamide gel electrophoresis.

INTRODUCTION

Cryptosporidium parvum, a protozoan parasite having worldwide distribution, is an enteric pathogen causing diarrhea in humans and a variety of other animals. Despite some recent progress (Riggs *et al.* 1999), consistently effective therapy against this parasite remains an enigma. The high rate of infection among immunocompromised humans and young animals, in large part, is due to the tenacious resistance of oocysts in the natural environment (Campbell *et al.* 1982, Madore *et al.* 1987, Peeters *et al.* 1989, Korich *et al.* 1990). Consequently, oocysts and their associated antigens remains the subject of scientific investigations.

Address for correspondence: Mark C. Healey, Department of Animal, Dairy, and Veterinary Sciences, Utah State University, 4815 Old Main Hill, Logan, UT 84322-4815, USA; Fax: (435) 797-2118; E-mail: mchealey@cc.usu.edu

Antigenic profiles of *C. parvum* oocysts have been summarized (Lumb *et al.* 1988, Current and Garcia 1991). The water industry relies heavily on treatment plants to make drinking water safe. Moreover, chemical treatment is routinely used to decontaminate the oocyst surface prior to cell culture inoculation in scientific investigations (Yang *et al.* 1996, Upton 1997, Zhang *et al.* 1998). Many standard disinfection procedures do not necessarily reduce *C. parvum* oocyst viability, but frequently alter oocyst wall antigens (Campbell *et al.* 1982, Korich *et al.* 1990). Consequently, any knowledge of antigen liability to oxidizing conditions and chemical disinfectants can be very useful.

Commercial bleach (Clorox®) containing sodium hypochlorite is the most common disinfectant used to decontaminate the surface of *C. parvum* oocysts. The present study analyzed oocyst protein patterns and antigen profiles before and after bleach treatment. Results indicated that certain oocyst antigens and epitopes were sensitive to 20% bleach treatment for 30 min while others were not. Therefore, polyclonal and Mab probes used to detect oocysts should be selected on the basis of their target epitopes and the sensitivity of these epitopes to known chemical exposure.

MATERIALS AND METHODS

Oocyst amplification and purification

Cryptosporidium parvum oocysts, originally isolated from Holstein calves (Iowa isolate), were amplified by using C57BL/6N mice (B&K Universal, Fremont, CA, USA) immunosuppressed with dexamethasone as described by Yang and Healey (1993). The mice (4 ~ 6 wk old) were inoculated *per os* with 10^6 oocysts/mouse, housed in wire-floored cages, and allowed to consume drinking water *ad libitum* containing 14 µg/ml dexamethasone phosphate throughout the experiment. Mouse feces were collected daily, beginning on day 3 postinoculation, from steel trays underlying the cage floor. The fecal pellets were collected in 2.5% potassium dichromate ($K_2Cr_2O_7$) solution and stored at 4°C prior to oocyst purification.

A salt flotation technique (Petry *et al.* 1995) and the cesium chloride gradient centrifugation technique (Kilani and Sekla 1987) were combined to purify the oocysts from feces. Briefly, fecal pellets were crushed and sieved sequentially through 3 screens with a final mesh of 400 (38 µm porosities), and then suspended in 20 volumes of water to sediment for 45 min. The supernatant was decanted and the sediment resuspended. This procedure was repeated 3 times. All the decanted supernatants were centrifuged at 1900 g for 10 min (unless otherwise specified all centrifugations were at 1900 g for 10 min). The oocyst-rich pellets were combined and suspended in 10 volumes of saturated NaCl solution with 1 volume of water overlaid and then centrifuged. Following centrifugation, the oocyst-containing interphase was removed and washed once with phosphate buffered saline (PBS, 25 mM, pH 7.2). The oocysts were washed and then diluted with 50 mM Tris-10 mM EDTA buffer to a suspension of 1 x 10^8 oocysts/ml. A CsCl gradient was prepared in 14 x 89 mm Ultra-Clear™ tubes (Beckman Instruments, Inc., Palo Alto, CA, USA). Gradient densities were 1.40, 1.10, and 1.05 g/ml in the bottom, middle, and top 3 ml, respectively. One ml of oocyst suspension was layered on the top of the gradient. Gradient tubes were ultra-centrifuged at 16000 g for 1 h at 4°C. Purified oocysts were harvested from the top band, washed with deionized water by centrifugation, resuspended in the desired amount of PBS or lysis buffer (formula provided below), and stored at -20°C.

Oocyst treatment and homogenate preparation

Approximately 2.5 x 10^9 purified oocysts in a 50 ml conical tube were centrifuged to produce an oocyst pellet. The supernatant was removed by aspiration. A commercial bleach preparation (Clorox®) containing 5.25% sodium hypochlorite was diluted with distilled deionized water (ddH_2O) to make a 20% working solution of 1.05% sodium hypochlorite. Ten ml of this solution was poured onto the oocyst pellet and vortexed. The tube was then incubated for 30 min at 4°C with limited agitation every 5 min. Oocysts were washed 4 times by centrifugation with PBS to remove residual bleach.

Bleach and non-bleach-treated oocysts were each suspended in a lysis buffer to a concentration of approximately 9.0 x 10^8 oocysts/ml. The lysis buffer consisted of 25 mM PBS, 50 mM Tris, 5 mM EDTA, 1% (w/v) octyl glucoside, 10 µg/ml α_1-antitrypsin, 100 µg/ml aprotinin, 0.5 mM diisopropylfluorophosphate, 5 mM iodoacetamide, 10 µg/ml leupeptin, 1 mM phenylmethylsulfonyl fluoride, 0.1 mM Nα-tosyl-L-lysylchoromethyl ketone, and 1 mM L-*trans*-epoxysuccinyl-leucylamido-(4-guanidino)-butane (Luft *et al.* 1987, Riggs *et al.* 1997). The oocyst suspension was snap-frozen in liquid nitrogen and thawed in a 37°C water bath for 12 cycles. It was then sonicated on ice with a Virsonic 50 Cell Disrupter (VirTis Company, Gardiner, NY, USA) for 20 s/sonication x 15 sonications at 50% power output with 1-min intervals. Samples of the resultant *C. parvum*-oocyst homogenate (CPOH) were examined by indirect IFA to ensure that more than 95% of the oocysts were disrupted. The CPOH was then divided into 200 µl aliquots and stored at -80°C until used.

Antibody production and screening

Murine polyclonal antibodies. Hyperimmune mouse serum (HMS) against *C. parvum* was produced in 7 adult BALB/c mice. Each mouse received 5 intramuscular injections of CPOH in Freund's incomplete adjuvant at monthly intervals. Each injection contained about 5x10^6 oocysts in a 50µl suspension. Five days after the last injection, blood was collected from the orbital sinus. Antibody titers against CPOH were measured by the enzyme-linked immunosorbent assay (ELISA) reported by Forney *et al.* (1996). Serum samples were pooled and stored at -20°C.

Murine monoclonal antibodies: Splenic lymphocytes harvested from CPOH-hyperimmunized BALB/c mice were fused with SP2/0 myeloma cells in a 50% polyethylene glycol solution. The presence of Mabs produced by resultant hybridomas was confirmed by ELISA as before. Hybridomas determined to be positive were cloned by limiting dilution, isotyped with a sub-isotyping kit (HyClone® Laboratories, Inc., Logan, UT, USA), and cryopreserved in liquid nitrogen.

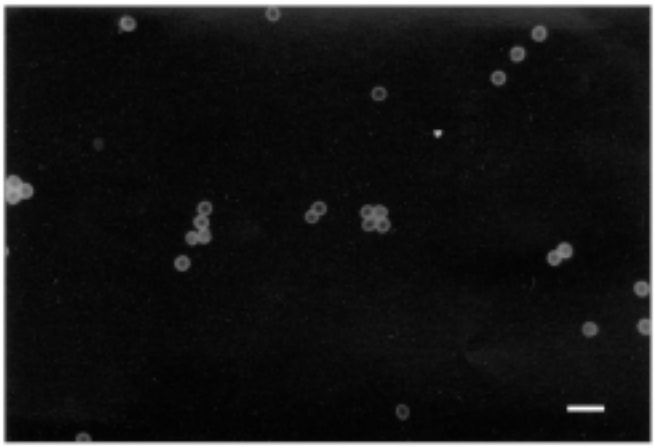

Fig. 1. Bleach-treated *Cryptosporidium parvum* oocysts examined by an indirect immunofluorescent assay using Mab 6B4. Oocysts appear brightly stained with hollow centers. Scale bar - 12 μm

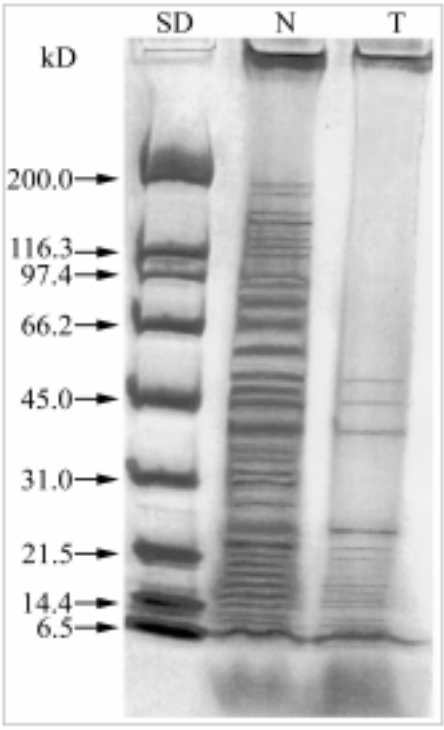

Fig. 2. Profile of *Cryptosporidium parvum*-oocyst homogenate (CPOH) proteins resolved by SDS-PAGE and stained by GelCode® blue reagent. Molecular weight standards are shown in lane SD and labeled in kilodaltons (kD) in the left-hand margin. Non-bleach-treated CPOH demonstrate at least 33 protein bands, with molecular weights ranging from 6.5 to 187 kD (Lane N). Beach-treated CPOH reduced the number of protein bands to 15, with molecular weights ranging from 6.5 to 55 kD (Lane T)

Indirect immunofluorescent assay (IFA)

A modified Mab-based IFA (Garcia *et al.* 1987, Arrowood and Sterling 1989) was used to examine oocysts and intermediate stages of *C. parvum* by employing different Mabs generated in our laboratory. Individual samples (either oocysts in feces, purified oocysts, or CPOH) were applied to the surface of pre-cleaned microscope slides, air-dried at 25°C for 30 min, and fixed by gentle flaming. Samples were incubated with one of the candidate Mabs (60 μl/application) for 30 min in a 100% humidified chamber at 37°C, followed by an additional 30 min with fluorescein isothiocyanate (FITC)-conjugated goat anti-mouse immunoglobulin (Sigma Chemical Company, St. Louis, MO, USA) diluted at 1:100 (50 μl/application). Following incubation, samples were thoroughly washed with PBS, covered with 2 drops of non-drying mounting medium (50% glycerol in PBS), and examined under a Zeiss epifluorescence microscope equipped with an ultraviolet lamp. To evaluate Mabs against intermediate parasitic stages, *C. parvum*-infected cell cultures growing on coverslips were subjected to the same procedure as described above for oocysts.

Dot blot assay

Mabs and HMS reacting with respective native and denatured CPOH were discerned by a dot-blot microfiltration apparatus in accordance with the manufacturer's instructions (Bio-Rad Laboratories, Richmond, CA, USA). Denaturation of CPOH was done by the same procedure as described for SDS-PAGE (below). The intensity of reaction was scored as: - = negative, 1+ = light, 2+ = moderate, 3+ = strong, and 4+ = very strong. Mabs for use in Western blot analysis were selected by the results of this assay.

Sodium dodecyl sulfate-polyacrylamide gel electrophoresis (SDS-PAGE)

A commercially available 4 ~ 20% gradient gel and Mini-PROTEAN® II dual slab cell (Bio-Rad Laboratories) were employed in SDS-PAGE. One part of solubilized CPOH was diluted with 2 parts (v/v) of sample buffer [2% SDS, 5% (v/v) β-mercaptoethanol, 0.0125% bromophenol blue, and 0.25% (v/v) glycerol in 62.5 mM Tris-HCl, pH 6.8] and boiled for 5 min before loading 30 μl into each gel lane. Prestained and non-prestained molecular weight standards (broad range, Bio-Rad Laboratories) were incorporated into the control gel lanes to determine the relative molecular weights of the resolved proteins. Electrophoresis was performed with a discontinuous buffer system (Laemmli 1970) at 175 V until the dye front reached the bottom of the slab gel (approximately 50 min). Following electrophoresis, GelCode® blue stain reagent (Pierce Chemical Company, Rockford, IL, USA), which employs the colloidal properties of Coomassie® blue G-250 for protein staining, was used to visualize CPOH protein bands in the slab gels.

Western blot analysis

Following SDS-PAGE, CPOH protein bands were electrophoretically transferred (Towbin *et al.* 1979) to the polyvinylidene difluoride (PVDF) membrane using a Mini Trans-Blot® Transfer Cell (Bio-Rad). Transfer was carried out overnight at 4°C at 30 V, followed by 60 V for 2 h. Transfer efficiency was monitored by observing the prestained molecular weight standards. Following transfer, the membrane sheets were rinsed with ddH_2O and dried with a cold air stream. Nonspecific sites on the sheets were blocked for 18 h with a solution

Table 1. Dot-blot assay scores for polyclonal and monoclonal antibodies against native and denatured *Cryptosporidium parvum*-oocyst homogenate (CPOH)

Antibody[1]	HMS	9D10	2C5	2F8	3F11	9G12	2B7	2C12	8B1	D8	6B4	8C6	9F11
Isotype[2]	ND[3]	IgM	ND	IgM	IgA	ND	IgG2b	IgA	ND	ND	IgM	ND	ND
Native[4]	4+	3+	3+	3+	3+	3+	4+	4+	4+	4+	4+	4+	ND
Denatured[5]	4+	2+	3+	1+	1+	1+	1+	1+	1+	1+	2+	2+	1+

[1] Polyclonal (HMS - hyperimmune mouse serum) and monoclonal antibody designations; [2]Isotyping was done on only select Mabs; [3]ND - not done; [4]Native - score for non-denatured CPOH; [5]Denatured - score for denatured CPOH.

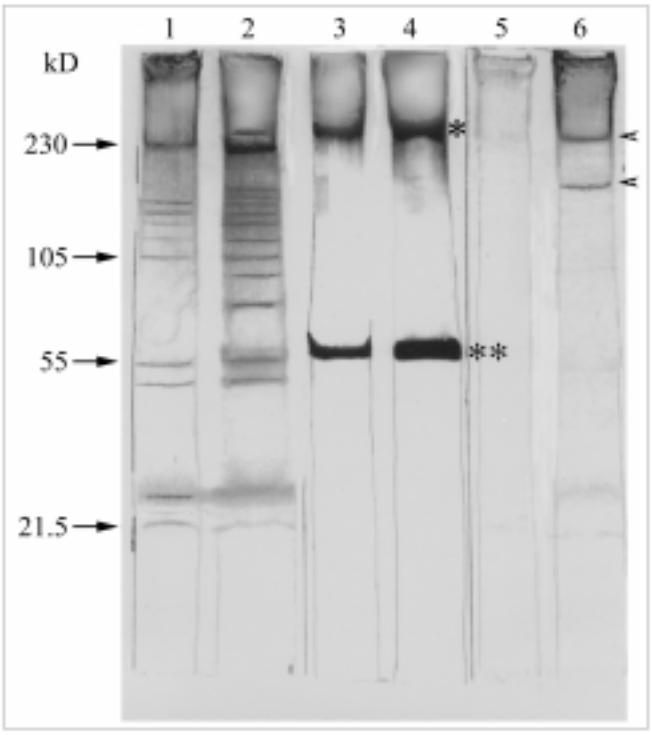

Fig. 3. Western blot analysis of bleach and non-bleach-treated *Cryptosporidium parvum*-oocyst homogenate (CPOH) using HMS and Mabs (6B4 and 9D10). Prior to bleach treatment, HMS recognized 15 protein bands with molecular weights ranging from 21.5 to 246 kD (Lane 2). Following bleach treatment, 10 protein bands remain with molecular weights ranging from 21.5 to 230 kD (Lane 1). Prior to and following bleach treatment, Mab 6B4 recognized 2 protein bands having molecular weights of 55 kD (**) and 246 kD (*) (Lanes 4 and 3, respectively). Similarly, Mab 9D10 recognized two protein bands before bleach treatment. The respective molecular weights are 168 kD and 230 kD (arrowheads) (Lane 6). Following bleach treatment, Mab 9D10 failed to recognize either band (Lane 5)

of 5% bovine serum albumin in 0.05 M Tris Buffered Saline (BSA-TBS, pH 7.4). The blocked sheet was cut into strips and incubated with either HMS (1:3000) or a Mab for 2 h, washed with PBS + 0.05% Tween 20 (PBS-T), and incubated for 1.5 h with biotinylated anti-mouse IgG goat serum (Sigma) diluted at 1:1000 in 1% BSA-TBS. The strips were further reacted with ExtrAvidin-Alkaline Phosphatase (Sigma) for 1.5 h after washing with PBS-T. Color development was accomplished by using an Alkaline Phosphatase Conjugate Substrate Kit (Bio-Rad) and stopped by washing with ddH_2O.

RESULTS

Antibody screening

ELISA showed that more than 70 hybridomas producing Mabs against *C. parvum* were generated. IFA determined that some Mabs (6B4 and 9D10) were against epitopes present on the oocyst stage (Fig. 1), while others (such as 2C5) were against epitopes on intermediate parasitic stages (data not shown).

Bleach treatment on oocysts

Prior to bleach treatment, oocysts reacted strongly with Mabs 6B4 and 9D10 as determined by IFA. Oocysts appeared brightly stained with hollow centers (Fig. 1). Following bleach treatment, oocysts lost their reaction with Mab 9D10, but retained their reaction with Mab 6B4 showing bright apple green fluorescence.

Dot blotting

Dot blot assay revealed that HMS had very strong reactions with both native and denatured CPOH (Table 1). The optimal concentration of HMS used in Western blotting was 1:3000, as determined by serial-dilution in dot blotting. Almost all Mabs reacted with native (non-denatured) CPOH antigens, with reaction intensity varying from 1+ to 4+. Following CPOH denaturation, only 12 Mabs continued to react with CPOH antigens (Table 1). Based on reaction intensity (2+ ~ 3+), 4 Mabs (6B4, 9D10, 2C5, and 8C6) were selected for further analysis in Western blotting.

SDS-PAGE of CPOH

The profile of CPOH proteins resolved by SDS-PAGE and stained by GelCode® blue reagent is shown in Fig. 2. Non-bleach-treated CPOH demonstrated at least 33 protein bands (Lane N). The molecular weights of these proteins ranged from 6.5 kD to 187 kD. Proteins with molecular weights below 6.5 kD

or over 200 kD could not be clearly discerned. Bleach treatment of oocysts reduced the number of protein bands to 15, with molecular weights ranging from 6.5 kD to 55 kD (Lane T).

Western blotting

The majority of CPOH protein bands in the gradient gels were transferred to PVDF membranes as noted by the disappearance of prestained standards in the gels and also by light staining of gels with GelCode® blue reagent following transfer. Western blot analysis of bleach- and non-bleach-treated CPOH using HMS and Mabs (6B4 and 9D10) are illustrated in Fig. 3. Prior to bleach treatment, HMS recognized 15 protein bands with molecular weights ranging from 21.5 kD to 246 kD (Lane 2). Following bleach treatment, 10 protein bands remained with molecular weights ranging from 21.5 kD to 230 kD (Lane 1). No bands were observed when normal mouse serum was used (data not shown).

Prior to and following bleach treatment of oocysts, Mab 6B4 recognized 2 protein bands from CPOH having molecular weights of 55 kD and 246 kD (Lanes 4 and 3, respectively). The band having the lowest molecular weight (55 kD) appeared much more intense (Lanes 4 and 3, respectively). Similarly, Mab 9D10 recognized two protein bands before bleach treatment. The respective molecular weights were 168 kD and 230 kD (Lane 6). However, following bleach treatment, Mab 9D10 failed to recognize either band (Lane 5). No protein bands were visible following incubation with Mab 2C5, Mab 8C6, and cell culture medium (negative control) (data not shown).

DISCUSSION

Cryptosporidium parvum is an undisputed waterborne pathogen of humans and other animals. This intestinal protozoan has been responsible for outbreaks of cryptosporidiosis traced back to surface and potable water sources (MacKenzie *et al.* 1994, Wallis *et al.* 1996). Because low numbers of oocysts present a potential risk for infection, the challenge has been to develop immunofluorescent and flow cytometric assays capable of detecting only a few oocysts (Vesey and Slade 1990, Vesey *et al.* 1993). A confounding factor is the effect that water disinfectants may have on oocyst detection. It has been reported that oocyst viability or infectivity is not affected by exposure of oocysts to 1.05 ~ 3% sodium hypochlorite (equivalent to 20 ~ 60% commercial bleach) for up to 18 h at 4 or 37°C, and only 70 ~ 100% commercial bleach can destroy oocyst infectivity (Campbell *et al.* 1982, Korich *et al.* 1990, Sterling 1990). Our results regarding the alteration of oocyst antigens following bleach treatment not only support the notion that the routine chlorination of drinking and recreation water has little or no effect on oocyst viability (Madore *et al.* 1987, Peeters *et al.* 1989, Current and Garcia 1991, Moore *et al.* 1998), but also suggest that routine chlorination may lead to a false-negative detection if an improper antibody is used in the assay. Moore *et al.* (1998) reported that 4 commercially available antibodies recognized a similar set of immunodominant epitopes on the oocyst wall. Unfortunately, these epitopes were labile to chlorine treatment and oxidizing conditions. Specifically, sodium hypochlorite and sodium meta-periodate reduced the ability of antibodies to detect the oocysts. This problem could have been circumvented by using *Cryptosporidium*-specific antibodies that recognize non-labile antigens on the oocyst wall. We report herein the generation of a panel of Mabs, the relative molecular weights of their target antigens, and the ability of at least one Mab to react with an epitope on the oocyst wall before and after treatment with 20% commercial bleach (1.05% sodium hypochlorite) for 30 min.

From 17 to 51 protein bands have been identified in electrophoretic profiles of freeze-thawed *C. parvum* oocysts, with molecular weights ranging from less than 6.5 to larger than 330 kD (Lazo *et al.* 1986, Luft *et al.* 1987, Lumb *et al.* 1988, Tilley and Upton 1990, Bonnin *et al.* 1991, Nina *et al.* 1992, Peeters *et al.* 1992). We demonstrated at least 33 protein bands in the electrophoretic analysis of non-bleach-treated CPOH, with molecular weights ranging from 6.5 to 187 kD (Fig. 2). Nine additional weak bands appeared in Western blotting, extending the band number to 42 and the molecular weight to 246 kD (Fig. 3). Our findings are, for the most part, in agreement with those reported by investigators cited above. Slight differences are likely due to the varying percentage of acrylamide gels used and the staining methods employed. In addition, the number of protein bands counted can be somewhat arbitrary. We enumerated protein bands by linear and exponential regression analysis. Bleach treatment reduced the number of protein bands in CPOH from 33 to 15, underscoring the effect that the sodium hypochlorite treatment has on oocyst wall proteins (Fig. 2).

Luft *et al.* (1987) demonstrated that antisera from orally infected mice consistently recognized 4 oocyst

antigens with molecular weights ranging from 72 kD to greater than 100 kD. Current and Garcia (1991) reported several Mabs specific for *C. parvum* oocyst/sporozoite antigens, with molecular weights ranging from approximately 48 kD (Nina *et al.* 1992) to more than 200 kD (Arrowood and Sterling 1989, Bonnin *et al.* 1991). However, the sensitivity of these antigens to bleach treatment was not evaluated. In the present study, HMS recognized 15 CPOH protein bands before and 10 bands after oocysts were treated with bleach, again signaling protein sensitivity to sodium hypochlorite exposure (Fig. 3). Not surprisingly, epitopes recognized by Mabs produced to CPOH showed variable susceptibility to bleach. Whereas Mabs 9D10, 2C5, and 8C6 reacted with labile epitopes, the epitope recognized by Mab 6B4 was clearly not sensitive to bleach treatment (Fig. 3).

Moore *et al.* (1998) predicted that the development of antibodies targeted to antigens that were not sensitive to sodium hypochlorite treatment was unlikely. Although we agree that commercially available antibodies specific for *Cryptosporidium* antigens either fail to react or react very weakly with oocysts following sodium hypochlorite treatment, Mab 6B4 from our panel recognizes an epitope that resists exposure to 20% bleach for at least 30 min, while Mab 9D10 recognizes an epitope that does not resist such an exposure. This is particularly relevant for investigators studying the life cycle of *C. parvum* in vitro because there is a measured advantage in discriminating between oocysts used to inoculate cell culture (decontaminated with bleach) and oocysts produced in cell culture as the parasite completes its life cycle (not exposed to bleach) (Healey *et al.* 1997, Upton 1997). Moreover, the water industry has a dedicated interest in antibodies capable of detecting *C. parvum* oocysts that have been exposed to various disinfection procedures (Campbell *et al.* 1982). Such procedures frequently reduce oocyst detection by antigenic alteration, but rarely reduce oocyst viability (Korich *et al.* 1990).

The importance of *C. parvum* oocyst antigenic liability to disinfectants, sanitizing treatments, and naturally occurring oxidizing conditions is uncontested from the vantage point of antibody-mediated oocyst detection. The next step will be to develop Mabs capable of specifically identifying *C. parvum* in samples containing different species of *Cryptosporidium*.

Acknowledgements. This research was supported in part by the Utah Agricultural Experiment Station and approved as journal paper no. 7223. The protocol for this study was approved by the Utah State University Institutional Animal Care and Use Committee.

REFERENCES

Arrowood M. J., Sterling C. R. (1989) Comparison of conventional staining methods and monoclonal antibody-based methods for *Cryptosporidium* oocyst detection. *J. Clinic. Microbiol.* **27:** 1490-1495

Bonnin A., Dubremetz J. F., Camerlynck P. (1991) Characterization and immunolocalization of an oocyst wall antigen of *Cryptosporidium parvum* (Protozoa: Apicomplexa). *Parasitology* **103:** 171-177

Campbell I., Tzipori S., Hutchison G., Angus K. W. (1982) Effect of disinfectants on survival of *Cryptosporidium* oocysts. *Vet. Rec.* **111:** 414-415

Current W. L., Garcia L. S. (1991) Cryptosporidiosis. *Clin. Microbiol. Rev.* **4:** 325-358

Forney J. R., Yang S., Healey M. C. (1996) Interaction of the human serine protease inhibitor α-1-antitrypsin with *Cryptosporidium parvum*. *J. Parasitol.* **82:** 469-502

Garcia L. S., Brewer T. C., Bruckner D. A. (1987) Fluorescence detection of *Cryptosporidium* oocysts in human fecal specimens by using monoclonal antibodies. *J. Clin. Microbiol.* **25:** 119-121

Healey M. C., Yang S., Du C., Liao S-F. (1997) Bovine fallopian tube epithelial cells, adult C57BL/6 mice, and non-neonatal pigs as models for cryptosporidiosis. *J. Euk. Microbiol.* **44:** 64S-65S

Kilani R. T., Sekla L. (1987) Purification of *Cryptosporidium parvum* oocysts and sporozoites by cesium chlorite and Percoll gradients. *J. Trop. Med. Hyg.* **36:** 505-508

Korich D. G., Mead J. R., Madore M. S., Sinclair N. A., Sterling C. R. (1990) Effects of ozone, chlorine dioxide, chlorine, and monochloramine on *Cryptosporidium parvum* oocyst viability. *Appl. Environ. Microbiol.* **56:** 1423-1428

Laemmli U. K. (1970) Cleavage of structural proteins during the assembly of the head of bacteriophage T4. *Nature* (London) **227:** 680-685

Lazo A., Barriga O. O., Redman D. R., Bech-Nielsen S. (1986) Identification by transfer blot of antigens reactive in the enzyme-linked immunosorbent assay (ELISA) in rabbits immunized and a calf infected with *Cryptosporidium* sp. *Vet. Parasitol.* **21:** 151-163

Luft B. J., Payne D., Woodmansee D., Kim C. W. (1987) Characterization of the *Cryptosporidium* antigens from sporulated oocysts of *Cryptosporidium parvum*. *Infec. Immun.* **55:** 2436-2441

Lumb R., Lanser J. A., O'Donoghue P. J. (1988) Electrophoretic and immunoblot analysis of *Cryptosporidium* oocysts. *Immunol. Cell Biol.* **66:** 369-376

MacKenzie W. R., Hoxie N. J., Gradus M. E., Blair K. A., Peterson D. E., Kazmierczak J. J., Addiss D. G., Fox K. R., Rose J. B., Davis J. P. (1994) A massive outbreak in Milwaukee of *Cryptosporidium* infection transmitted through the public water supply. *N. Engl. J. Med.* **331:** 161-167

Madore M. S., Rose J. B., Gerba C. P., Arrowood M. J., Sterling C. R. (1987) Occurrence of *Cryptosporidium* oocysts in sewage effluents and selected surface waters. *J. Parasitol.* **73:** 702-705

Moore A. G., Vesey G., Champion A., Scandizzo P., Deere D., Veal D., Williams K. L. (1998) Viable *Cryptosporidium parvum* oocysts exposed to chlorine or other oxidizing conditions may lack identifying epitopes. *Int. J. Parasitol.* **28:** 1205-1212

Nina J. M. S., McDonald V., Deer R. M. A., Wright S. E., Dyson D. A., Chiodini P. L., McAdam K. P. W. J. (1992) Comparative study of the antigenic composition of oocyst isolates of *Cryptosporidium parvum* from different hosts. *Parasite Immunol.* **14:** 227-232

Peeters J. E., Mazás E. A., Masschelein W. J., Martinez de Matueana I. V., Debacker E. (1989) Effect of disinfection of drinking water with ozone or chlorine dioxide on survival of *Cryptosporidium parvum* oocysts. *Appl. Environ. Microbiol.* **55:** 1519-1522

Peeters J. E., Villacorta I., Vanopdenbosch E., Vandergheynst D., Naciri M., Ares-Mazás E., Yvoré P. (1992) *Cryptosporidium parvum* in calves: kinetics and immunoblot analysis of specific serum and local antibody responses (Immunoglobulin A [IgA],

IgG, and IgM) after natural and experimental infections. *Infec. Immun.* **60:** 2309-2316

Petry F., Robinson H. A., McDonald V. (1995) Murine infection model for maintenance and amplification of *Cryptosporidium parvum* oocysts. *J. Clin. Microbiol.* **33:** 1922-1924

Riggs M. W., Stone A. L., Yount P. A., Langer R. C., Arrowood M. J., Bentley D. L. (1997) Protective monoclonal antibody defines a circumsporozoite-like glycoprotein exoantigen of *Cryptosporidium parvum* sporozoites and merozoites. *J. Immunol.* **158:** 1787-1795

Riggs M. W., McNeil M. R., Perryman L. E., Stone A. L., Scherman M. S., O'Connor R. M. (1999) *Cryptosporidium parvum* sporozoite pellicle antigen recognized by a neutralizing monoclonal antibody is a β-mannosylated glycolipid. *Infec. Immun.* **67:** 1317-1322

Sterling C. R. (1990) Waterborne cryptosporidiosis. In: Cryptosporidiosis of Man and Animals, (Eds. J. P. Dubey, C. A. Speer and R. Fayer.). CRC Press, Inc., Boca Raton, FL, USA, 51-58

Tilley M., Upton S. J. (1990) Electrophoretic characterization of *Cryptosporidium parvum* (KSU-1 isolate) (Apicomplexa: Cryptosporidiidae). *Can. J. Zool.* **68:** 1513-1519

Towbin H., Staehelin T., Gordon J. (1979) Electrophoretic transfer of proteins from polyacrylamide gels nitrocellulose sheets: Procedure and some applications. *Proc. Nat. Acad. Sci.* USA **76:** 4350-4354

Upton S. J. (1997) *In vitro* cultivation. In: Cryptosporidium and Cryptosporidiosis, (Ed. R. Fayer). CRC Press, Inc., Boca Raton, FL, USA, 181-207

Vesey G., Slade J. S. (1990). Isolation and identification of *Cryptosporidium* from water. *Water Sci. Technol*. **24:** 165-167

Vesey G., Slade J. S., Byrne M., Shepard K., Dennis P. J., Fricker C. R. (1993). Routine monitoring of *Cryptosporidium* oocysts in water using flow cytometry. *J. Appl. Bacteriol.* **75:** 87-90

Wallis P. M., Erlandsen S. L., Isaac-Renton J. L., Olson M. E., Robertson W. J., van Keulen H. (1996) Prevalence of *Giardia* cysts and *Cryptosporidium* oocysts and characterization of *Giardia* spp. isolated from drinking water in Canada. *Appl. Environ. Microbiol.* **66:** 2789-2797

Yang S., Healey M. C. (1993) The immunosuppressive effects of dexamethasone administered in drinking water to C57BL/6N mice infected with *Cryptosporidium parvum*. *J. Parasitol.* **79:** 626-630

Yang S., Healey M. C., Du C., Zhang J. (1996) Complete development of *Cryptosporidium parvum* in bovine fallopian tube epithelial cells. *Infec. Immun.* **64:** 349-354

Zhang J., Yang S., Healey M. C. (1998) Effect of bleach pretreatment on the *in vitro* excystation of *Cryptosporidium parvum* oocysts. *Chin. J. Zoonoses.* **14:** 53-55

Received on 2nd March, 2001; accepted on 19th July, 2001

Acta Protozool. (2001) 40: 281 - 289

ACTA
PROTOZOOLOGICA

Haemosporida of Birds of Prey and Owls from Germany

Oliver KRONE[1], Jürgen PRIEMER[1], Jürgen STREICH[1], Paul SÖMMER[2], Torsten LANGGEMACH[3] and Olaf LESSOW [4]

[1] Institute for Zoo and Wildlife Research, Berlin; [2] Brandenburg State Institution for Large Protected Areas, Nature Centre Woblitz, Himmelpfort; [3] Brandenburg State Environmental Agency, Bird Conservation Centre, Buckow; [4] NABU Bird Station Leiferde, Leiferde, Germany

Summary. A total of 1149 free-living birds of prey from Germany were examined for blood parasites. The prevalence of infection was 11% (adult birds 18%, immature birds 16%, nestlings 4%). Among the Falconiformes 11% of 976 birds were infected, and 13% of 173 Strigiformes. Out of 17 falconiform species nine were infected with blood parasites whereas the Eurasian buzzard (*Buteo buteo*) had the highest prevalence for haematozoa; i.e. *Leucocytozoon toddi* (31%), the highest prevalence (25%) for *Haemoproteus* sp. was found in the hobby (*Falco subbuteo*). Eight species of owls were examined for blood parasites; the tawny owl (*Strix aluco*) had the highest prevalence with *Haemoproteus syrnii* (22%). In the one pygmy owl (*Glaucidium passerinum*) examined *Trypanosoma avium* and *Plasmodium (Giovannolaia) fallax* were detected. The white-tailed sea eagle (*Haliaeetus albicilla*) was found to be a host of *L. toddi* for the first time. Differences in the prevalence of blood parasites were found in the seasons and age classes of the birds but not between birds admitted to a rehabilitation centre or samples in the wild, the sexes, bird orders and the regions.

Key words: Falconiformes, Haematozoa, *Haemoproteus, Leucocytozoon*, Plasmodiidae, raptors, Strigiformes.

INTRODUCTION

Blood parasites were first described by Danilewsky in 1885 when he examined blood of Accipitridae, Laniidae and Corvidae. Since then avian haemosporidians have been recorded in about 68% of avian species examined and these have been found to be cosmopolitan (Atkinson and Van Riper III 1991). Bennett *et al.* (1994) listed 72 bird families in which *Haemoproteus*, *Leucocytozoon* or *Hepatozoon* were described. Most species of *Haemoproteus* and *Leucocytozoon* are relatively host-specific and restricted to bird species of the same family (Fallis *et al.* 1974, Atkinson 1986). This is in contrast to species of avian *Plasmodium*, which have a much broader host specific and occur in several avian families by changing their character (Bennett *et al.* 1982).

Since the first extensive study on the life cycle of *Haemoproteus tinnunculi* originated from Germany (Wasielewski and Wülker 1918), no systematic study on the prevalence and intensity of blood parasites from Falconiformes and Strigiformes from this country was conducted. Scattered information on blood parasites in raptors from Germany are found in the literature: Koch (1899) found hobby (*F. subbuteo*) nestlings taken from a nest near Berlin were heavily infected

Address for correspondence: Oliver Krone, Institute for Zoo and Wildlife Research, Postfach 601103, D-10252, Berlin, Germany; Fax: +49 (0) 30 51 26104; E-mail: krone@izw-berlin.de

with *Haemoproteus* sp. Mayer (1911) described *Haemoproteus* sp. in 2 of 3 tawny owls (*Strix aluco*) from Lübeck. Information on *Leucocytozoon* spp. is not reliable due to possible confusion with *Trypanosoma* spp. in the early studies of haematozoan research (Schaudin 1904; Mayer 1910, 1911; Moldovan 1913).

This study considers the prevalence and intensity of the genera *Haemoproteus*, *Leucocytozoon* and *Plasmodium*, in falconiform and strigiform birds from Germany.

MATERIALS AND METHODS

The birds examined in this study from 1996-2000 were wild birds admitted to rehabilitation centres sampled during the first two days after admission or birds sampled during ringing. Birds originated from mainly three different locations in Germany: Baden-Württemberg (BW) (47°50' to 49°25' N, 8°50' to 9°75' E), Lower Saxony (LS) (52°00' to 53°00' N, 9°50' to 11°00' E) and Berlin-Brandenburg (BB) (52°00' to 53°25' N, 11°50' to 14°50' E). Twenty-five different species of raptors in 5 families were subject to this study (Table 2). Identification of the bird species and the age categories was based on the descriptions by Baker (1993), Forsman (1999) and Glutz von Blotzheim (1971). The ageing of the pulli was performed by using the descriptions of Heinroth and Heinroth (1927) and the tables of growth for the falconiformes (Bijlsma 1997). A total of 976 blood smears from falconiform and 173 from strigiform birds were examined for the presence of blood parasites.

Samples were taken from the brachial vein. Blood films were air dried, fixed in absolute methanol and stained with Giemsa´s solution for 40 minutes. The scanning time was 10 min for every blood smear examined. They were scanned at x25 for 0.5 min, x100 for 1,5 min, x200 for 2 min, and x400 for 6 min. The oil immersion (x1000) was only used when the blood smear contained parasites. Measurements were performed with a Zeiss Axioplan microscope attached *via* a video camera to a PC with AnalysisPro 2.1 as software. Intensities of parasites were calculated by counting them in fields of 300-400 erythrocytes in 10 fields.

Species identification was based on the descriptions by Peirce *et al.* (1990) for *Haemoproteus brachiatus, H. tinnunculi, H. elani* and *H. nisis*, but for *H. buteonis* by Valkiűnas (1997), and by Bishop and Bennett (1989) of strigiform birds; for *Leucocytozoon* of Falconiformes by Greiner and Kocan (1977) and of Strigiformes by Bennett *et al.* (1993), for *Plasmodium* by Garnham (1966). *Trypanosoma avium* from the pygmy owl (*Glaucidium passerinum*) was described previously by Krone (1996).

The age (three classes: nestling, immature bird, adult bird), sex, origin (seven regions), order (Falconiformes or Strigiformes), bird species (25 species), and a possible injury or disease (birds admitted to rehabilitation centres) were regarded as variables potentially influencing its parasite burden (two categories: infected/not infected). Logistic regression (Hosmer and Lemeshow 1989) was used in order to analyse the effect of multiple variables on the parasite load. Categorical variables were compared by means of chi-square test or Fisher's exact test. Adjusted standardised residuals were used to identify the categories responsible for a significant chi-square test (Everitt 1977). Standardised residuals beyond ± 1.96 indicate a significant deviation from the expected values. The McNemar test (Bortz *et al.* 1990) served to compare prevalences for samples with related parasite information. A potential trend for the prevalences of the age classes was tested using Pfanzagl's trend test (Bortz *et al.* 1990). The significance level was generally set to $\alpha = 0.05$. All statistical calculations were performed using the SPSS 9.0 software.

RESULTS

A total of 11% (n=1149; 95% CI: 10, 13) of blood smears from birds of prey were positive for haematozoa. A similar prevalence was found in Falconiformes (n=976, 11%; 9, 13) and Strigiformes (n=173, 13%; 8, 19). The nestlings (pulli) had the lowest, whereas adult birds had the highest prevalences.

Of 17 hawk species examined, 9 were found to be infected with haemoparasites (Table 1). In comparison only 3 of 8 owl species examined were infected (Table 2).

No haematozoa were found in the osprey (*Pandion haliaetus*, pulli n=40, immature n=5, adult n=28), honey buzzard (*Pernis apivorus*, n=13), black kite (*Milvus migrans*, n=11), marsh harrier (*Circus aeruginosus,* pulli n=16, immature n=6, adult n=4), hen harrier (*Circus cyaneus,* n=1), montagu´s harrier (*Circus pygargus*, pulli n=31), merlin (*Falco columbarius*, n=1) and peregrine falcon (*Falco peregrinus,* pulli n=36, immature n=1, adult n=7).

No blood parasites were found in the barn owl (*Tyto alba*, pulli n=25, immature n=6, adult n=31), Tengmalm´s owl (*Aegolius funereus*, n=1), short-eared owl (*Asio flammeus*, n=1), little owl (*Athene noctua,* n=1) and eagle owl (*Bubo bubo,* n=8).

The hawks were mainly infected with *Leucocytozoon toddi* (9.5%, n=976) and only a few with *Haemoproteus* spp. (1.9%, n=976) while an equal number of owls were infected with *L. ziemanni* (10.4%, n=173) and *H. syrnii* (9.2%, n=173). *Plasmodium fallax* and *Trypanosoma avium* were only detected in the single pygmy owl examined. Measurements of the blood parasites are presented from infected birds in which large numbers of haemoparasites were found (Table 3).

A logistic regression was performed using the age, order, origin, season, and the admission to a rehabilitation centre as independent and the infection state as dependent variable. The sex was known only for 547 out of 1149 birds. Therefore, the influence of sex was separately tested, in order to use the full data set in the

Table 1. Prevalences and intensities of blood parasites in Falconiformes. ad. - adult, immat. - immature, max - maximal value, min - minimal value, n - sample size, pull. - pulli, SD - standard deviation, x - mean

Species	n	*Leucocytozoon*	*Haemoproteus*	*Leuco. + Haemo.*
Accipiter gentilis	227	21 (9%)	1	1 (0.4 %)
pull.	185	13		
intensity x (min-max) SD		1.43 (0.1-5) 1.65		
immat.	17	4		
intensity x (min-max) SD		0.33 (0.2-0.5) 0.13		
ad.	25	3	1	1
intensity x (min-max) SD		0.52 (0.05-1.4) 0.77	0.05%	
Accipiter nisus	132	7 (5 %)		
pull.	68			
immat.	20	3		
intensity x (min-max) SD		0.23 (0.05-0.4) 0.16		
ad.	44	4		
intensity x (min-max) SD		0.1 (0.05-0.2) 0.04		
Aquila pomarina	20	1		
pull.	9			
ad.	11	1		
intensity		0.05%		
Buteo buteo	189	59 (31%)	9 (5%)	3 (2 %)
pull.	15	2		
intensity x (min-max) SD		0.23 (0.1-0.35) 0.18		
immat.	62	14	5	1
intensity x (min-max) SD		1.29 (0.05-13.5) 3.32	1.35 (0.05-3.1) 1.1	
ad.	112	43	4	2
intensity x (min-max) SD		0.39 (0.05-8.9) 1.38	1.44 (0.35-2.15) 0.8	
Buteo lagopus	7	1		
immat.	3	1		
intensity		0.10%		
ad.	4			
Falco subbuteo	28		7	
pull.	3			
immat.	1			
ad.	24		7	
intensity x (min-max) SD			2.31 (0.05-6.6) 2.24	
Falco tinnunculus	136	1	3	
pull.	14			
immat.	48	1	1	
intensity		0.05%	2.75%	
ad.	74		2	
intensity x (min-max) SD			1.28 (0.95-1.6) 0.46	
Haliaeetus albicilla	15	1		
pull.	4	1		
intensity		0.45%		
immat.	3			
ad.	8			
Milvus milvus	24	2		
pull.	13	2		
intensity x (min-max) SD		1.7 (0.9-2.5) 1.13		
immat.	2			
ad.	9			

multiple analysis. No significant differences in the infection state of the sexes occurred (Fisher's exact test, P=0.358, n=547). The logistic regression revealed significant differences between the age classes (P<0.001, n=1146) and the seasons (P<0.001, n=1146), but not for the bird orders (p=0.365, n=1146), rehabilitation station (P=0.483, n=1149), and the regions (p=0.162, n=1146). For a more detailed analysis, the significant variables were subsequently tested using chi-square and standardised residuals. Seasonal differences were confirmed (chi-square test, p<0.001, n=1149), whereat the infection rate is below average in summer (standardised

Table 2. Prevalences and intensities of blood parasites in Strigiformes; for abbreviations see Table 1

Species	n	*Leucocytozoon*	*Haemoproteus*	*Leuco.* + *Haemo.*	other
Asio otus	25	1			
pull.	4	1			
intensity		0.40%			
immat.	1				
ad.	20				
Glaucidium passerinum	1				*T. avium*
ad.	1				*P.fallax*
intensity					0.15%
Strix aluco	73	16 (21.9%)	17 (23.3%)	12 (16.4%)	
pull.	33	1			
intensity		0.05%			
immat.	11	2	2	1	
intensity m (min-max) SD		0.2 (0.05-0.35) 0.21	12.2 (0.15-24.25) 17		
ad.	29	13	15	11	
intensity m (min-max) SD		0.35 (0.05-0.8) 0.28	9.22 (0.15-34.4) 9.5		

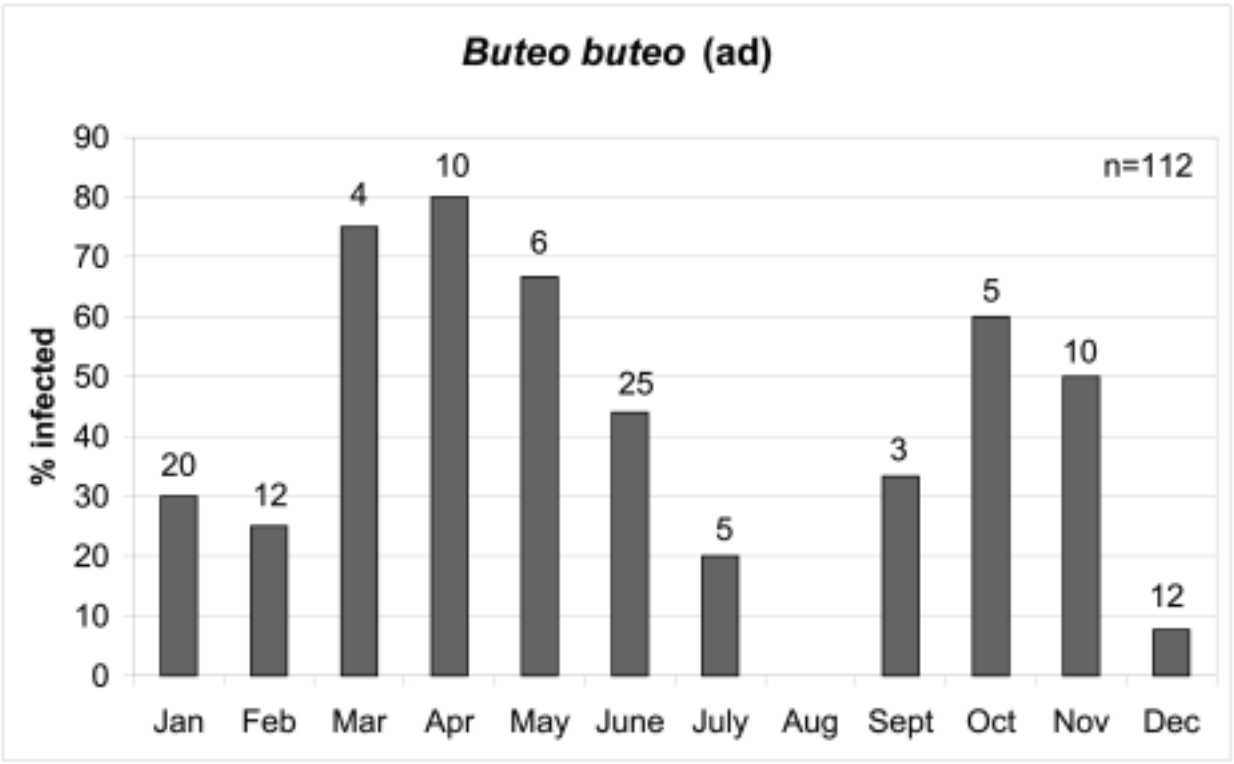

Fig. 1. Prevalence of blood parasites in adult Eurasian buzzards over the year (numbers above the bars are birds examined)

residual SR=-4.4) and above average in spring (SR=2.7) and autumn (SR=3.5). Differences between the age classes were also confirmed (chi-square test, $p<0.001$, n=1149) with pulli (SR=-7.2) showing a below-average infection rate as opposed to immature (SR=3.0) and adult birds (SR=5.0). A trend was detected (Pfanzagl's test, $P<0.001$, n=1149) demonstrating an increase in the prevalence with increasing age.

Hawks and owls differed in their prevalence for *Haemoproteus* spp. ($P<0.001$, Fisher´s exact test, n=1149) but not for *Leucocytozoon* spp. (P=0.677, Fisher´s exact test, n=1149). The hawks had a signifi-

Table 3. Measurements (mean in μm, standard deviation in parentheses) of *Haemoproteus* spp. found in Falconiformes and Strigiformes; ACGE - *Accipiter gentilis*, BUBT - *Buteo buteo*, FATI - *Falco tinnunculus*, FASU - *Falco subbuteo*, STAL - *Strix aluco*

Host species	ACGE	BUBT	FASU	FATI	STAL
Parasite species	*H. elani*	*H. buteonis*	*H. tinnunculi*	*H. tinnunculi*	*H. syrnii*
Uninfected erythrocyte	n = 20	n = 20	n = 20	n = 20	n = 20
Length	12.73 (0.55)	13.29 (0.97)	11.70 (0.55)	12.80 (0.62)	12.48 (0.66)
Width	7.02 (0.42)	7.02 (0.51)	6.43 (0.43)	6.93 (0.46)	7.37 (0.39)
Area	70.28 (3.84)	75.30 (7.46)	62.69 (3.55)	71.82 (4.45)	74.97 (5.81)
Uninfected erythrocyte nucleus	n = 20	n = 20	n = 20	n = 20	n = 20
Length	6.59 (0.25)	5.83 (0.49)	6.45 (3.89)	6.07 (0.42)	6.01 (0.53)
Width	2.48 (0.18)	2.50 (0.14)	2.34 (0.27)	2.64 (0.20)	3.04 (0.29)
Area	13.76 (1.03)	12.62 (0.93)	12.89 (1.73)	13.83 (1.19)	16.36 (2.22)
% area of erythrocyte	19.58	16.76	20.56	19.26	21.82
Erythrocyte infected by macrogametocyte	n = 20	n = 20	n = 20	n = 20	n = 20
Length	14.09 (0.72)	14.00 (0.89)	13.03 (0.44)	13.05 (0.73)	13.87 (0.99)
Width	7.08 (0.49)	6.98 (0.67)	7.43 (0.24)	7.39 (0.54)	7.43 (0.93)
Area	84.42 (4.88)	81.37 (9.77)	78.55 (5.07)	78.96 (4.75)	87.83 (8.38)
Infected erythrocyte nucleus	n = 20	n = 20	n = 20	n = 20	n = 20
Length	6.13 (0.74)	5.90 (0.64)	6.23 (0.28)	5.40 (0.37)	5.47 (0.64)
Width	2.35 (0.17)	2.54 (0.36)	2.11 (0.33)	2.74 (0.18)	2.94 (0.27)
Area	12.91 (1.22)	13.50 (1.49)	11.93 (0.84)	13.40 (1.08)	14.84 (2.02)
% area of erythrocyte-parasite complex	15.29	16.59	15.19	16.97	16.90
Macrogametocyte	n = 20	n = 20	n = 20	n = 20	n = 20
Length	13.23 (0.57)	15.08 (1.07)	16.40 (0.53)	15.67 (0.47)	15.27 (0.33)
Width	2.60 (0.34)	2.61 (0.16)	4.06 (0.21)	3.92 (0.22)	3.15 (0.27)
Area	53.57 (7.11)	54.51 (6.21)	57.63 (6.01)	55.21 (2.59)	53.42 (5.80)
% area of erythrocyte-parasite complex	63.46	66.69	73.36	69.92	60.82
Macrogametocyte nucleus	n = 20	n = 20	n = 20	n = 20	n = 20
Length	2.76 (0.34)	2.64 (0.17)	3.81 (0.20)	3.75 (0.25)	3.63 (0.43)
Width	2.04 (0.36)	2.14 (0.18)	2.88 (0.33)	2.87 (0.11)	2.19 (0.12)
Area	4.53 (0.91)	4.67 (0.39)	9.14 (0.49)	9.28 (0.46)	5.80 (0.88)
% area of gametocyte	8.46	6.97	15.86	16.81	10.86
Pigment granules	15.15 (1.59)	15.30 (2.03)	22.60 (2.60)	23.90 (2.83)	20.20 (3.71)
Nuclear displacement ratio	0.81 (0.09)	0.83 (0.10)	0.61 (0.09)	0.59 (0.11)	0.61 (0.13)
Erythrocyte infected by microgametocyte	n = 20	n = 20	n = 20	n = 20	n = 20
Length	13.42 (1.05)	14.66 (1.04)	12.96 (0.50)	13.00 (1.00)	14.07 (0.75)
Width	7.11 (0.46)	7.19 (0.34)	7.50 (0.52)	7.67 (0.66)	7.99 (0.50)
Area	79.92 (7.42)	88.03 (7.11)	82.56 (6.24)	80.66 (3.26)	94.11 (7.47)
Infected erythrocyte nucleus	n = 20	n = 20	n = 20	n = 20	n = 20
Length	6.38 (0.62)	5.81 (0.49)	6.19 (0.37)	5.78 (0.30)	5.62 (0.44)
Width	2.34 (0.25)	2.45 (0.25)	2.12 (0.19)	2.62 (0.21)	2.79 (0.24)
Area	12.66 (1.38)	12.59 (1.29)	12.54 (1.27)	13.70 (0.68)	14.25 (1.68)
% area of erythrocyte-parasite complex	15.84	14.30	15.19	16.98	15.14
Microgametocyte	n = 20	n = 20	n = 20	n = 20	n = 20
Length	16.26 (2.34)	15.92 (0.79)	14.62 (0.67)	15.32 (0.63)	15.38 (0.36)
Width	3.16 (0.16)	3.19 (0.31)	4.24 (0.31)	4.28 (0.44)	2.96 (0.35)
Area	55.37 (3.14)	57.72 (3.11)	60.11 (3.02)	59.77 (5.32)	52.03 (2.32)
% area of erythrocyte-parasite complex	69.28	64.89	72.81	74.10	55.29
Microgametocyte nucleus	n = 20	n = 20	n = 20	n = 20	n = 20
Length	10.17 (1.79)	10.24 (0.47)	9.56 (0.55)	9.57 (0.69)	5.73 (0.41)
Width	2.27 (0.21)	2.61 (0.21)	3.80 (0.30)	4.12 (0.48)	3.23 (0.26)
Area	28.07 (3.10)	29.74 (2.13)	40.40 (1.61)	38.90 (2.08)	15.31 (1.32)
% area of gametocyte	50.70	51.52	67.21	65.08	29.43
Pigment granules	14.70 (2.67)	15.60 (1.56)	21.75 (1.76)	22.15 (2.31)	15.75 (1.73)
Nuclear displacement ratio	0.83 (0.08)	0.85 (0.08)	0.62 (0.12)	0.50 (0.09)	0.69 (0.09)

Table 4. Prevalences of *Leucocytozoon* and *Haemoproteus* and number of birds examined in different regions of Europe (L - *Leucocytozoon,* H - *Haemoproteus)*

	Peirce and Marquiss (1983)	Mikaelian and Bayol (1991)	Peirce *et al*. (1983)		Sacchi and Prigioni (1984)	Svobodová and Votýpka (1998)	Kučera (1981a)
Region	Scotland	France	Britain	Spain	Italy	Czech Republic	Europe (literature review)
birds of prey (number of species)	60% (6) n = 235	31% (14) n = 150	20.3% (17) n = 54	14.2% (12) n = 28	21.9% (15) n = 114		
falconiform birds	60% (L,H) n = 229	35% (L,H) n = 83	2 (L,H) n = 33	3 (L,H) n = 25	22% (L,H) n = 91	24% (L) n = 459 9.3% (H) n = 495	2.5% (L) n = 334 53.1% (H) n = 178
strigiform birds	3 (L,H) n = 6	30% (L,H) n = 67	9 (L,H) n = 21	1 (L,H) n = 3	22% (L,H) n = 23		9.9% (L) n = 162 22.6% (H) n = 178
A. nisus	67% (L) 16% (H) n = 195	1 (H) n = 4	2 (L) 1 (H) n = 2		3 (L) n = 7	29% (L) 12% (H) n = 308	
B. buteo	2 (L) n = 3	46% (L) 61% (H) n = 26	0 (L,H) n = 3	1 (L,H) n = 9	9 (L) n = 39	38% (L) 9% (H) n = 99	
F. tinnunculus	0 (L,H) n = 6	20% (H) n = 35	0 (L,H) n = 12	0 (L,H) n = 1	1 (L) 5 (H) n = 20	0 (L) 1.5% (H) n = 66	
F. peregrinus	0 (L,H) n = 25		0 (L,H) n = 3	0 (L,H) n = 2			
F. subbuteo		2 (H) n = 4					
S. aluco	3 (L) 0 (H) n = 4	14% (L) 50% (H) n = 22	6 (L) 2 (H) n = 12		2 (L) 1 (H) n = 7		
A. otus	0 (L,H) n = 2	45% (H) 1 8% (L) n = 11	0 (L,H) n = 1		0 (L,H) n = 6		
T. alba		0 (L,H) n = 17	0 (L,H) n = 1	0 (L,H) n = 2	0 (L,H) n = 5		

cantly higher prevalence for *L. toddi* than for *H. elani* (P<0.001, McNemar test, n=976), whereas no differences could be found between prevalences of different blood parasites within the owls (P<0.754, McNemar test, n=173).

In order to analyse potential differences between the species, the subsequent analysis was restricted to adult birds of those species with at least 20 adult animals in the sample. A difference was found among adult birds of the species: *A. gentilis, A. nisus, B. buteo, F. subbuteo,*

F. tinnunculus, P. haliaetus concerning the infection rates with *Haemoproteus* spp. (P<0.001, chi-square test, n=299). The hobby was infected above average (SR=6.2).

Adult hawks (*A. gentilis, A. nisus, B. buteo, F. subbuteo, F. tinnunculus, P. haliaetus*) parasitised by *L. toddi* differed significantly in the species' prevalences (P<0.001, chi-square test, n=299). The Eurasian buzzard was most frequently parasitised (SR=7.2) compared to all others and the hobby (SR=-2.2), kestrel (SR=-4.3), and osprey (SR=-2.4) were infected below average.

More detailed analysis was done on the Eurasian buzzard for which sufficient data were available. A logistic regression test revealed differences between the seasons (P<0.001, n=189) but not between the age classes (P=0.108, n=189), rehabilitation stations (P=0.790, n=189), and between the regions (P=0.168, n=189). The seasonal differences were confirmed by a subsequent analysis (chi-square test, P=0.001, n=189), with an above-average infection rate in spring (SR=3.3) and a below-average infection rate in winter (SR=-3.2). A bias could be suspected because of the inclusion of pullis in the spring. However, the same analysis restricted to the adult buzzards revealed the same results (chi-square test, P=0.003, n=112, SR (spring)=3.0, SR (winter)=-3.3).

A seasonal change in prevalence was found. Peaks of infection occurring in both spring and autumn are shown in Fig. 1. Of all adult Eurasian buzzards examined, 38% were infected with *L. toddi* and only 4% with *H. buteonis* (n=112).

No differences could be found between the sexes of Eurasian buzzards (Fisher's exact test, P=0.185, n=44).

From the nestlings (pulli) sampled, the minimum age of infection with *Leucozytozoon toddi* in the goshawk (*Accipiter gentilis*, n=13) was 17 days, in the red kite (*Milvus milvus*, n=13) 24 days, in the Eurasian buzzard (n=14) 36 days, white-tailed sea eagle (n=4) 40 days and with *Leucozytozoon ziemanni* in the tawny owl (n=33) 15 days.

DISCUSSION

Prevalences of blood parasites in European birds of prey varied considerably, depending on bird species, geographic region (Table 4) and season.

The prevalences for *Plasmodium* spp. in birds of prey are generally low. Kučera (1981b) found a prevalence of 2.3% in Strigiformes (n=178), but did not diagnose the parasite in Falconiformes (n=333). In this survey only the pygmy owl was infected with *P. fallax*.

The low prevalence of *Haemoproteus* spp. in hawks (1.9%, n=976) in this study might be explained due to the different abundance of the vectors in the habitats of hawks and owls or due to a possible difference in susceptibility. The low prevalence of 5.3% with *L. toddi* in sparrow-hawks (n=132) in this survey could be a result of the choice of the breeding area, which often consists of young coniferous trees in a dry habitat, which is less suitable for vectors.

Wiehn *et al.* (1999) found a significantly higher prevalence of *Haemoproteus* spp. in females than in males during the nestling period in common kestrels from Finland in one of three years of investigations, whereas no differences between the sexes could be found in this study.

The differences in the prevalence of blood parasites between age classes are consistent with results by Ashford *et al.* (1990).

Parasitaemic intensities of *H. tinnunculi* in American kestrels (*Falco sparverius*) increased during the nestling cycle in females, indicating that blood parasitism, immunity and kestrel reproduction are interrelated and are possibly linked allocation of metabolizable energy in the host (Apanius 1993). The youngest birds of prey infected with blood parasites were nestlings of sparrow-hawks in Scotland infected with *L. toddi* at an age of 14 days (Peirce and Marquiss 1983). Only a few white-tailed sea eagles (*Haliaeetus albicilla*) had previously been examined for haematozoa, with all being negative (Nikitin and Artemenko 1927, Peirce 1980). This study showed for the first time that the white-tailed sea eagle could be infected with *L. toddi*. The bird was 40 days old. Stuht *et al.* (1999) found the youngest nestling of a bald eagle (*Haliaeetus leucocephalus*) to be infected with *L. toddi* at an age of 25 days.

Cheke *et al.* (1976) detected a seasonal variation in the prevalence of blood parasites in wild birds from England, with a peak in May. Kučera (1981b) revealed two significant peaks in the prevalence of *Haemoproteus* spp., one in May and another in September. For *Leucocytozoon* he only found a peak in spring (Kučera 1981a). He attributed the spring peak to an increase of sexual hormones during the breeding and rearing of young. It was suggested that the autumn peak

was due to a high proportion of young birds in the population with acute infections due to incomplete immunity. Research on raptors during their breeding period revealed a "spring relapse" of haemoparasites in the blood of adult birds, facilitating the infection of the youngsters in the nest by an insect vector (Ashford *et al.* 1990). As this study shows there is an increase of infection in Eurasian buzzards during spring and autumn (Fig. 1). The peak in spring reflects the so called "spring relapse" and the peak in autumn is consistent with the idea of Peirce (1989) that relapses with increased parasitaemia may occur, that are triggered by hormonal activity during breeding, migration or stress. Migrating birds of prey, mainly steppe buzzards (*Buteo buteo vulpinus*) sampled in Israel had a high prevalence (64%) of blood parasites (Cooper *et al.* 1993).

Measurements of *H. elani* from the goshawk, *H. buteonis* from the Eurasian buzzard and *H. tinnunculi* from the hobby and common kestrel are lower than given by Peirce *et al.* (1990). These and the lower dimensions of *H. syrnii* from the tawny owl compared to the results of Bishop and Bennett (1989) can probably be explained due to smaller erythrocytes measured in this study containing smaller parasites. In addition results presented in Table 3 indicate a broader range for *Haemoproteus* than given by Peirce *et al.* (1990) and Bishop and Bennett (1989). We followed the separation of the species *H. elani* and *H. buteonis* on the basis of morphological characteristics indicated by Valkiű`nas (1997). A cross-transmission experiment would be applicable to proof the species separation.

Acknowledgements. We are grateful to the "Deutscher Falkenorden" for supporting this study financially. We would like to thank R. Altenkamp, D. Haas, A. Hallau, N. Kenntner, P. Lepom, B.-U. Meyburg, C. Rohde, W. Scheller, D. Schmidt and M. Streitz for their co-operative work in collecting blood smears and providing us with back ground information about the sampled birds. We are also grateful to M.A. Peirce for verification of species identification and constructive advises, to M. East for reading the manuscript and to K. Ernst for her technical assistance.

REFERENCES

Apanius V. (1993) Blood parasitism, immunity and reproduction in American kestrels (*Falco sparverius*). In: Biology and Conservation of Small Falcons, (Eds. M. K. Nicholls and R. Clarke). Proceedings of the Hawk and owl Trust Conference, London, 117-125

Ashford R. W., Wyllie I., Newton I. (1990) *Leucocytozoon toddi* in British sparrowhawks *Accipiter nisus*: observations on the dynamics of infection. *J. Nat. Hist.* **24:** 1101-1107

Atkinson C. T. (1986) Host specificity and morphometric variation of *Haemoproteus meleagridis* Levine, 1961 (Protozoa: Haemosporina) in gallinaceous birds. *Can. J. Zool.* **64:** 2634-2638

Atkinson C. T., Van Riper III C. (1991) Pathogenicity and epizootiology of avian haematozoa: *Plasmodium*, *Leucocytozoon*, and *Haemoproteus*. In: Bird-parasite Interaction, (Eds. J. E. Loye and M. Zuk). Oxford University Press, New York, 19-48

Baker K. (1993) Identification Guide to European Non-passeriformes. BTO Guide 24, Norfolk

Bennett G. F., Whiteway M., Woodworth-Lynas C. B. (1982) A host-parasite catalogue of the avian haematozoa. Occasional papers in biology, No. 5, Memorial University of Newfoundland

Bennett G. F., Earlé R. A., Peirce M. A. (1993) The Leucocytozoidae of South African birds. The Falconiformes and Strigiformes. *Ostrich* **64:** 67-72

Bennett G. F., Peirce M. A., Earlé R. A. (1994) An annotated checklist of the valid avian species of *Haemoproteus*, *Leucocytozoon* (Apicomplexa: Haemosporida) and *Hepatozoon* (Apicomplexa: Haemogregarinidae). *Syst. Parasitol*. **29:** 61-73

Bijlsma R. G. (1997) Handleiding veldonderzoek Roofvogels. KNNV Uitgeverij, Utrecht

Bishop M. A., Bennett G. F. (1989) The haemoproteids of the avian order Strigiformes. *Can. J. Zool*. **67:** 2676-2684

Bortz J., Lienert G. A., Boehnke K. (1990) Verteilungsfreie Methoden in der Biostatistik. Springer, Berlin, Germany

Cheke R. A., Hassall M., Peirce M. A. (1976) Blood parasites of British birds and notes an their seasonal occurrence at two rural sites in England. *J. Wildl. Dis*. **12:** 133-138

Cooper J. E., Gorney-Labinger E., Ion F. (1993) Parasitological and other studies on migrating raptors. In: Raptor Biomedicine, (Eds. P. T. Redig, J. E. Cooper, J. D. Remple and B. Hunter). University of Minnesota Press, Minneapolis, 28-31

Danilewsky B. (1885) Zur Parasitologie des Blutes. *Biol. Zentrabl.* **5:** 529-537

Everitt B. S. (1977) The Analysis of Contingency Tables. Chapman and Hall, London

Fallis A. M., Desser S. S., Kahn R. A. (1974) On species of *Leucocytozoon*. *Adv. Parasitol*. **12:** 1-67

Forsman D. (1999) The Raptors of Europe and the Middle East. T&AD Poyser, London

Garnham P. C. C. (1966) Malaria Parasites and other Haemosporidia. Blackwell Scientific Publications, Oxford

Glutz v. Blotzheim U. N. (Eds.) (1971) Handbuch der Vögel Mitteleuropas. Band 4 Falconiformes. Akademische Verlagsgesellschaft, Frankfurt am Main

Greiner E. C., Kocan A. A. (1977) *Leucozytozoon* (Haemosporida; Leucozytozoidae) of the Falconiformes. *Can. J. Zool.* **55:** 761-770

Heinroth O., Heinroth M. (1927) Die Vögel Mitteleuropas. Band II. Hugo Bermühler Verlag, Berlin

Hosmer D. W., Lemeshow S. (1989) Applied Logistic Regression. John Wiley & Sons, N. Y.

Koch R. (1899) Über die Entwicklung der Malariaparasiten. *Z. Hyg. Infektionskr.* **32:** 1-24 (I-IV)

Krone O. (1996) The pygmy owl (*Glaucidium passerinum*) as a new host for the rare haematozoon *Trypanosoma avium*. *Appl. Parasitol*. **37:** 300-301

Kučera J. (1981a) Blood parasites of birds in central Europe. 2. Leucocytozoon. *Folia Parasitol*. **28:** 193-203

Kučera J. (1981b) Blood parasites of birds in central Europe. 3. Plasmodium and Haemoproteus. *Folia Parasitol*. **28:** 303-312

Mayer M. (1910) Über die Entwicklung von Halteridium. *Arch. Schiffs. Tropenhyg*. **14:** 197-202

Mayer M. (1911) Über ein Halteridium und Leucocytozoon des Waldkauzes und deren Weiterentwicklung in Stechmücken. *Arch. Protistenkd*. **21:** 232-254

Mikaelian I., Bayol P. (1991) Blood Protozoa found in birds of prey undergoing rehabilitation. *Point Vet*. **22:** 857-860

Moldovan J. (1913) Über die Entwicklung von *Leukozytozoon ziemanni*. *Zentbl. Bak. Parasit. Infektionskr*. **71:** 66-69

Nikitin S. A., Artemenko W. D. (1927) Protozoa in the blood of vertebrates of the Southern Ukraine. *Russ. Zh. Trop. Med*. **5:** 654-664 (in Russian)

Peirce M. A. (1980) Haematozoa of British birds: post-mortem and clinical findings. *Bull. Br. Ornithiol. Club* **100:** 158-160

Peirce M. A. (1989) The significance of avian haematozoa in conservation strategies. In: Diseases and threatened birds, (Ed. J. E. Cooper). ICBP Technical Publication No. 10, Cambridge 69-78

Peirce M. A., Marquiss M. (1983) Haematozoa of British birds. VII. Haematozoa of raptors in Scotland with a description of *Haemoproteus nisi* sp. nov. from the sparrow-hawk (*Accipiter nisus*) *J. Nat. Hist*. **17:** 813-821

Peirce M. A., Greenwood A. G., Cooper J. E. (1983) Haematozoa of raptors and other birds from Britain, Spain and the United Arab Emirates. *Avian Pathol*. **12:** 447-459

Peirce M. A., Bennett G. F., Bishop M. (1990) The Haemoproteus of the avian order Falconiformes. *J. Nat. Hist*. **24:** 1091-1100

Sacchi L., Prigioni C. (1984) Occurrence of *Leucocytozoon* and *Heamoproteus* (Apicomplexa, Haemosporina) in Falconiformes and Strigiformes of Italy. *Ann. Parasitol. Hum. Comp*. **59:** 219-226

Schaudin F. (1904) Generations- und Wirtswechsel bei Trypanosoma und Spirochaete. *Arb. K. GesundhAmt.* **20:** 387-439

Stuht J. N., Bowerman W. W., Best D. A. (1999) Leucocytozoonosis in nestling Bald Eagles in Michigan and Minnesota. *J. Wild. Dis*. **35:** 608-612

Svobodová M., Votýpka J. (1998) Occurrence of blood protists in raptors (Falconiformes). *Buteo* **10:** 51-56 (in Czech)

Valkiűnas G. (1997) Bird haemosporida. *Acta Zool. Lituanica*, 3-5 (monograph)

Wasielewski T., Wülker G. (1918) Die *Haemoproteus*-Infektion des Turmfalken. *Arch. Schiffs. Tropenhyg*. **22:** 3-100, I-IV

Wiehn J., Korpimäki E., Pen I. (1999) Haematozoan infections in the Eurasian kestrel: effects of fluctuating food supply and experimental manipulation of parental effort. *Oikos* **84:** 87-98

Received on 30th January, 2001; accepted on 18th July, 2001

Acta Protozool. (2001) 40: 291 - 296

ACTA
PROTOZOOLOGICA

Fine Structure and Biometric Characterization of the Shell in the Rare Testacean Species *Hyalosphenia punctata* Penard (Protozoa: Testacealobosia)

Júlia Katalin Török

Department of Systematic Zoology and Ecology of the Eötvös Loránd University, Budapest

Summary. *Hyalosphenia punctata* Penard was described from the sediment of Swiss lakes. Following its recognition this species was only sparsely detected, especially out of the area of its description. Because of its rare occurrence fine structure of its shell has been unknown. The present study gives new insights into the shell composition of *H. punctata* on the occasion of its occurrence in the Hungarian section of the River Danube and suggests a change of its generic position in the future, possibly into genus *Nebela*. Biometric characterization of the shells from different populations shows a negligible fluctuation within the range of the shell size.

Key words: biometric characterization, fine structure, *Hyalosphenia*, morphology, taxonomy, testate amoebae.

INTRODUCTION

The majority of testate amoeba species can be identified exclusively on the basis of the shell morphology. However, in certain species some morphological details were overseen or failed to be concerned as a determining trait at the time of the original description. The improved microscopic techniques provide the opportunity to reveal some new peculiarities in the fine structure of such species and it becomes possible to add them to the morphological description of the species.

According to composition, main types of the shell in testate amoebae are proteinaceous, agglutinate, siliceous and calcareous. Besides composing material there is an organic matrix that plays a determining role: it either forms a continuous sheet constructing the whole shell (in which the shell material may be embedded), or represents merely a binding material, which connects the building units (Ogden 1990).

The genus *Hyalosphenia* Stein, 1857 is characterized by a proteinaceous shell, where organic cement forms a continuous sheet, without external elements.

The aquatic testacean species *Hyalosphenia punctata* Penard, 1891 has turned up quite rarely since its description, only few papers report its appearance (Bhatia, Forel, Günthert, Monti; see Grospietsch 1965; Opravilova 1974, 1980). It is said to prefer the deep water zone of cold, alpine lakes (Penard 1891, 1902; Grospietsch 1965). However, it has also been found in a swamp (Penard 1902) and running waters (Opravilova

Address for correspondence: Júlia Katalin Török, Department of Systematic Zoology and Ecology, Eötvös Loránd University, Budapest, Hungary; E-mail: torokjuli@cerberus.elte.hu

1974, 1980). I have also encountered this species in lotic environment, during a survey of benthic testaceans in the main channel of the Szigetköz-section of the River Danube. Since three distinct samples harboured considerable numbers of specimens, it became possible to examine, whether they represent the same population or not.

My microscopic observations revealed that this species has a unique shell structure within the genus, which has been referred to as "punctuated" (see species name).

Since this rare species is very poorly documented in the scientific literature, it seemed to be reasonable to publish these new observations on this species, supplemented with taxonomic remarks and a biometric characterization of the shell.

MATERIALS AND METHODS

Hyalosphenia punctata Penard, 1891 was found in core samples, collected from the sediment of the main channel of the Szigetköz-Danube within the frame of a three-year study on benthic protozoans of the River Danube carried out between 1995-98. For sampling details see Török (1997). *H. punctata* was found in the sediment samples originating from the 1812, 1813, 1828, 1843 and 1846 river km. Table 1 shows the characteristics of the samples comprising considerable numbers of specimens.

Sediment samples were fixed and stained with Bereczky's method (Bereczky 1985).

First the tests were investigated under light microscope using bright field, phase and Nomarski optics. The first observations were made on the wet material and afterward certain tests were embedded into Euparal as permanent slides. Since this species has an extraordinary fragile shell, it has always collapsed or lost its original form when exposed to air. To avoid this, the light micrographs of *H. punctata* were made on wet material.

For scanning electron microscopic (SEM) study shells were air dried, then coated with gold. SEM investigation was made with a HITACHI S-2360N machine operating at 9 kV electron beam acceleration voltage.

Measurements and biometric characterization were made according to Schönborn *et al.* (1983).

RESULTS

The shell was transparent, made up from small, nearly circular building units of *ca* 1µm diameter each, which did not seem to overlap (Figs 1-9). Using the highest light microscopic magnification, they could be seen next to the pseudostome as well (Figs 6, 9). The shell structure seemed to fade toward the pseudostome. There was a narrow lip around the pseudostome (Figs 1, 4, 6). The coloration of the detected specimens varied slightly: one specimen showed a yellowish hue throughout the whole test, while another one was yellow at the aboral and the middle part and colourless near the pseudostome. In some of the cells the plasma filled up almost the whole shell. No epipodia were found (Figs 10-11). Food content consisted of bacteria, and algae, especially diatoms (Figs 10-12). A single nucleus with a large globular nucleolus was clearly visible in some of the cells (Figs 13, 14).

Biometric characterization of 51 shells was carried out. The values are represented together with those measured by other authors (Table 2). To compare the shell parameters in the three populations with considerable number of specimens to the rest of the shells I carried out their separate morphometric analyses (Table 3).

DISCUSSION

Morphology

Besides its rare occurrence, the lack of data on *H. punctata* fine structure may be attributed to its fragile test which is seemingly structureless, hyalin at low magnification. Moreover, it might get damaged or disappear in course of any kinds of manipulation (e.g. flotation, filtration) of the sample. Owing to its transparency and relatively small size, it is easy to oversee the shells in a turbid sediment sample. In the scanning electron micrographs the building units at the aboral part were much better visible than those toward the pseudostome, suggesting that the units are coated with an outer homogeneous organic layer which is getting more pronounced toward the adoral part (Figs 7-9).

The unique composition of the shell reminds me of *Arcella* shells, which are composed of proteinaceous building units bound together with organic cement, resulting a honeycomb pattern and deposit iron progressively with age. A thin outer and inner cement sheet covers the joined units (Netzel 1975, 1977). In *H. punctata*, in higher magnification building units and their arrangement are very similar to those of *Arcella* species, since both light and SEM micrographs suggest that the surface of the shell is covered with an outer - presumably organic - layer, especially at the adoral part, thus fading the underlying shell structure. Transmission electron micrographs would settle the question.

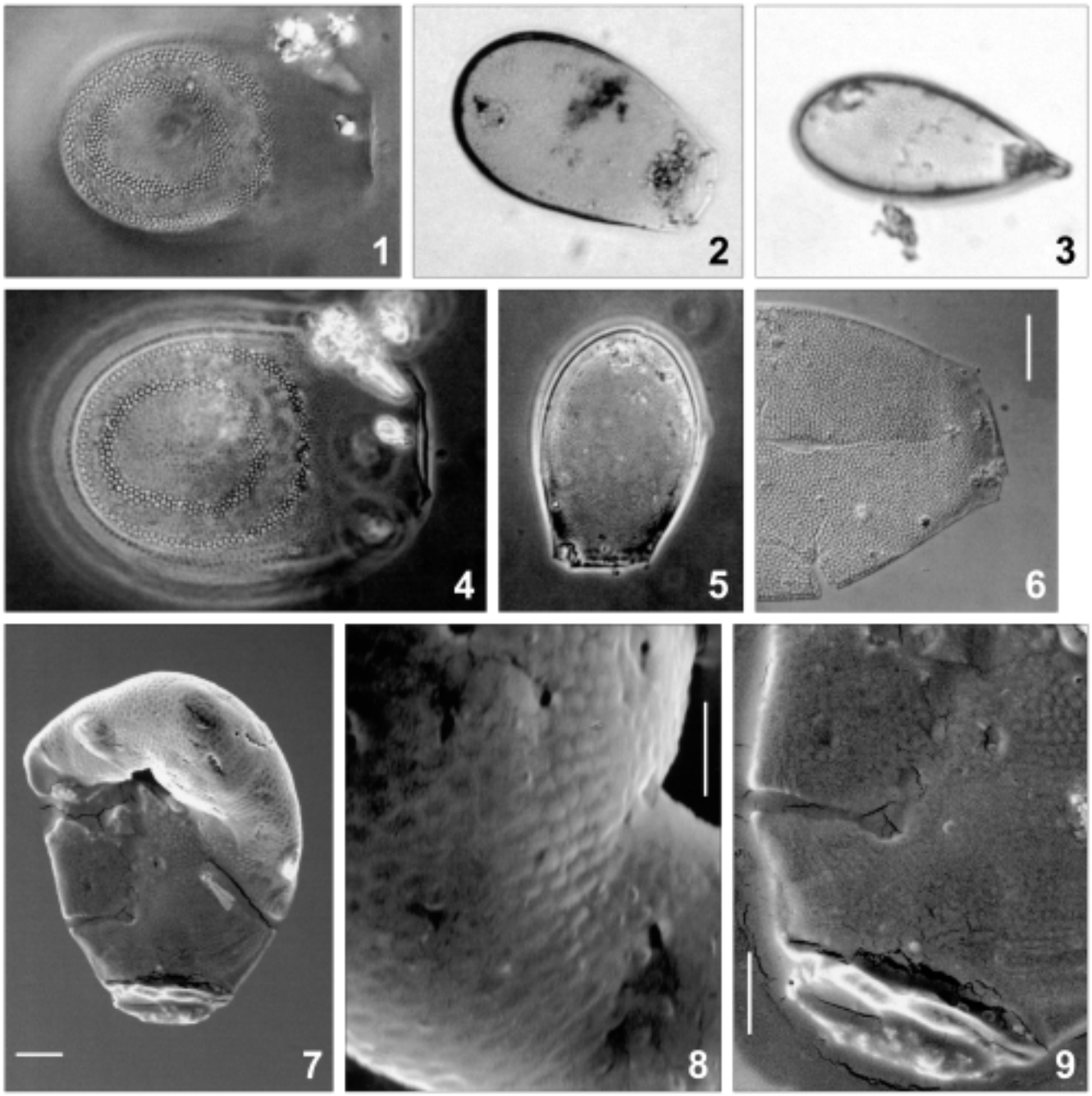

Figs 1-9. Empty shells of *Hyalosphenia punctata*. **1** - aboral punctuation of the shell, frontal view, length 75 µm (Nomarsky differential interference contrast); **2** - frontal view of another specimen, length 75 µm (bright field); **3** - lateral view of the shell in Fig. 1 (bright field); **4** - same specimen as in Figs 1, 3 with emphasized pseudostome (phase contrast); **5, 6** - frontal view of another specimen, length 92 µm (phase contrast), with detailed adoral shell structure, scale bar - 20 µm (Nomarsky differential interference contrast); **7-9** - frontal view showing the building units, with details of the aboral and adoral parts, scale bars - 10 µm, 5 µm, 7 µm, respectively (scanning electron micrographs)

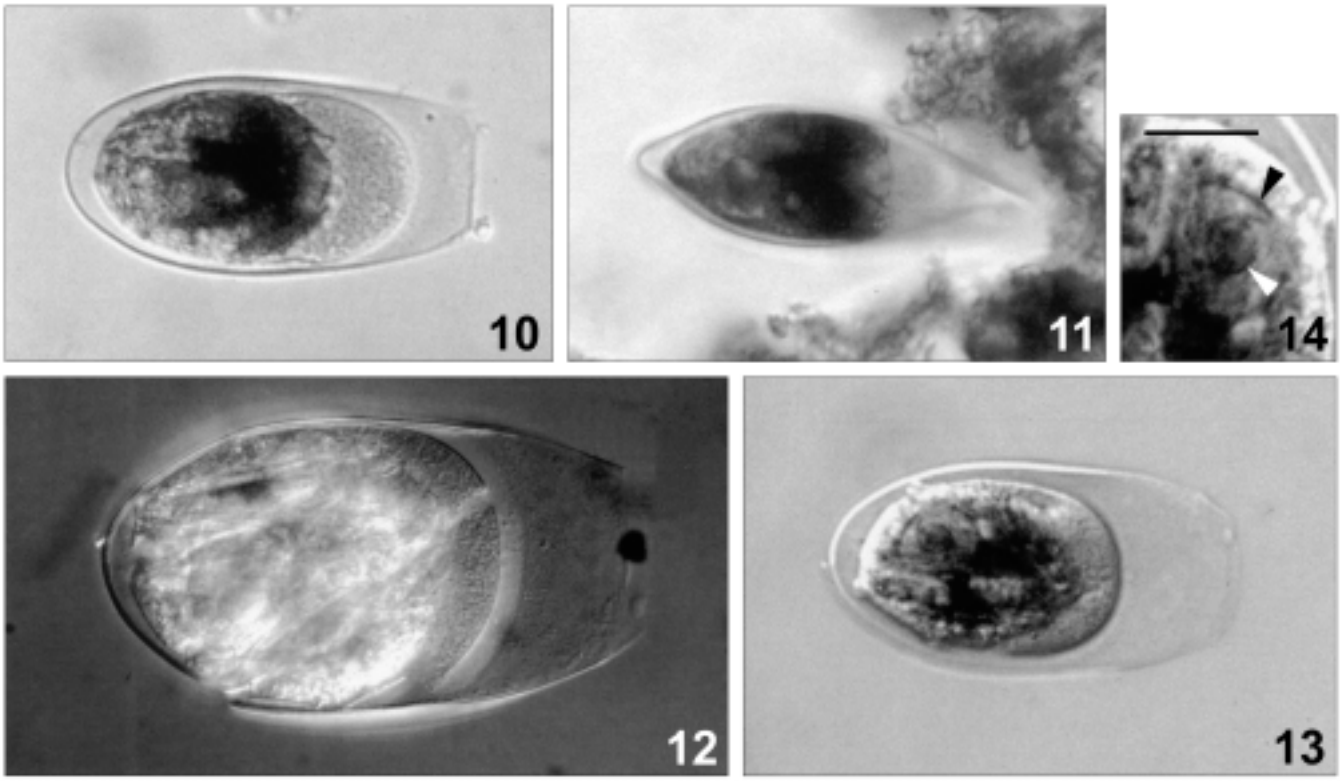

Figs 10-14. Full shells of *Hyalosphenia punctata*. **10, 11** - frontal and lateral view of a specimen fixed and stained alive, length 74 µm (bright field); **12** - specimen with ingested diatoms, length 71µm (bright field); **13** - specimen with clearly visible nucleus, length 63 µm (bright field); **14** - detail of Fig.13, showing nucleolar envelope (black arrowhead) and single globular nucleolus (white arrowhead), scale bar - 10 µm (bright field)

Table 1. Samples inhabited by populations with a considerable number of specimens of *Hyalosphenia punctata*

Sample	Location	Date of collection	Microhabitat	Living specimens (%)
RAo/10/96	1812 river km, near the right side bank	October, 1996	surface of the sediment	55.5
LAo/10/96	1813 river km, near the left side bank	October, 1996	surface of the sediment	5
LAo/10/97	1813 river km, near the left side bank	October, 1997	surface of the sediment	100

Cyphoderia species with the same size of building units possess siliceous scales arranged in more regular rows, not similar to the structure of *H. punctata*. Penard (1902) has demonstrated that the scales *H. punctata* are insoluble in sulphuric acid and concluded that they are siliceous. An X-ray microanalysis in the future could prove this observation.

My measurements of the shells (Table 2) correspond well with the values given in the literature, although the references on the shell size are restricted only to the shell length (Penard 1902, Opravilova 1974). Majority of the specimens I saw were originating from three distinct samples. The separate morphometric analysis of the three samples with living specimens resulted quite homogeneous median values for the main classical features (length, breadth of the shell and shell breadth over the aperture) (Table 3). Populations 2 and 3, the richest ones in specimens, resulted from a consecutive sampling from the same locality. They share almost the same median values, only the shell breadth over the pseudostome varies slightly. This fact suggests that the two populations are identical, i.e. *H. punctata* survives there over

Table 2. Biometric characterization of *Hyalosphenia punctata* Penard, based on pooled data of the present study, including measurements from other experts to compare. ($\bar{x}$ - arithmetic mean, M - median, s - standard deviation, $s_{\bar{x}}$ - deviation of the arithmetic mean, CV - coefficient of variation, Min - minimum, Max - maximum, N - number of specimens, Ps denotes the breadth of shell over the pseudostome, shell measurements are in μm)

	$\bar{x}$	M	s	$s_{\bar{x}}$	CV	Min	Max	N
Length								
Penard	-	-	-	-	-	55	90	-
Opravilova	-	-	-	-	-	69	93	8
Present work	75.54	75	9.42	6.14	12.5	35	95	51
Breadth	38.97	40	7.14	4.31	18.3	16	54	47
Depth	26.75	25	4.05	2.75	15.1	25	35	6
Ps	25.15	25	3.01	2.49	11.9	15	32	44

Table 3. Separate biometric characterization of three populations and randomly found specimens of *Hyalosphenia punctata* Penard detected in course of the present work. (P1 - population from the 1812 river km, sample RAo/10/96; P2 - population from the 1813 river km, sample LAo/10/96; P3 - population from the 1813 river km, sample LAo/10/97; Rs - randomly found specimens from all localities. Values of the three populations are also included in group Rs, as specimens, represented by their median values). For further explanation see Table 2

	$\bar{x}$	M	s	$s_{\bar{x}}$	CV	Min	Max	N
P1								
Length	82	82.5	7.18	5.56	8.76	73	95	9
Breadth	40.11	40	5.05	3.37	12.59	32.5	51	9
Ps	24.75	25	2.49	1.56	10.06	22	30	8
P2								
Length	76.97	75	5.11	3.92	6.64	70	90	19
Breadth	39.36	40	3.83	2.43	9.73	35	52	18
Depth	25.12	25	0.25	0.19	0.99	25	25.5	4
Ps	24.91	25	2.15	1.38	8.63	20	27.5	17
P3								
Length	76.38	75	5.14	4.49	6.73	70	85	13
Breadth	39.21	40	2.59	2.06	6.60	34.5	42.5	12
Ps	26.25	26	2.14	1.62	8.15	22	30	12
Rs								
Length	68.81	75	14.35	11.08	20.85	35	85	13
Breadth	39.88	40	8.99	5.19	22.55	16	54	12
Ps	24.50	25	6.08	4.20	24.81	15	37	10

longer periods of time. Population 1 has somewhat larger length dimensions.

Ecology and distribution

Although *Hyalosphenia punctata* was listed already in Penard's first large monograph on the Swiss lakes (Penard 1891), most information referring to this species still originate from the same author (Penard 1891, 1902). Some more, scattered references are also available from other experts, but all of them are confined to establish the presence of the species (Bhatia, Forel, Güntert, Monti; see Grospietsch 1965). Opravilova published some size and ecological data (1974, 1980).

In the Danube sediment *H. punctata* was found only occasionally, which suggests its low individual abundance. This is not astonishing under the severe conditions reinforced by the irregular water regime of this river section. However, the longer survival of the same testacean population (P2 and P3 in Table 3) at the same geographic locality is of great significance. Low abundance with either very few detected specimens (8) or low dominance and frequency values was also found by

Opravilova (1974, 1980). These support the author's view that it is reasonable to regard *H. punctata* as a rare testate amoeba species.

Regarding its typical habitat, *H. punctata* was considered among the typical inhabitants of the deep-water benthos of cold, alpine lakes (Penard 1902, Grospietsch 1965). However, the specimens in the studies of Opravilova and the present study were found in running waters. Bityska Brook and Bobrav Stream are small streams with a maximum of 0.3 and 1.5 m depth, and 5 and 10 m width, respectively (Opravilova 1974, 1980). On the contrary, the sampled region of the Danube has about three - four hundred m^3/s mean water discharge. This is with more than one order of magnitude larger than the two streams studied by Opravilova. The found specimens can either be accidental elements in the local species assemblages of the lotic environment or can originate from the lentic habitats of the extended side arm systems of the Danube (Szigetköz and Csallóköz). It is regrettable that there was no reference to the exact microhabitat type where *H. punctata* occurred in the Bobrav Stream (Opravilova 1974). In the Bityska Brook *H. punctata* was found exclusively in one sampling locality, the sediment (Opravilova 1980).

Reflections on taxonomy

The revealed particular shell structure of *H. punctata* makes questionable the present generic position of the species since the revealed structure conflicts with the general definition of the genus which declares that shells are composed of homogeneous proteinaceous material. The general form of the shell and the rim around the pseudostome are arguments to the advantage of *Hyalospheniidae* Schulze, 1877. However, the observed composition of the shell suggests that this species might be rather a member of genus *Nebela* than a *Hyalosphenia*. Further observations, including more living specimens and recognition of the origin and chemical nature of the composing shell units might result in placing *H. punctata* into the genus *Nebela*. But, before making this change, the Filosean origin of the building units has to be proved.

Acknowledgements. I am very grateful to Dr. Z. Kristóf for making the SEM micrographs, Mr. M. Balogh for his help with the SEM preparation and Dr. M. Cs. Bereczky for comments on the manuscript. This study was financed by the Hungarian Scientific Research Foundation (OTKA, T-17708).

REFERENCES

Bereczky M. Cs. (1985) Fixations- und Färbungsschnellverfahren bei quantitativen ökologischen Untersuchungen von Protozoen in Binnengewässern. *Arch. Protistenkd.* **129:** 187-190

Grospietsch Th. (1965) Monographische Studie der Gattung *Hyalosphenia* Stein. *Hydrobiologia* **26:** 211-241

Netzel H. (1975) Die Entstehung der hexagonalen Schalenstruktur bei der Thekamöbe *Arcella vulgaris* var. *multinucleata* (Rhizopoda, Testacea). *Arch. Protistenkd*. **117:** 321-357

Netzel H. (1977) Morphogenesis in the shelled rhizopod *Arcella dentata*. *Protistologica* **13:** 299-319

Ogden C. G. (1990) The structure of the shell wall in testate amoebae and the importance of the organic cement matrix. In: Scanning Electron Microscopy in Taxonomy and Functional Morphology, (Ed. D. Claugher). Systematics Association Special Volume, Clarendon Press, Oxford, **41:** 235-257

Opravilova V. (1974) Testacea (Protozoa: Rhizopoda) of the River Bobrava in Moravia. *Vestn. Cesk. Spol. Zool.* **38:** 127-147

Opravilova V. (1980) Prispevek k poznani ekologie krytenek (Rhizopoda, Testacea) Potoka Bityska (Morava, CSSR). *Acta Sci. Nat. Mus. Morav. Occid. Trebic* **11:** 5-16 (in Czech)

Penard E. (1891) Contributions à l'étude des Rhizopodes du Léman (Bibliothéque Universelle). *Arch. Sci. Phys. Nat. ser.* 3, **26:** 134-156

Penard E. (1902) Faune rhizopodique du bassin du Léman. H. Kündig, Geneve

Schönborn W., Foissner W., Meisterfeld R. (1983) Licht- und rasterelektronenmikroskopische Untersuchungen zur Schalenmorphologie und Rassenbildung bodenbewohnender Testaceen (Protozoa: Rhizopoda) sowie Vorschläge zur biometrischen Charakterisierung von Testaceen-Schalen. *Protistologica* **19:** 553-566

Török J.K. (1997) Distribution and coenotic composition of benthic testaceans (Protozoa, Rhizopoda) in the abandoned main channel of River Danube at Szigetköz (NW-Hungary). *Opusc. Zool. Budapest* **29-30:** 141-154

Received on 8th May, 2001; accepted on 4th September, 2001

Acta Protozool. (2001) 40: 297 - 301

ACTA
PROTOZOOLOGICA

Trichodina porocephalusi sp. n. (Ciliophora: Trichodinidae) from an Indian Flathead Sleeper, *Ophiocara porocephalus* (Valenciennes) (Eleotrididae)

Ghazi S. M. ASMAT

Department of Zoology, University of Chittagong, Chittagong, Bangladesh

Summary. A population of trichodinids (Ciliophora: Trichodinidae) was found on the gills of an Indian estuarine flathead sleeper, *Ophiocara porocephalus* collected from the Hooghly River in West Bengal, India and was described as a new species. The species is characterized by the shape of denticles having broad and rectangular blades with truncated distal margins, parallel borders, apexes with distinct notches in the lower border of the anterior margins; robust, conical central parts; backwardly directed short, stumpy rays with prominent ray apophyses and grooves; and argentophobic central areas which are somewhat elevated from the rest of the adhesive disc and contains few to many argentophilic dots or patches. The body diameter ranged from 32.5-50.5 (42.3 ± 5.2) μm, whilst the denticle number was 20-27 (24.3 ± 1.5). This ciliophoran infested approximately 20.8% of the host fishes (54 out of 240) on their gills during March 1996 to December 1997, sometimes along with *Trichodina acuta* Lom, 1961 and *Tripartiella copiosa* Lom, 1959. The highest percentage of infestation was recorded in October 1997 (90%). The variation of the adhesive disc is recorded and discussed.

Key Words: Ciliophora, estuarine fish, gills, India, *Ophiocara porocephalus*, *Trichodina porocephalusi* sp. n., trichodinid.

INTRODUCTION

In India, studies on the trichodinid ciliophorans, relatively few so far, is gaining momentum recently in various aspects. As a result, 12 species of trichodinid ciliophorans representing the genera *Trichodina* Ehrenberg, 1838; *Paratrichodina* Lom, 1963; and *Tripartiella* Lom, 1959 were reported from different freshwater and estuarine Indian fishes (Hagargi and Amoji 1979; Mukherjee and Haldar 1982; Das and Haldar 1987; Das *et al.* 1987; Mishra and Das 1993; Saha *et al*. 1995 a, b; Saha and Haldar 1996, 1997; Asmat and Haldar 1998; Asmat 2001a, b). During the present study on the biodiversity of the trichodinid ciliophorans inhabiting the freshwater and estuarine fishes, a new species of *Trichodina* was found on the gills of an estuarine flathead sleeper, *Ophiocara porocephalus*.

MATERIALS AND METHODS

The host fishes (4.5-8.0 cm, 20-50 g) were collected by fishing nets from different rivulets of the Hooghly River in the Hooghly District of West Bengal during March 1996 to December 1997. Gill scrapings were made at the riverside. Air-dried gill scrapings were transported to the laboratory. The slides with trichodinid

Address for correspondence: Ghazi S. M. Asmat, Department of Zoology, University of Chittagong, Chittagong 4331, Bangladesh; Fax: 880-31-726310; E-mail: asmat@globalctg.net

ciliophorans were impregnated with Klein's dry silver impregnation technique (Klein 1958). Examinations of prepared slides were made under the Olympus phase-contrast microscope at x100 magnification. Measurements were made according to the recommendations of Lom (1958), Wellborn (1967), Arthur and Lom (1984) and Van As and Basson (1989, 1992).

RESULTS

Trichodina porocephalusi sp. n. (Figs 1-16, Table 1)

This is a medium-sized and bell-shaped trichodinid, 32.5-50.5 (42.3 ± 5.2) µm, having unique adhesive disc surrounded by a finely striated border membrane. The centre of the disc is argentophobic, somewhat elevated from the rest of the disc (Fig. 8), contains few to many argentophilic dots or patches and surrounded by undulated or notched border. The denticulate ring consists of 20-27 (24.3 ± 1.5) rectangular, medium-sized denticles. The interblade space is medium. The number of radial pins per denticle is 6-9 (7.4 ± 1.0).

Typically, the blade is broad and rectangular. The distal margin is truncated, runs parallel to the border membrane or slightly curved. The gap between the distal margin of blade and border membrane is moderate to large. The tangent point is blunt, rarely forms a line with y-axes, situated lower than the distal margin. The anterior margin angularly curves down and forms a shallow apex at the base of blade that rarely extends beyond the y+1 axis (Figs 9-12). A notch is present just below the apical cone in the anterior margin. The anterior blade apophysis is sometimes prominent (Figs 3-6). The curve of posterior margin forms a shallow crescent with deepest point at the same level as apex (Figs 9-12). The posterior blade apophysis is absent. The blade connection is thin.

The central part of denticle is robust, wide and sharply triangular. The tip rarely extends halfway past the y-1 axis and interposed firmly into the preceding denticle (Figs 9-12). Shapes of the central part above and below the x-axis are similar. Indentation on the lower central part sometimes prominent (Figs 4, 6).

The ray connection is short and broad bearing distinct ray apophysis directed antero-distally (Figs 1-8). The ray is much shorter than the blade, stumpy, crooked at the base, broad with prominent central groove and slightly bent in backward direction. Lateral margins of the ray are parallel, ending in a round or truncated point that almost touches the y-1 axis (Figs 10-12). The space between the tip of ray and the central clear area forms a narrow impregnated ring.

The adoral zone of cilia spirals about 380-390°.

Intraspecific variability

Remarkable variation in the denticle morphology was recorded in the present study. Based on the denticle shape three types of specimens could be identified. These are designated here as Type I, Type II and Type III.

In Type I, the blades are larger, robust with crescent-shaped blade and shorter and slightly arched ray. In these cases the ray base is barely distinguishable from the central part (Fig. 1). These ciliates are big in size.

In Type II, the blade is elongated, sickle-shaped with more or less parallel borders, relatively longer rays and distinct ray connection (Fig. 2). These are medium sized trichodinid.

In Type III, the denticle consists of more slender and shorter blades with parallel margins and truncated distal margin and more arched and slender rays (Figs 3-8). These are small sized members of this species. The specimens of Type III were found to be greater in number in each population, while Type I was rather rare. Whether these variations are due to adaptation of trichodinids to face unfavorable condition in host body or related to the age of individual specimens or to the seasons of the year or other reasons are matter of future studies. All the types mentioned above were found not only in the same population but also on the same host fish on many occasions.

Type host: *Ophiocara porocephalus* (Valenciennes) (Eleotrididae).

Type locality: Hooghly River (Latitude 22°00'N, Longitude 88°07'E) of Hooghly District, West Bengal, India.

Location: gills.

Etymology: named after the specific name of the host fish, *Ophiocara porocephalus* (Valenciennes).

Type specimens: holotype, slide OP-1 prepared on 05-10-1996; paratypes, slide OP-2 prepared on 05-10-1996 and slide OP-3 prepared on 15-1-1997 are in the collection of the Department of Zoology, University of Chittagong, Chittagong 4331, Bangladesh.

DISCUSSION

The centre of the adhesive disc in the described species possesses an undivided clear area with a rounded

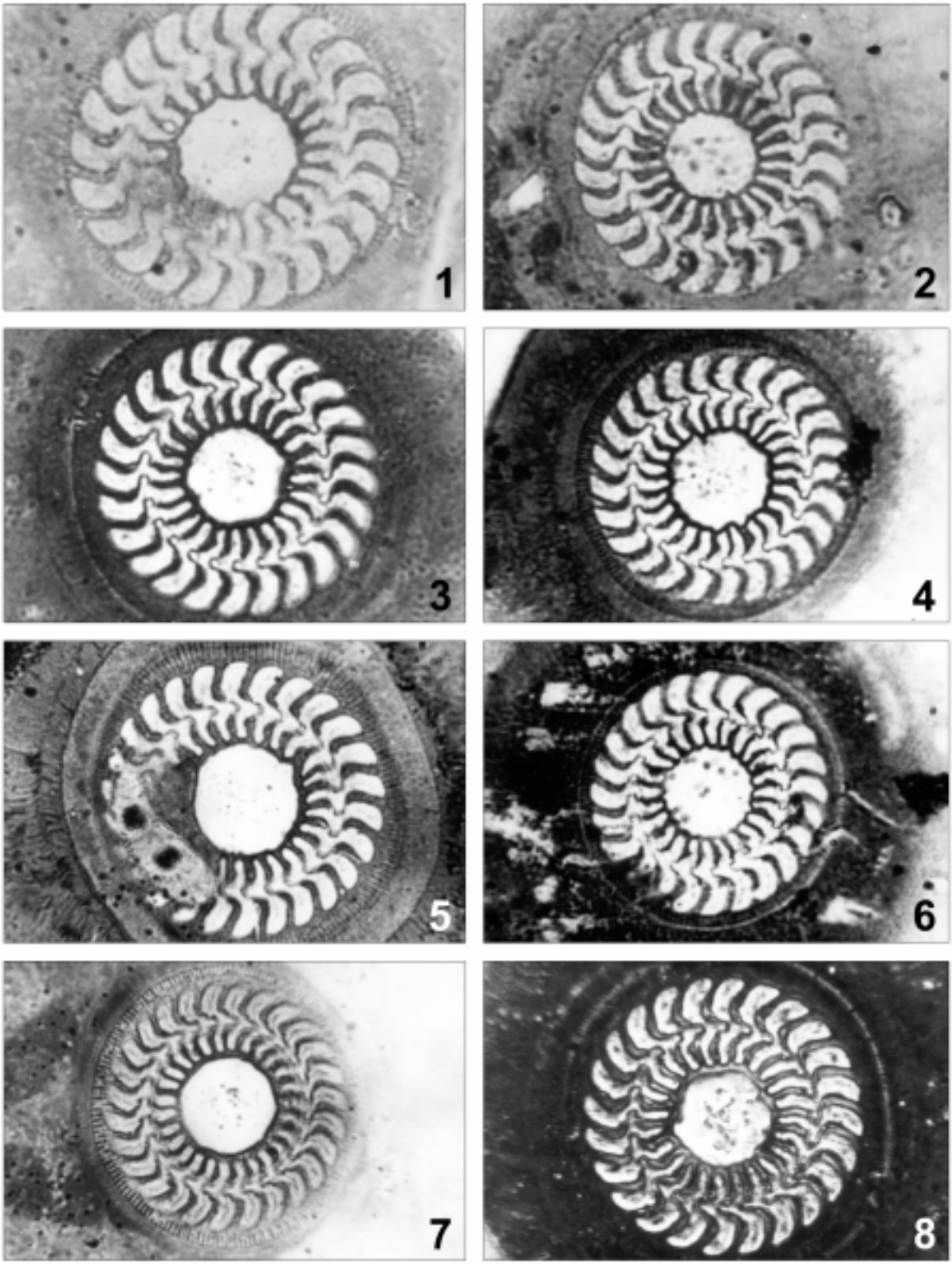

Figs 1-8. Photomicrographs of *Trichodina porocephalusi* sp. n. from *Ophiocara porocephalus* showing the variation in the structure of denticle

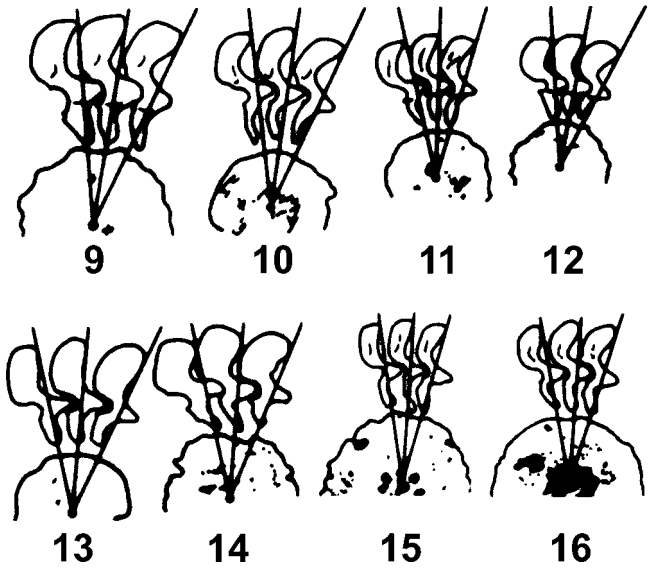

Figs 9-16. Diagramatic drawings of denticles of trichodinids. **9-12 -** *Trichodina porocephalusi* sp. n. from India; **13, 14 -** *T. jadranica noblei* Lom, 1970 redrawn from Lom (1970); **15, 16** -*Trichodina* sp. 2 of Grupcheva *et al*. (1989) redrawn from Grupcheva *et al*. (1989)

or slightly notched perimeter containing a few to a large number of dark granules, which rarely form patches. Based on this character and the unique shape and variability of the denticles among the silver impregnated specimens of the present species, it may be said that to a lesser extent, it resembles *T. jadranica noblei* Lom, 1970 and *Trichodina* sp. 2 of Grupcheva *et al.* (1989).

Lom (1970) described *T. jadranica noblei* from the gills of a marine fish, *Eleotris sandwicensis* in Oahu, Hawaii. The character of central clear area in some specimens of the presently studied species with clumps of irregular dark materials in the middle (Figs 6, 8) is similar to *T. j. noblei* but the denticle morphology distinctly differs in two species. The shape of blade in *T. j. noblei* is somewhat broad, oval, and shorter than the ray (Figs 13, 14). The ray is almost straight in *T. j. noblei* (Fig. 13). Lom (1970) mentioned his Fig. 2 of Plate V (Fig. 14 in the present paper) as an atypical specimen. The shape of denticle in the species under discussion is significantly different from that of *T. j. noblei* in having considerably larger denticles with rather rectangular blades, backwardly bent rays, which are almost half of the size of blade. The two species also differs in morphometrical data (Table 1).

In considering the shape of denticles, the members of the specimens of Type II in the present work having denticles with elongated, sickle-shaped blades and relatively longer rays are somewhat similar to *Trichodina* sp. 2 of Grupcheva *et al.* (1989) as shown by them in Figs 1A, B. They collected the specimens from the gills of the Mediterranean *Gobius niger. Trichodina* sp. 2 differs from the presently studied trichodinid in lacking of distinct notch at the anterior margin and truncated tip of

Table 1. Morphometric (in µm) comparison of *Trichodina porocephalusi* sp. n. with *T. jadranica noblei* Lom, 1970 and *Trichodina* sp. 2 of Grupcheva *et al*. (1989)

Species	*Trichodina jadranica noblei*	*Trichodina* sp. 2 (n=31)	*Trichodina porocephalusi* sp. n. (n=20)
Host	*Eleotris sandwicensis*	*Gobius niger*	*Ophiocara porocephalus*
Locality	Oahu, Hawaii	Mediterranean, Banyuls, France	Hooghly, West Bengal, India
Location	Gills	Gills	Gills
References	Lom (1970)	Grupcheva *et al*. (1989)	Present paper
Diameter of body	26 - 40 (32)	63-110 (79)	32.5-50.5 (42.3 ± 5.2)
of adhesive disc	21- 29 (25)	41-61 (51)	27.0-42.3 (35.2 ± 4.8)
of denticulate ring	13 - 17 (14)	25-38 (32)	16.3-26.0 (20.9 ± 2.8)
of central area	-	-	7.1-17.4 (12.4 ± 2.6)
of clear area	-	-	6.1-15.3 (10.4 ± 2.5)
Width of border membrane	2.5	4.8-5.8	2.0-4.8 (3.5 ± 0.7)
Number of denticles	21 - 25 (23)	28-32 (30)	20-27 (24.3 ± 1.5)
of radial pins/denticle	6	8-9	6-9 (7.4 ± 1.0)
Span of denticle	-	-	8.2-10.7 (9.7 ± 0.7)
Length of denticle	4	3.8-6.7 (5.5)	2.5-5.6 (4.7 ± 0.8)
of ray	2.5-3	3.8-5.8 (4.6)	2.5-4.1 (3.0 ± 0.5)
of blade	2	4.3-6.7 (5.7)	3.1-5.1 (4.2 ± 0.6)
Width of central part	1.2	1.9-3.4 (2.4)	1.5-3.1 (2.5 ± 0.6)
Degree of adoral ciliature		-	380-390^0

blade, ray apophysis and in having not much variation in the shape of denticles, and rays sometimes having slightly broadened tips. The clear central area of *Trichodina* sp. 2 is larger than the present species and contains dense black patches at the centre (Figs 15, 16). The described species also differs from *Trichodina* sp. 2 in having the smaller diameter of the adhesive disc and the denticulate ring as well as in the denticle dimensions (Table 1).

Acknowledgements. The work was carried out in the Department of Zoology, University of Kalyani, West Bengal, India. The author is grateful to Mr. Saugata Basu, Assistant Master, Uttarpara Govt. High School, Hooghly 712258, West Bengal, India for his help in collecting the host fishes on several occasions. I am indebted to Professor Qamar Banu, Department of Zoology, University of Chittagong for useful advice in improving the manuscript.

REFERENCES

Arthur J. R., Lom J. (1984) Trichodinid Protozoa (Ciliophora: Peritrichida) from freshwater fishes of Rybinsk Reservoir, USSR. *J. Protozool.* **31:** 82-91

Asmat G. S. M. (2001a) *Trichodina cancilae* sp. n. (Mobilina: Trichodinidae) from the gills of a freshwater gar, *Xenentodon cancila* (Hamilton) (Belonidae). *Acta Protozool.* **40:** 141-146

Asmat G. S. M. (2001b) *Trichodina canningensis* sp. n. (Ciliophora: Trichodinidae) from an Indian estuarine fish, *Mystus gulio* (Hamilton) (Bagridae). *Acta Protozool.* **40:** 147-151

Asmat G. S. M., Haldar D. P. (1998) *Trichodina mystusi*- a new species of trichodinid ciliophoran from Indian estuarine fish, *Mystus gulio* (Hamilton). *Acta Protozool.* **37:** 173-177

Das M. K., Haldar D. P. (1987) Urceolariid ciliates of the genus *Tripartiella* invading gills of freshwater cultured carps in India. *Arch. Protistenkd*. **134:** 169-178

Das M. K., Pal R. N., Das P. B. (1987) Preliminary observations on the ecology of animal parasites in estuarine fishes of Deltaic West Bengal. *J. Indian Soc., Coastal Agric. Res.* **5:** 319-323

Grupcheva G., Lom J., Dykova I. (1989) Trichodinids (Ciliata: Urceolariidae) from gills of some marine fishes with the description of *Trichodina zaiki* sp. n. *Folia Parasitol*. **36:** 193-207

Hagargi S. S., Amoji S. D. (1979) Occurrence of *Trichodina pediculus* Ehrenberg 1838 on freshwater carps, *Barbus* spp. *Curr. Sci*. **48:** 789-790

Klein B. M. (1958) The dry silver method and its proper use. *J. Protozool*. **5:** 99-103

Lom J. (1958) A contribution to the systematics and morphology of endoparasitic trichodinids from amphibians, with a proposal of uniform specific characteristics. *J. Protozool*. **5:** 215-263

Lom J. (1970) Trichodinid ciliates (Peritricha, Urceolariidae) from some marine fishes. *Folia Parasitol*. **17:** 113-125

Mishra R. K., Das M. K. (1993) Urceolariid ciliate, *Trichodina reticulata* infesting gills of *Catla catla* in India. *J. Inland. Fish. Soc. India*. **25:** 54-56

Mukherjee M., Haldar D. P. (1982) Observations on the urceolariid ciliates of the genera *Trichodina* and *Tripartiella* in freshwater teleosts. *Arch. Protistenkd.* **126:** 419-426

Saha B. S., Haldar D. P. (1996) First record of *Tripartiella bursiformis* (Davis, 1947) Lom, 1959 (Protozoa: Urceolariidae) from the gills of *Xenentodon cancila* (Hamilton) in the Indian subcontinent. *J. Beng. Nat. Hist. Soc. (NS*) **15:** 11-17

Saha B. S., Haldar D. P. (1997) Observations on the urceolariid ciliates of the genus *Tripartiella* Lom, 1959 parasitising the gills of three freshwater edible fishes of West Bengal, India. *J. Inland Fish. Soc. India* **29:** 28-36

Saha B. S., Bandopadhyay P. K., Haldar D. P. (1995a) Biodiversity of trichodinid ciliates in freshwater fishes of West Bengal. *Environ. Ecol.* **13:** 814-823

Saha B. S., Bandopadhyay P. K., Haldar D. P. (1995b) First record of *Paratrichodina* sp. (Protozoa: Urceolariidae) from the gills of *Notopterus notopterus* (Pallas) from the Indian subcontinent. *J. Beng. Nat. Hist. Soc. (NS)* **4:** 35-42

Van As J. G., Basson L. (1989) A further contribution to the taxonomy of the Trichodinidae (Ciliophora: Peritrichida) and a review of the taxonomic status of some fish ectoparasitic trichodinids. *Syst. Parasitol*. **14:** 157-179

Van As J. G., Basson L. (1992) Trichodinid ectoparasites (Ciliophora: Peritrichida) of freshwater fishes of the Zambesi River system, with a reappraisal of host specificity. *Syst. Parasitol*. **22:** 81-109

Wellborn T. L., Jr. (1967) *Trichodina* (Ciliata: Urceolariidae) of freshwater fishes of the Southern United States. *J. Protozool*. **14:** 399-412

Received on 13th February, 2001; accepted on 30th August, 2001

Acta Protozool. (2001) 40: 303 - 309

ACTA
PROTOZOOLOGICA

Three New Species of Gregarines (Apicomplexa: Sporozoea: Porosporidae) in the Estuarine Crabs from Kerala, India

Puthampurayil K. PRASADAN[1] and Kuniyil P. JANARDANAN[2]

[1]Department of Zoology, Mary Matha Arts & Science College, Vemom (P.O.), Mananthavady; [2]Parasitology Laboratory, Department of Zoology, University of Calicut, Kerala, India

Summary. Different development stages of 3 new species of cephaline gregarines, *Nematopsis messor, N. quadratum* and *N. annulipes* infecting the crabs, *Metapograpsus messor* (Forskäl), *Sesarma quadratum* (Fabricius) and *Uca annulipes* Edwards respectively are described and their systematic position discussed.

Key words: crabs, gregarines, *Metapograpsus messor, Nematopsis annulipes* sp. n., *N. quadratum* sp. n., *N. messor* sp. n., *Sesarma quadratum, Uca annulipes.*

Abbreviations: DW - deutomerite width, LA - length of association, PL - protomerite length, PW - protomerite width, TL - total length.

INTRODUCTION

All cephaline gregarines known to inhabit crabs are included in only 4 genera: *Nematopsis* Schneider, 1892; *Cephaloidophora* Mavrodiadi, 1908; *Pachyporospora* Théodoridès, 1961 and *Stephanospora*, Prema and Janardanan, 1989. Extensive survey of estuarine crabs in Kerala revealed the presence of 3 species of cephaline gregarines belonging to the genus *Nematopsis.* Detailed studies proved that they represent new species. The present paper provides their description.

Address for correspondence: Puthampurayil K. Prasadan, Department of Zoology, Mary Matha Arts & Science College, Vemom (P.O.), Mananthavady-670645, Kerala, India; E-mail: drprasadan@yahoo.co.in

MATERIALS AND METHODS

The crabs, *Metapograpsus messor* (Forskäl), *Sesarma quadratum* (Fabricius) and *Uca annulipes* Edwards, collected from sandy and rocky shores of estuaries and river banks in Kerala, were examined for the presence of gregarine parasites. The carapace of each crab was removed, the alimentary tract was then transferred onto a slide and examined for gregarines. Trophozoites and sporadins were recovered from the midgut and gametocyts from the hindgut or from fecal matter. Gametocysts recovered at various stages of development were maintained in moist chamber for further development. The cysts completed development and extruded spores by simple rupture of the cyst wall in 24 h.

Structural details of development stages were studied following the method reported by Prema and Janardanan (1989). Illustrations were made with the aid of a camera lucida; descriptions and measurements are based on a minimum of 20 live specimens. All measurements are in micrometers (μm); mean values are underlined.

Types of all parasites (stained specimens on slides) and their host crabs are deposited in the parasite collections, Parasitology Laboratory, Department of Zoology, University of Calicut, Kerala (India).

RESULTS

Nematopsis messor sp. n. (Fig. 1, Table 1)

Description

Sporadins (Fig.1.1): biassociative; association caudofrontal; colour milky-white. Syzygy early, linear.

Primites: protomerite shape hemispherical, wider than long, maximum width at posterior end; transparent lens-shaped structure present at anterior end; epicyte uniformly thick, striated; endocyte granular. Septum circular, convex toward deutomerite; constriction at septum inconspicuous. Deutomerite ovoid, narrow behind septum, gradually widens caudally, posterior end broadly rounded; maximum width in posterior half; epicyte uniformly thick; endocyte granular. Nucleus spherical, faintly visible in fresh sporadins, variable in position; endosome single, spherical.

Satellites: lengths on average slightly shorter than primites. Protomerite shape hemispherical, wider than long; epicyte uniformly thick, striated; endocyte granular with transparent lens-shaped structure at anterior end. Septum similar to primite (see above). Deutomerite ovoid, narrow behind septum, gradually widens caudally, posterior end broadly rounded; maximum width at posterior half. Nucleus and endosome similar to primite (see above).

Gametocysts (Fig. 1.2): shape spherical; colour milky-white. Cyst wall double; epicyst thick, hyaline, width uneven, 6.6-11.5; endocyst thin, width uniformly even, 1.6.

Gymnospores (Fig. 1.3): shape spherical; diameter 4.5-5.3; uninucleated bodies arranged radially in rosette pattern around central, hyaline cytoplasm.

Trophozoites (Figs 1.4-1.6): development extracellular. Smallest observed trophozoite (Fig. 1.4) has a hemispherical protomerite and ovoid deutomerite. In an association measuring 129.6 long (Fig. 1.6), the primite measured 70.7 by 37.1 and satellite 58.6 by 37.1.

Taxonomic summary

Type specimens: syntypes, No.Z/Par/G/101; deposited in the parasite collections, Parasitology Laboratory, Department of Zoology, University of Calicut, Kerala, India.

Type host: *Metapograpsus messor* (Forskäl) (Arthropoda: Crustacea: Grapsidae). Symbiotype: host crab preserved in the Parasitology Laboratory (see address above). Additional hosts: None.

Type locality: India, Kerala, Malppuram district, Kadalundi Estuary, sandy and rocky intertidal. Additional localities in India: Kannur district, Mavilayi and Muzhappilangad; Kozhikode district, Iringal and Kizhariyur (all sandy and rocky river banks).

Collection dates: 1988 (February, March, November, December); 1989 (October through December); 1990 (January through April).

Site of infection: intestine.

Prevalence: in 8 of 22 crab hosts examined.

Etymology: named after the species of crab host.

Remarks

Nematopsis messor sp. n. resembles most to *N. raoudi* Vivárès, 1971 from the crab *Portunus latipes*. However, it differs in several significant ways, including the shape of primites and satellites; and in the presence of (1) a prominent lens-shaped structure at the anterior part of the protomerite, (2) a spherical nucleus and (3) a protomerite in the satellites. In addition, the species described above is from a different host and a different geographical locality. This is the first report of gregarines from *Metapograpsus messor* (Forskäl).

Nematopsis quadratum sp. n. (Fig. 2, Table 1)

Description

Sporadins (Fig. 2.1): biassociative, association caudofrontal; colour milky-white. Syzygy early, linear.

Primites: always larger than satellites. Protomerite shape hemispherical with a plano-convex to biconvex lens-shaped structure at anterior part; epicyte uniformly thick, striated; endocyte granular. Septum circular, convex toward deutomerite. Deutomerite elongate ovoid, narrow behind septum gradually widens caudally, posterior end broadly rounded; maximum width in posterior half; epicyte hyaline; endocyte granular; a transparent lens-shaped structure at posterior part. Interlocking mechanism between primite and satellite well developed. Nucleus spherical to ovoid.

Satellites: protomerite and septum similar to that of primite (see above). Deutomerite widest behind septum, gradually tapers caudally, posterior end rounded. Nucleus

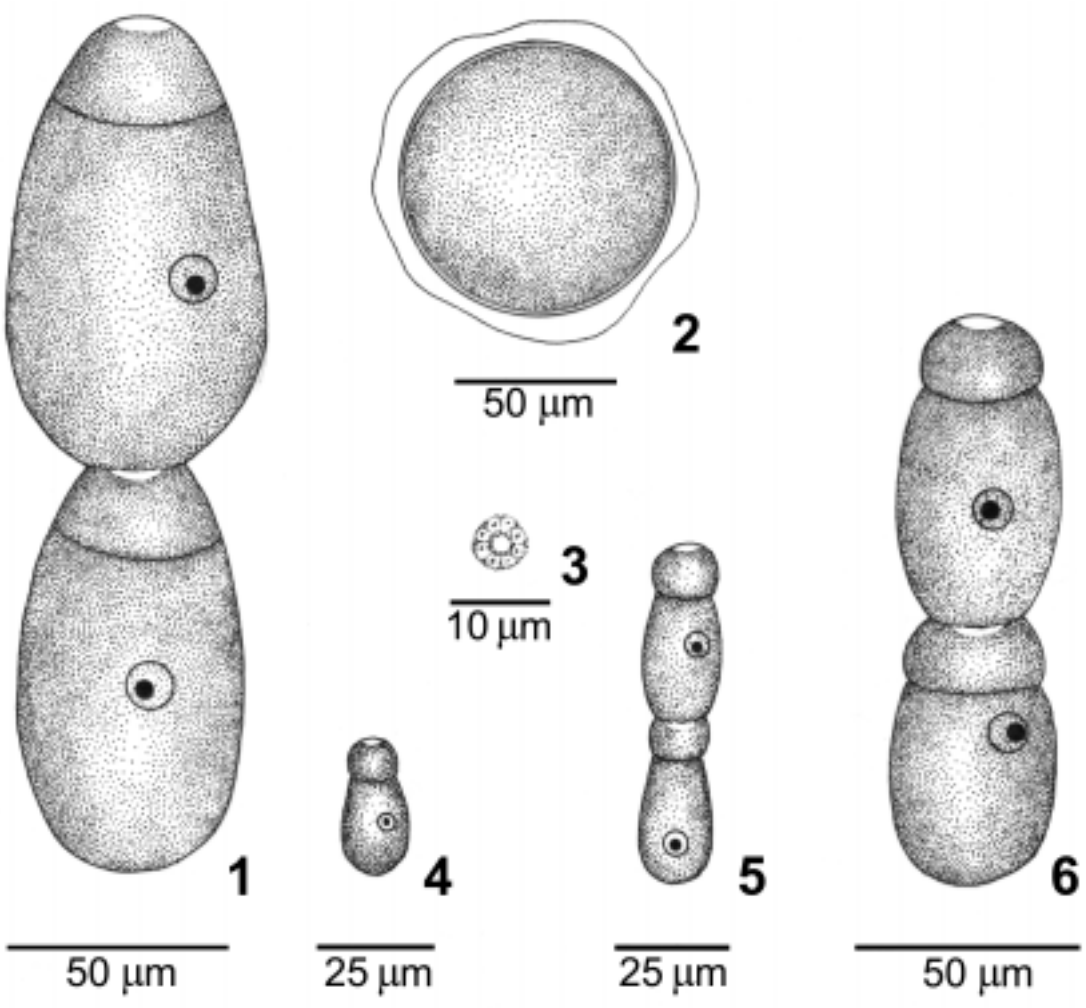

Figs 1.1-1.6. *Nematopsis messor* sp. n.; **1.1** - sporadins; **1.2** - gametocyst; **1.3** - gymnospore; **1.4** - early trophozoites; **1.5, 1.6** - early associations. Scale bars - **1.1, 1.2, 1.6** - 50 µm; **1.4, 1.5** - 25 µm ; **1.3** - 10 µm

spherical to ovoid, faintly visible in fresh sporadins, variable in position; endosome single, round to ovoid.

Gametocysts (Fig. 2.2): shape spherical; colour milky-white, opaque. Cyst wall double; epicyst thick, hyaline, width uneven, 20.4 - 40.

Gymnospores (Fig. 2.3): shape spherical; diameter 7.5; uninucleated bodies arranged radially in rosette pattern around central, hyaline cytoplasm.

Trophozoites: development extracellular. Smallest observed trophozoite (Fig. 2.4) has a hemispherical, protomerite and cylindrical deutomerite. Largest observed trophozoite was elongate, almost cylindrical, with hemispherical protomerite and elongated deutomerite.

Taxonomic summary

Type specimens: syntypes; No.Z/Par/G/102; deposited in the parasite collections, Parasitology Laboratory, Department of Zoology, University of Calicut, Kerala, India.

Type host: *Sesarma quadratum* (Fabricius) (Arthropoda: Crustacea: Grapsidae). Symbiotype: host crab preserved in the Parasitology Laboratory (see address above). Additional host: none.

Type locality: India, Kerala, Malappuram district, Olippuram rocky river banks. Additional localities in India: Kannur district, Mavilayi and Muzhappilangad; Kozhikode district, Feroke and Ramanattukara;

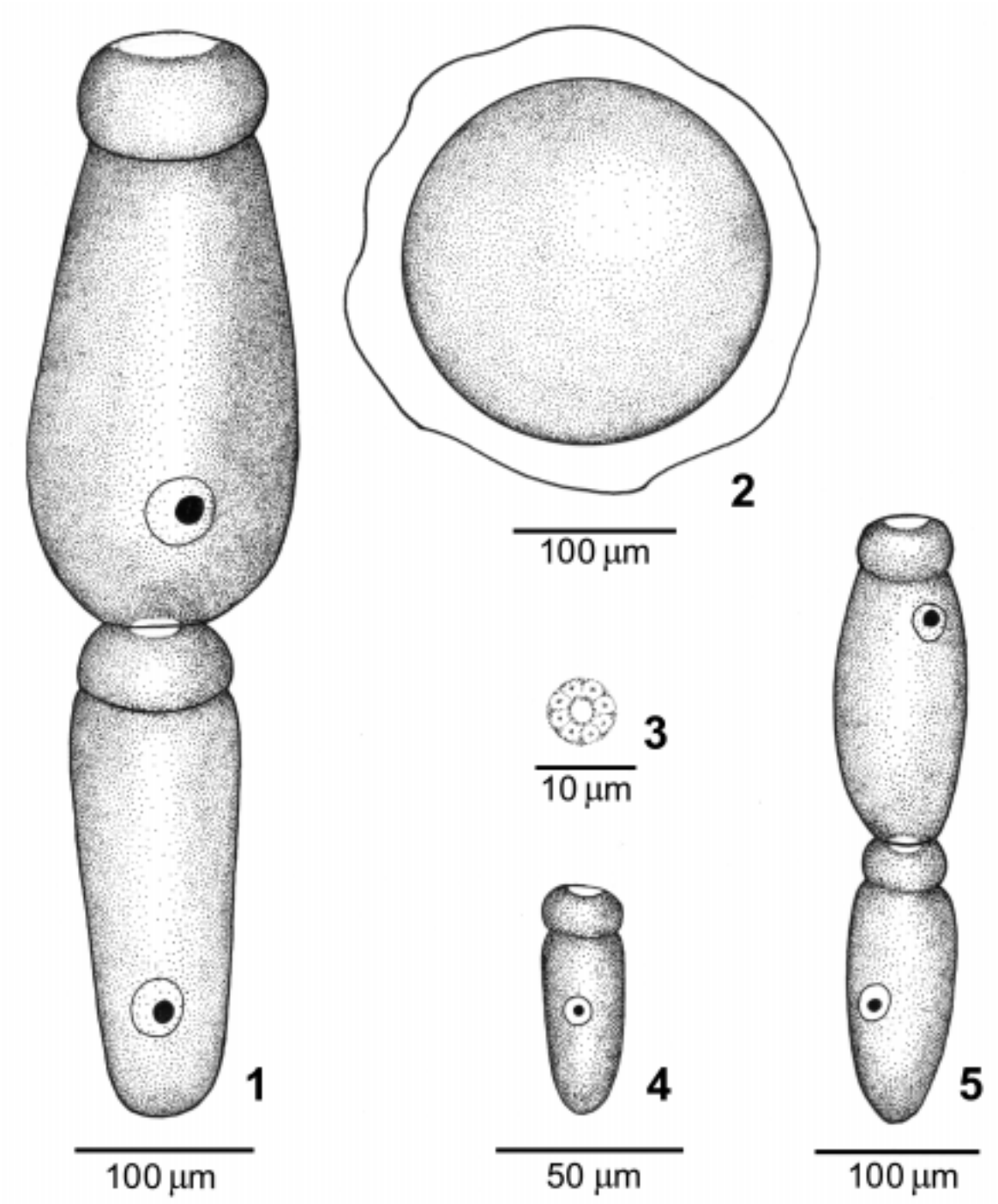

Figs 2.1-2.5. *Nematopsis quadratum* sp. n.; **1.1** - sporadins; **1.2** - gametocyst; **1.3** - gymnospore; **1.4** - early trophozoites; **1.5 -** early association. Scale bars - **1.1, 1.2, 1.5** - 100 µm; **1.4** - 50 µm; **1.3** - 10 µm

Malappuram district, Vazhakkad (all rocky and sandy river banks) and Ernakulam district, Vallarpadam sandy and rocky intertidal.

Collection dates: 1988 (February - March); 1989 (October through December); 1991 (January through April).

Site of infection: intestine.

Prevalence: in 6 of 31 crab hosts examined.

Etymology: named after the species of crab host.

Remarks

Nematopsis quadratum sp. n. does not resemble any known species of *Nematopsis*. In comparison with

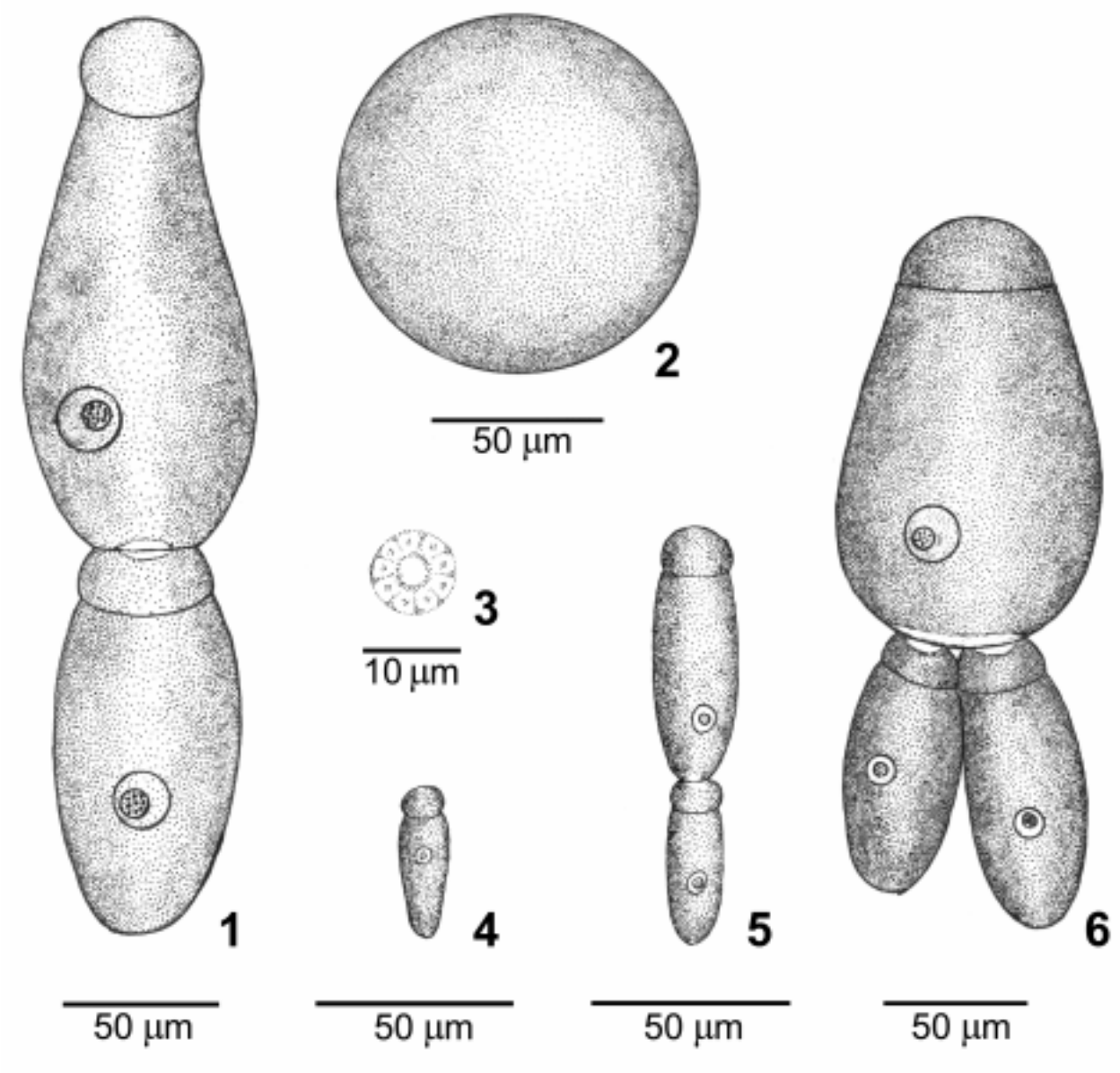

Figs 3.1-3.6. *Nematopsis annulipes* sp. n.; **1.1** - sporadins; **1.2** - gametocyst; **1.3** - gymnospore; **1.4** - early trophozoites; **1.5 -** early association; **1.6** - association of three sporadins. Scale bars - **1.1, 1.2, 1.4-1.6 -** 50 µm; **1.3** - 10 µm

Nematopsis messor sp. n. (see above) it differs in having (1) larger sporadins, trophozoites, gametocysts and gymnospores, (2) a lens-shaped granule-free structure at the posterior part of primite deutomerite and (3) spherical to ovoid nucleus. The present species is recovered from a different host and this forms the first report of a cephaline gregarine from *Sesarma quadratum* (Fabricius).

***Nematopsis annulipes* sp. n. (Fig. 3, Table 1)**

Description

Sporadins (Fig. 3.1): biassociative, association caudofrontal; colour milky-white. Syzygy early, linear; occasionally two satellites in syzygy with a primite.

Primites: protomerite shape subspherical to ovoid; epicyte uniformly thick, striated; endocyte granular. Sep-

Table 1. Measurements and ratios of three new species of gregarines of the genus *Nematopsis* found in estuarine crabs in Kerala, India. All measurements taken from fresh specimens; means are underlined

Measurements	*N. messor*	*N. quadratum*	*N. annulipes*
Association Length	114-140.9-178	404-492.7-678	213-259.9-317
Primites:			
Total length	59-72.7-94	177-285.3-370	86-138.4-185
Deutomerite width	30-40.3-58	89-128.1-162	38-59-94
Protomerite length	13-18.6-23	50-59.7-69	17-28.5-36
Protomerite width	23-34-43	54-90.8-121	33-39.9-56
Ratio: PL:TL	1 : 3.9	1 : 4.8	1 : 4.9
Ratio: PW : DW	1 : 1.2	1 : 1.4	1 : 1.5
Satellites:			
Total length	51-68-86	152-207.3-308	101-121.4-147
Deutomerite width	25-33.9-46	50-83.1-117	26-49.2-79
Protomerite length	13-16-20	30-41-56	17-22.1-30
Protomerite width	18-29.9-40	50-74.1-102	25-36.3-43
Ratio: PL : TL	1 : 4.3	1 : 5.1	1 : 5.5
Ratio: PW : DW	1 : 1.1	1 : 1.1	1 : 1.3
Gametocyst (Diameter)	54-66.7-86	139-206.4-246	112-115.5-119
Gymnospore (Diameter)	4.5-5.3	7.5	9
Trophozoites:			
Smallest observed:			
Length:	31.3	56.1	37.1
Protomerite length	9.9	13.2	7.4
Deutomerite length	21.4	42.9	29.7
Largest observed:			
Length:	103.9	300	140
Protomerite length	28	62	28
Deutomerite length	75.9	238	112
Smallest observed			
Association Length:	75.9	385	107
Primite length	39.6	200	66
Satellite length	36.3	185	41

tum circular, convex toward deutomerite. Deutomerite narrow behind septum gradually dilates caudally, posterior end broadly round or flat; epicyte longitudinally striated; endocyte granular with a transparent lens-shaped structure at posterior end. Nucleus spherical, variable in position; endosome single, spherical, contains 8-12 granules.

Satellites: protomerite shape rectangular, broader than long; anterior margin flat; deutomerite shape elongate ovoid, which is widest at the middle; epicyte uniformly thick; endocyte granular. Nucleus and endosome similar to primite (see above).

Association of 3 sporadins (Fig. 3.6): two satellites in syzygy with a primite. Primite ovoid, measured 151.8; one satellite 87.5 and the other satellite 102.3 in length.

Gametocysts (Fig. 3.2): shape spherical to ovoid; colour milky-white; cyst wall single, hyaline.

Gymnospres (Fig. 3.3): shape spherical, uninucleated bodies arranged radially in a rosette pattern around a central, hyaline cytoplasm.

Trophozoites: development extracellular. Smallest observed trophozoite (Fig. 3.4) narrow, elongate ovoid.

Taxonomic summary

Type specimens: syntypes; No. Z/Par/G/103; deposited in the parasite collection, Parasitology Laboratory, Department of Zoology, University of Calicut, Kerala, India.

Type host: *Uca annulipes* Edwards (Arthropoda: Crustacea: Ocypodidae). Symbiotype: host crabs preserved in the Parasitology Laboratory (see address above). Additional host: none.

Type locality: India, Kerala, Malappuram district, Olippuram River, muddy and sandy shores. Additional localities in India: Kannur District, Mavilayi and

Muzhappilangad; Kozhikode district, Chaliyam and Malappuram district, Ramanattukara Kadalundi and Vazhakkad (all sandy and muddy river banks).

Collection dates: 1988 (February-March); 1989 (October through December); 1991 (January through April).

Site of infection: intestine

Prevalence: in 9 of 44 crab hosts examined.

Etymology: named after the species of crab host.

Remarks

Nematopsis annulipes recovered from *Uca annulipes* Edwards, also does not resemble any known species in the genus that have been described from crabs. In some characters it superficially resembles *Nematopsis quadratum* sp. n. (see above). From a comparative study of characters, it is evident that unlike *N. quadratum* the present form has (1) subspherical to ovoid primite protomerite without lens-shaped structure, (2) elongate ovoid satellite deutomerite which is widest at the middle, (3) spherical nuclei, (4) spherical to ovoid and single walled gametocysts and (5) larger gymnospores.

DISCUSSION

Cephaline gregarines infecting crabs are grouped into two families, namely the Porosporidae Labbé, 1899 and Cephaloidophoridae Kamm, 1922. The gregarines recovered from estuarine crabs in the present study have extracellular development and their gametocysts formed gymnospores. These characters warrant placing the gregarines in the family Porosporidae. Members of the Porosporidae are heteroxenous and molluscs are the only known intermediate hosts. Sporogonic development in the intermediate hosts of many species remains unknown. In cases where sporogony is unknown generic placement is based on the morphology of vegetative stages in the digestive tract of crustacean hosts. Molluscan hosts of the present gregarines could not be discovered even after repeated attempts. Hence generic designation was based on the morphology of the trophozoites, sporadins and gymnospores. The family Porosporidae includes four genera, *Porospora, Nematopsis, Pachyporospora* and *Stephanospora.* Amongst these the genus *Porospora* has not been reported from crabs. Trophozoites and sporadins of the present gregarines do not resemble either *Pachyporospora* or *Stephanospora* but bear the requisite characters of *Nematopsis* and are, therefore, assigned to this genus.

Acknowledgements. The authors express their sincere thanks to Dr. Maya deb, (Zoological Survey of India, Kolkatta) for taxonomic identification of host specimens. The University Grants Commission, New Delhi provided the financial assistance in the form of a major research grant (F-3-79/86 SR II).

REFERENCES

Mavrodiadi P.A. (1908) The barnacles of the Black Sea and their gregarine parasites. Preliminary note. *Zapiski Novoross. Obsh. Estestrois.* **32:** 101-132

Prema S., Janardanan K. P. (1989) Observations on *Stephanospora paratelphusae* gen. n., sp. n. (Apicomplexa: Cephalina) from the freshwater crab, *Paratelphusa hydrodromous* (Herbst). *Acta Protozool*. **28:** 303-310

Schneider A. (1892) Signalement d'un nouvean sporozoaire. *Tabl. Zool.* **2:** 209-210

Théodoridès J. (1961) Sur la distinction entre les grégarines des familles des Cephaloidophoridae et des Porosporidae parasites des crustacés décapodes. *C. R. Acad. Sci*. **252:** 3640-3642

Vivárès C. P. (1971) Les grégarines Porosporidae parasites des crustacés décapodes brachyoures Méditerranéens. *Vie Milieu* **22:** 55-68

Received on 19th March, 2001; accepted on 30th August, 2001

Acta Protozool. (2001) 40: 311 - 315

ACTA
PROTOZOOLOGICA

Short Communication

Light Regulation of Protein Phosphorylation in *Blepharisma japonicum*

Hanna FABCZAK, Bożena GROSZYŃSKA and Stanisław FABCZAK

Department of Cell Biology, Nencki Institute of Experimental Biology, Polish Academy of Sciences, Warszawa, Poland

Summary. We demonstrate alterations in protein phosphorylation levels in light-exposed *Blepharisma* using immunological and densitometric methods. The examinations show that cell illumination elicited a two-fold enhancement of phosphorylation of a 46 kDa protein and a marked decrease in the phosphorylation of a 28 kDa protein over that measured in dark-adapted cells. The observed light-dependent changes in the phosphorylation levels of both proteins were entirely reversible. In contrast, no alteration in protein phosphorylation was detected in cells treated by external potassium, which depolarizes the cell membrane. These observations suggest that both the 28 kDa and 46 kDa proteins might be involved in the light transducing mechanism, which results in the photophobic response of *Blepharisma.*

Key words: *Blepharisma japonicum,* ciliate, phosphorylation and dephosphorylation, phosphoserine, phosphoprotein, photophobic response, phototransduction.

INTRODUCTION

The ciliate *Blepharisma japonicum* possess a photoreceptor system that renders the cells capable of avoiding light. The pigment granules located just beneath the plasma membrane, containing pink-colored quinones - blepharismin, are believed to function as the photosensor units of the cellular light-sensitive system (Giese 1973, Tao *et al.* 1994, Maeda *et al*. 1997, Song 1997a, Matsuoka *et al*. 2000). On account of this feature, the ciliates exhibit photodispersal as they tend to move predominantly toward shady or dark regions (Mast 1906, Fabczak H. 2000a). The light-avoiding behavior of *Blepharisma japonicum* results largely from their motile behavior (step-up photophobic response) to a sudden increase in light intensity (Kraml and Marwan 1983). During prolonged intense illumination, an increase in forward movement (positive photokinesis) and a marked elongation of the cell body also occur (Kraml and Marwan 1983, Ishida *et al.* 1989). The cell photophobic response consists of a delayed cessation of forward swimming, a period of backward movement (ciliary reversal) followed by restoration of forward swimming, usually in an altered direction (Fabczak H. *et al.* 1993, Fabczak S. *et al.* 1993). The ciliary reversal during photophobic response is mediated by a Ca^{2+}/K^{+} action potential elicited by the light-induced receptor potential (Fabczak S. *et al.* 1993). The photoreceptor system in *Blepharisma japonicum* seems to be coupled to membrane potential and photomotile changes *via* a sensory transduction pathway (Fabczak H. *et al.* 1993,

Address for correspondence: Hanna Fabczak, Department of Cell Biology, Nencki Institute of Experimental Biology, Polish Academy of Sciences, ul. Pasteura 3, 02-093 Warszawa, Poland; Fax: (4822) 8225342; E-mail: hannafab@nencki.gov.pl

Song 1997b). It involves, as is the case in invertebrate or vertebrate photoreceptor cells (Rayer *et al.* 1990), cGMP and inositol trisphosphate as the possible second messengers (Fabczak H. *et al.* 1993, 1998, 1999; Fabczak H. 2000b).

One of the most important mechanisms in the regulation of cellular metabolism or cell function is the process of protein phosphorylation (Greengard 1978, Cohen 1982, Bünemann and Hosey 1999, Dickman and Yarden 1999, Graves and Krebs 1999). In the photoreceptor rod of vertebrate retina, there is evidence that phosphorylated proteins may participate in the regulation of visual function. Of particular relevance are proteins that exhibit light-dependent changes in the extent of their phosphorylation (Polans *et al.* 1979, Hermolin *et al.* 1982, Lee *et al.* 1984, Hamm 1990). In the present study using immunological and densitometer methods, we demonstrate that protein phosphorylation or dephosphorylation occurs in the ciliate when light is applied. These observations indicate that the light-dependent processes of protein phosphorylation may be involved in the control of the photophobic behavior of *Blepharisma japonicum*.

MATERIALS AND METHODS

Cell culture

Cells of *Blepharisma japonicum* were grown in 100 ml glass vessels containing Pringsheim solution (pH 7.0) at room temperature in darkness (Fabczak H. *et al.* 1993). The cells were fed with axenically cultured cells of *Tetrahymena pyriformis*. Prior to experiments, the cells were starved for at least 24 h before the organisms were collected, washed in an excess of fresh culture medium and subsequently used for assays after a further 12 h incubation in fresh culture medium in darkness.

Cell stimulation

Before each experiment, 200 µl samples of dark-adapted cells were first left at rest for about 10 min to avoid mechanical disturbances. They were subsequently exposed to light or ionic stimulation. The cell samples were illuminated for 2 s with light afforded by a 150 W fiberoptic light source (MLW, Germany) equipped with an electromagnetic programmable shutter (model 22-841, Ealing Electro-Optics, England). Ionic stimulation was performed by cell incubation for 2 s in external 4 mM K^+ solution prepared by gentle addition of the proper amount 0.1 M KCl to the cell suspension.

Immunoblotting assay

In order to quantify protein phosphorylation levels, samples of control (dark-adapted) cells and cells following treatment with light or potassium ions were immediately mixed after exposure with sample buffer containing 2% SDS, 5% 2-mercaptoethanol, 10% glycerol, 1.0 mM EDTA and 62.5 mM Tris at pH 6.8 (Laemmli 1970) supplemented with protease or phosphatase inhibitors (50 mM NaF, 2 mM phenylmethylsulfonylfluoride, 1 µM okadaic acid, 10 µg/ml aprotinin or 50 µM leupeptin) and then boiled for 5 min. The equal amounts of cell proteins (30 µg) were separated on 10% SDS-polyacrylamide gels (SDS-PAGE) with the use of the Hoefer System (Amersham, USA) and transferred to nitrocellulose filters for 1 h at 100 V in transfer buffer consisting of 192 mM glycine, 20% methanol and 25 mM Tris at pH 8.3 (Towbin *at al.* 1979). For detection of phosphoserine-containing proteins, the blots were incubated in blocking solution composed of 2% BSA in TBS (50 mM NaCl, 25 mM Tris, pH 8.0) and 0.05% Tween-20 (BSA-Tris-Tween) for 2 h at room temperature. After the blocking procedure, the blots were incubated with the primary antibody (Alexis, Switzerland) against phosphoserine overnight at a concentration of 0.05 µg/ml in 0.3% BSA-TBS-Tween at 4 ^{0}C. The nitrocellulose filters were finally washed several times in TBS with 0.05% Tween (TBS-Tween). After washing, the blots were treated for 1h with anti-mouse IgG-horseradish peroxidase conjugates at a dilution of 1:10 000 (Calbiochem) prepared in the blocking buffer. Immunoreactive bands were developed using an Amersham Enhanced Chemiluminescence (ECL) detection system. Their intensities were quantified using a molecular dynamics personal laser densitometer and ImageQuant software. Molecular weights of polypeptides were determined based on their relative electrophoretic mobilities using prestained molecular weight standards (BioRad). In a control set of experiments, incubation with primary antibodies was omitted. The concentration of cell proteins in individual samples was estimated by a method reported elsewhere (Bradford 1976).

RESULTS AND DISCUSSION

Detection of phosphorylated proteins in cell samples were made using three different monoclonal antibodies, Pser-7F12, Pser-4A9 and Pser-1C8, which may specifically recognize phosphorylated serine epitopes. Two of the applied antibodies, Pser-7F12 and Pser-4A9, revealed marked protein phosphorylation levels of similar patterns (Figs 1 A; 2 A), while the Pser-1C8 antibody indicated a lower number of phosphoproteins (Fig. 3 A), possibly due to lower amino acid sequence specificity. It is well known that antibody specificity depends on phosphorylation of the amino acid and on the surrounding amino acid sequence. If one of these two criteria is unfulfilled, the antibody will not detect the phosphorylation site. Most labeled cell proteins were unaffected by illumination, except for proteins of a molecular weight of about 46 kDa (Figs 1 A, B; 2 A) and proteins below 28 kDa (Figs 1 A, B; 2 A; 3 A). The increased phosphorylation of the 46 kDa protein on illumination (Figs 1 A; 2 A and lanes 1, 2) lasts up to 180 s after illumination (Figs 1 A, B; 2 A and lanes 1 to 4). In the

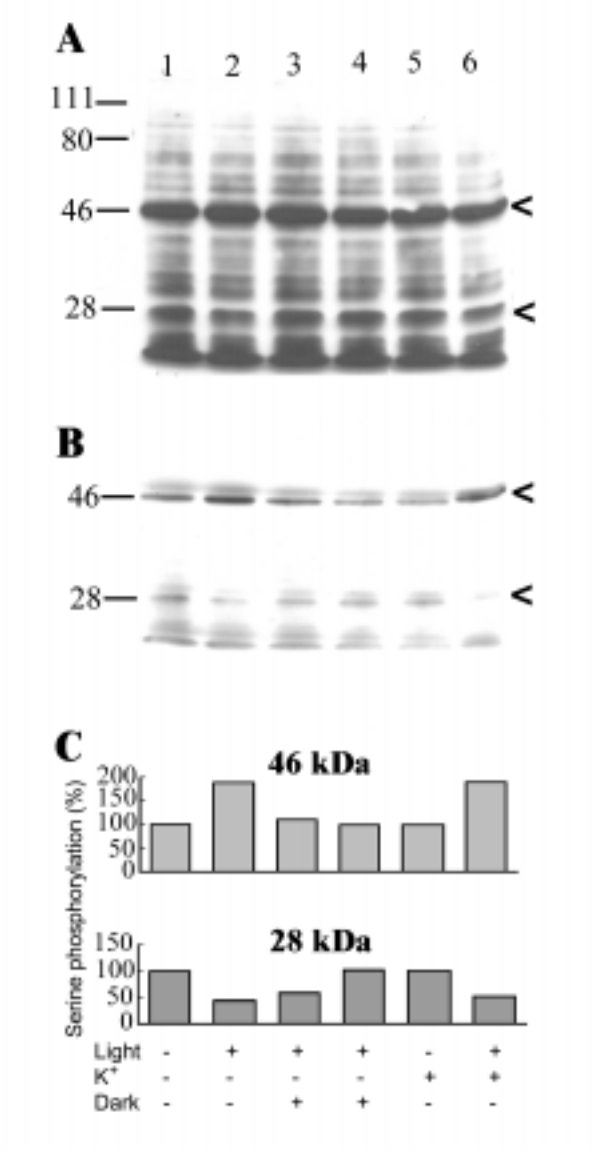

Figs 1 A-C. Detection of light-induced protein phosphorylation in *Blepharisma* by monoclonal antibody, Pser-7F12**. Lane 1:** cells adapted to darkness (control); **Lane 2:** cells exposed to light for 2 s; **Lanes 3, 4:** cells exposed to light for 2 s and then kept in darkness for 180 s and 300 s, respectively; **Lane 5:** dark adapted cells stimulated by 4 mM K^+ for 2 s; **Lane 6:** dark-adapted cells stimulated by 4 mM K^+ and subsequently exposed to light for 2 s. The arrows indicate 46 kDa and 28 kDa proteins, of which phosphorylation levels were altered when illuminated. Immunoblot exposure to X-ray film for 10 s (**A)** and 2 s (**B**); **C** - quantification of protein phosphorylation intensity of bands from **B**. The phosphorylation values found for control cells were defined as 100%

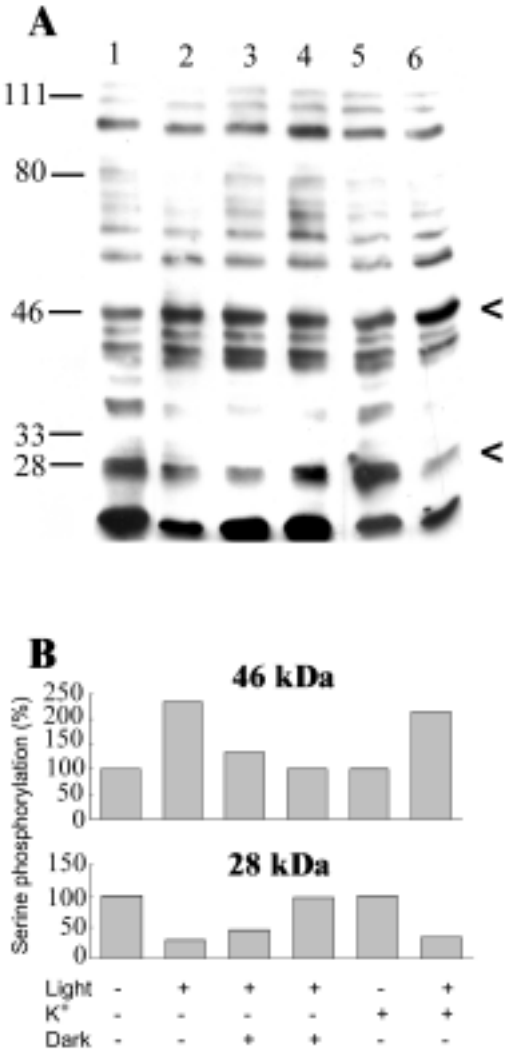

Figs 2 A, B. Detection of protein phosphorylation by light in *Blepharisma* by monoclonal antibody, Pser-4A9. **A -** 30 s exposure of immunoblot to X-ray film. **B** -quantification of serine phosphorylation of 46 kDa and 28 kDa proteins. Other details as in Fig. 1

dark, the most extensively labeled phosphoprotein had an apparent molecular weight of 28 kDa (Figs 1 A, B; 2 A; 3 A and lane 1) and the phosphorylation level of this protein was markedly reduced by illumination (Figs 1 A, B; 2 A; 3 A and lane 2). The light-induced dephosphorylation of 28 kDa protein was entirely reversible, as progressive phosphorylation of the protein was observed in dark-adapted cells for 180 s (Figs 1 A, B; 2 A; 3 A and lane 3) and after about 300 s the phosphorylation level reached the level observed in control cells (Figs 1 A, B; 2 A; 3 A and lane 4).

To test whether phosphorylation and dephosphorylation of cellular proteins in *Blepharisma* is specifically induced by light or is simply elicited by cell membrane

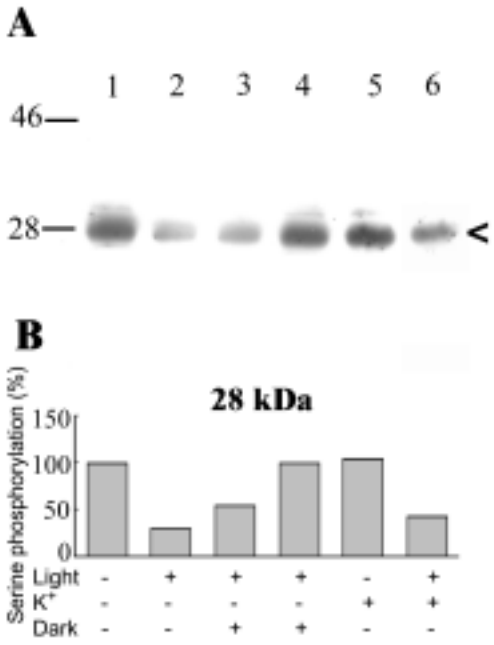

Figs 3 A, B. Detection of light-induced protein phosphorylation in *Blepharisma* by monoclonal antibody, Pser-1C8. **A -** 20 min. exposure of immunoblot to X-ray film. **B -** quantification of serine phosphorylation of the 28 kDa protein. Other details as in Fig. 1

depolarization, the effect of ionic stimulation was examined. These experiments indicate that the phosphorylation level of proteins of 28 kDa and 46 kDa was unaffected by membrane depolarization compared to cell samples exposed to light (Figs 1 A, B; 2 A; 3 A and lane 5). The pattern of protein phosphorylation in cell samples, which were first treated with K^+ and subsequently exposed to light (Figs 1 A, B; 2 A; 3 A and lane 6), was similar to that obtained for cells that were only illuminated (Figs 1 A; 2 A; 3 A and lane 2).

The results of semi-quantitative analysis of protein phosphorylation indicated that the level of phosphorylation of 46 kDa proteins by 2 s illumination caused a two-fold increase over the values found in dark-adapted cells (Figs 1 C; 2 B). In the case of the 28 kDa polypeptide, the level of phosphorylation is lower in all cell samples exposed to light. The phosphorylation levels for both these proteins returned to the control levels after about 300 s of cell incubation under dark conditions (Figs 1 C, 2 B, 3 B).

It has been shown that phosphorylation and dephosphorylation of cellular proteins play a crucial role in the regulation of various sensory transduction pathways (Greengard 1978, Cohen 1982, Bünemann and Hosey 1999, Dickman and Yarden 1999, Graves and Krebs 1999). In the visual system, light induces phosphorylation of photoreceptors (rhodopsin) by a protein kinase (Bownds *et al.* 1972, Kühn 1974, Frank *et al.* 1973). The higher light intensity causes a marked dephosphorylation of proteins of low molecular weight in intact rods (Polans *et al.* 1979, Lee *et al.* 1984, Bownds and Brewer 1986). In the present study, we showed that light is capable of influencing the level of protein phosphorylation in *Blepharisma japonicum*, as it takes place in the photoreceptor cells of vertebrates. In this ciliate, however, the proteins being phosphorylated or dephosphorylated by light have not yet been identified. It was recently shown that the photosensory pigment blepharismin in *Blepharisma japonicum* is associated with a 200 kDa membrane protein (Matsuoka *et al.* 2000). It is likely that the polypeptide of molecular weight of 46 kDa, which underwent highly specific phosphorylation on serine after light stimulation, is associated with the 200 kDa complex photoreceptor protein or it simply represents a fragment of the high molecular weight protein resulting from digestion by endogenous cellular proteases during detergent solubilization (Matsuoka *et al.* 2000). Further investigations are necessary regarding the identification of this protein and elucidation of the mechanism that governs the observed protein phosphorylation and dephosphorylation by light in protozoan ciliate *Blepharisma*.

Acknowledgements. This work was supported in part by grant no. 6P04C-057-18 from the Committee for Scientific Research and the statutory funding for the Nencki Institute of Experimental Biology.

REFERENCES

Binder B. M., Brewer E., Bownds M. D. (1989) Stimulation of protein phosphorylation in frog rod outer segments by protein kinase activators. *J. Biol. Chem.* **264:** 8857-8864

Bownds M. D., Brewer E. (1986) Changes in protein phosphorylations and nucleotide triphosphates during phototransduction. In: The Molecular Mechanism of Photoreception. (Ed. H. Stieves), Springer Verlag, New York Inc., New York, 159-169

Bownds M. D., Bawes J., Miller J., Stahlman M. (1972) Phosphorylation of frog photoreceptor membranes induced by light. *Nature New Biol.* **237:** 125-127

Bradford M. M. (1976) A rapid and sensitive method for the quantitation of microgram quantities of protein utilizing the principle of protein-dye binding. *Anal. Biochem.* **72:** 248-254

Bünemann M., Hosey M. M. (1999) G-protein coupled receptor kinases as modulators of G-protein signaling. *J. Physiol.* **517:** 5-23

Cohen P. (1982) The role of protein phosphorylation in neural and hormonal control of cellular activity. *Nature* **296:** 613-620

Dickman M. B., Yarden O. (1999) Serine/threonine protein kinases and phosphatases in filamentous fungi. *Fungal Gen. Biol.* **26:** 99-117

Fabczak H. (2000a) Protozoa as model system for studies of sensory light transduction: photophobic response in the ciliate *Stentor* and *Blepharisma*. *Acta Protozool.* **39:** 171-181

Fabczak H. (2000b) Contribution of the phosphoinositide-dependent signal pathway to photo motility in *Blepharisma*. *J. Photochem. Photobiol*. *B.* **55:**120-127

Fabczak H., Tao N., Fabczak S., Song P.-S. (1993) Photosensory transduction in ciliates. IV Modulation of the photomovement response of *Blepharisma japonicum* by cGMP. *Photochem. Photobiol*. **57:** 889-892

Fabczak H., Walerczyk M., Fabczak S. (1998) Identification of protein homologous to inositol trisphosphate receptor in ciliate *Blepharisma*. *Acta Protozool*. **37:** 209-213

Fabczak H., Walerczyk M., Groszyńska B., Fabczak S. (1999) Light induces inositol trisphosphate elevation in *Blepharisma japonicum*. *Photochem. Photobiol.* **69:** 254-258

Fabczak S., Fabczak H., Song P.-S. (1993) Photosensory transduction in ciliates. III. The temporal relation between membrane potentials and photomototile responses in *Blepharisma japonicum. Photochem. Photobiol.* **57:** 872-876

Frank R. N., Cavanagh H. D., Kenyon K. R. (1973) Light stimulated phosphorylation of bovine visual pigments by adenosine triphosphate. *J. Biol. Chem.* **248:** 596-609

Giese A. C. (1973) *Blepharisma.* The Biology of a Light-sensitive Protozoan. Stanford Univ. Press, Stanford

Grave J. D., Krebs E. G. (1999) Protein phosphorylation and signal transduction. *Pharmacol. Ther*. **82:** 111-121

Greengard P. (1978) Phosphorylated proteins as physiological effectors. *Science* **199:** 146-152

Hamm H. (1990) Regulation by light of cyclic nucleotide-dependent protein kinases and their substrates in frog rod outer segments. *J. Gen. Physiol.* **95:** 545-567

Hermolin J., Karell M. A., Hamm H. E., Bownds M. D. (1982) Calcium and cyclic GMP regulation of light-sensitive protein phosphorylation in frog photoreceptor membranes. *J. Gen. Physiol.* **79:** 633-655

Ishida M., Shigenaka Y., Taneda K. (1989) Studies on the mechanism of cell elongation in *Blepharisma japonicum.* I. Physiological mechanism how light stimulation evokes cell elongation. *Europ. J. Physiol.* **25:** 182-186

Kraml M., Marwan W. (1983) Photomovement responses of the heterotrichous ciliate *Blepharisma japonicum. Photochem. Photobiol.* **37:** 313-319

Kühn H. (1974) Light dependent-phosphorylation of rhodopsin in living frogs. *Nature (Lond).* **250:** 588-590

Laemmli U. K. (1970) Cleavage of structural proteins during the assembly of the head of bacteriophage T4. *Nature* **277:** 680-685

Lee R. H., Brown B. M., Lolley R. N. (1984) Light-induced dephosphorylation of a 33K protein in rod outer segments of rat retina. *Biochemistry* **23:** 1972-1977

Matsuoka T., Tokumori D., Kotsuki H., Ishida M., Matsushita M., Kimura S., Itoh T., Checcucci G. (2000) Analyses of structure of photoreceptor organelle and blepharismin-associated protein in unicellular eukaryote *Blepharisma. Photochem. Photobiol***. 72:** 709-713

Maeda M., Haoki H., Matsuoka T., Kato Y., Kotsuki H., Utsumi K., Tanaka T. (1997) Blepharismin 1-5, novel photoreceptor from the unicellular organism *Blepharisma japonicum. Tetrahedron Lett.* **38:** 7411-7414

Mast S. O. (1906) Light reactions in lower organisms. 1. *Stentor coeruleus. J. Exp. Biol.* **3:** 359-399

Polans A. S., Hermolin J., Bownds M. D. (1979) Light-induced dephosphorylation of two proteins in frog rod outer segments. *J. Gen Physiol.***74:** 595-613

Rayer B., Naynert M., Stieve H., (1990) Phototransduction; Different mechanisms in vertebrates and invertebrates. *J. Photochem. Photobiol*. *Part B*. **7:** 107-148

Song P.-S., (1997a). Light signal transduction in ciliate *Stentor* and *Blepharisma*. 1. Structure and function of the photoreceptors. In: Biophysics of Photoreception Molecular and Phototransductive Events (Ed. C. Taddei-Ferretti), World Sci., Singapore, New Jersey, London, Hong Kong, 48-66

Song P.-S., (1997b). Light signal transduction in ciliate *Stentor* and *Blepharisma*. 2. Transduction mechanism. In: Biophysics of Photoreception Molecular and Phototransductive Events (Ed. C. Taddei-Ferretti), World Sci., Singapore, New Jersey, London, Hong Kong, 76-82

Tao N., Diforce L., Romanowski M., Meza-Keuthen S., Song P.-S., Furuya M. (1994) *Stentor* and *Blepharisma* photoreceptors: structure and function. *Acta Protozool.* **33:** 199-211

Towbin H., Staehelin T., Gordon J. (1979) Electrophoretic transfer of proteins from polyacrylamide gels to nitrocellulose sheet: Procedure and some applications. *Proc. Natl. Acad. Sci. USA* **76:** 4350-4354

Received and accepted on 10th October, 2001

INSTRUCTIONS FOR AUTHORS

Acta Protozoologica is a quarterly journal that publishes current and comprehensive, experimental, and theoretical contributions across the breadth of protistology, and cell biology of lower Eukaryote including: behaviour, biochemistry and molecular biology, development, ecology, genetics, parasitology, physiology, photobiology, systematics and phylogeny, and ultrastructure. It publishes original research reports, critical reviews of current research written by invited experts in the field, short communications, book reviews, and letters to the Editor. Faunistic notices of local character, minor descriptions, or descriptions of taxa not based on new, (original) data, and purely clinical reports, fall outside the remit of *Acta Protozoologica.*

Contributions should be written in grammatically correct English. Either British or American spelling is permitted, but one must be used consistently within a manuscript. Authors are advised to follow styles outlined in The CBE Manual for Authors, Editors, and Publishers (6th Ed., Cambridge University Press). Poorly written manuscripts will be returned to authors without further consideration.

Research, performed by "authors whose papers have been accepted to be published in *Acta Protozoologica* using mammals, shall have been conducted in accordance with accepted ethical practice, and shall have been approved by the pertinent institutional and/or governmental oversight group(s)"; this is Journal policy, authors must certify in writing that their research conforms to this policy.

Nomenclature of genera and species names must agree with the International Code of Zoological Nomenclature (ICZN), International Trust for Zoological Nomenclature, London, 1999; or the International Code of Botanical Nomenclature, adopted by XIV International Botanical Congress, Berlin, 1987. Biochemical nomenclature should agree with "Biochemical Nomenclature and Related Documents" (A Compendium, 2nd edition, 1992), International Union of Biochemistry and Molecular Biology, published by Portland Press, London and Chapel Hill, UK.

Except for cases where tradition dictates, SI units are to be used. New nucleic acid or amino acid sequences will be published only if they are also deposited with an appropriate data bank (e.g. EMBL, GeneBank, DDBJ).

All manuscripts that conform to the Instructions for Authors will be fully peer-reviewed by members of Editorial Board and expert reviewers. The Author will be requested to return a revised version of the reviewed manuscript within four (4) months of receiving the reviews. If a revised manuscript is received later, it will be considered to be a new submission. There are no page charges, but Authors must cover the reproduction cost of colour illustrations.

The Author(s) of a manuscript, accepted for publication, must transfer copyrights to the publisher. Copyrights include mechanical, electronic, and visual reproduction and distribution. Use of previously published figures, tables, or brief quotations requires the appropriate copyright holder's permission, at the time of manuscript submission; acknowledgement of the contribution must also be included in the manuscript. Submission of a manuscript to *Acta Protozoologica* implies that the contents are original, have not been published previously, and are not under consideration or accepted for publication elsewhere.

SUBMISSION

Authors should submit manuscript to: Dr Jerzy Sikora, Nencki Institute of Experimental Biology, ul. Pasteura 3, 02-093 Warszawa, Poland, Fax: (4822) 8225342; E-mail: jurek@nencki.gov.pl or j.sikora@nencki.gov.pl.

At the time of submission, authors are encouraged to provide names, E-mails, and postal addresses of four persons who might act as reviewers. Extensive information on *Acta Protozoologica* is available at the website: **http://www.nencki.gov.pl/ap.htm**; however, please do not hesitate to contact the Editor.

Hard copy submission: Please submit three (3) high quality sets of text and illustrations (figures, line drawing, and photograph). When photographs are submitted, arranged these in the form of plate. A copy of the text on a disk or CD should also be enclosed, in PC formats, preferably Word for Windows version 6.0 or higher (IBM, IBM compatible, or MacIntosh). If they do not adhere to the standards of the journal the manuscript will be returned to the corresponding author without further consideration.

E-mail submission: Electronic submission of manuscripts by e-mail is acceptable in PDF format only. Illustrations must be prepared according to journal requirement and saved in PDF format. The accepted manuscript should be submitted as a hard copy with illustrations (two copies, one with lettering + one copy without lettering) in accordance with the standards of the journal.

ORGANIZATION OF MANUSCRIPTS

Text: Manuscripts must be typewritten, double-spaced, with numbered pages (12 pt, Times Roman). The manuscript should be organized into the following sections: Title, Summary, Key words, Abbreviations, Introduction, Materials and Methods, Results, Discussion, Acknowledgements, References, Tables, and Figure legends. Figure legends must contain explanations of all symbols and abbreviations used. The Title Page should include the title of the manuscript, first name(s) in full and surname(s) of author(s), the institutional address(es) where the work was carried out, and page heading of up to 40 characters (including spaces). The postal address for correspondence, Fax and E-mail should also be given. Footnotes should be avoided.

Citations in the text should be ordered by name and date but not by number, e.g. (Foissner and Korganova 2000). In the case of more than two authors, the name of the first author and *et al.* should be used, e.g. (Botes *et al.* 2001). Different articles by the same author(s) published in the same year must be marked by the letters a, b, c, etc. (Kpatcha *et al.* 1996a, b). Multiple citations presented in the text must be arranged by date, e.g. (Small 1967, Didier and Detcheva 1974, Jones 1974). If one author is cited more than once, semicolons should separate the other citations, e.g. (Lousier and Parkinson 1984; Foissner 1987, 1991, 1994; Darbyshire *et al.* 1989).

Please observe the following instructions when preparing the electronic copy: (1) label the disk with your name; (2) ensure that the written text is identical to the electronic copy; (3) arrange the text as a single file; do not split it into smaller files; (4) arrange illustrations as separate files; do not use Word files; *.TIF, *.PSD, or *.CDR graphic formats are accepted; (5) when necessary, use only italic, bold, subscript, and superscript formats; do not use other electronic formatting facilities such as multiple font styles, ruler changes, or graphics inserted into the text; (6) do not right-justify the text or use of the hyphen function at the end of lines; (7) avoid the use of footnotes; (8) distinguish the numbers 0 and 1 from the letters O and l; (9) avoid repetition of illustrations and data in the text and tables.

References: References must be listed alphabetically. Examples for bibliographic arrangement:

Journals: Flint J. A., Dobson P. J., Robinson B. S. (2003) Genetic analysis of forty isolates of *Acanthamoeba* group III by multilocus isoenzyme electrophoresis. *Acta Protozool.* **42:** 317-324

Books: Swofford D. L. (1998) PAUP* Phylogenetic Analysis Using Parsimony (*and Other Methods). Ver. 4.0b3. Sinauer Associates, Sunderland, MA

Articles from books: Neto E. D., Steindel M., Passos L. K. F. (1993) The use of RAPD's for the study of the genetic diversity of *Schistosoma mansoni* and *Trypanosoma cruzi*. In: DNA Fingerprinting: State of Science, (Eds. S. D. J. Pena, R. Chakraborty, J. T. Epplen, A. J. Jeffreys). Birkhäuser-Verlag, Basel, 339-345

Illustrations and tables: After acceptance of the paper, drawings and photographs (two copies one with lettering + one copy without) must be submitted. Each table and figure must be on a separate page. Figure legends must be placed, in order, at the end of the manuscript, before the figures. Figure legends must contain explanations of all symbols and abbreviations used. All line drawings and photographs must be labelled, with the first Author's name written on the back. The figures should be numbered in the text using Arabic numerals (e.g. Fig. 1).

Illustrations must fit within either a single column width (86 mm) or the full-page width (177 mm); the maximum length of figures is 231 mm, including the legend. Figures grouped as plates must be mounted on a firm board, trimmed at right angles, accurately mounted, and have edges touching. The engraver will then cut a fine line of separation between figures.

Line drawings should be suitable for reproduction, with well-defined lines and a white background. Avoid fine stippling or shading. Prints are accepted only in *.TIF, *.PSD, and *.CDR graphic formats (Grayscale and Colour - 600 dpi, Art line - 1200 dpi) on CD. Do not use Microsoft Word for figure formatting.

Photographs should be sharp, glossy finish, bromide prints. Magnification should be indicated by a scale bar where appropriate. Pictures of gels should have a lane width of no more than 5 mm, and should preferably fit into a single column.

PROOF SHEETS AND OFFPRINTS

After a manuscript has been accepted, Authors will receive proofs for correction and will be asked to return these to the Editor within 48-hours. Authors will be expected to check the proofs and are fully responsible for any undetected errors. Only spelling errors and small mistakes will be corrected. Twenty-five reprints (25) will be furnished free of charge. Additional reprints can be requested when returning the proofs, but there will be a charge for these; orders after this point will not be accepted.

Indexed in: Current Contents, Biosis, Elsevier Biobase, Chemical Abstracts Service, Protozoological Abstracts, Science Citation Index, Librex-Agen, Polish Scientific Journals Contents - Agric. & Biol. Sci. Data Base at: **http://psjc.icm.edu.pl**, Microbes.info "Spotlight" at **http://www.microbes.info**, and electronic version at Nencki Institute of Experimental Biology website in *.PDF format at http://www.nencki.gov.pl/ap.htm now free of charge.

ACTA
PROTOZOOLOGICA

ORIGINAL ARTICLES

SHORT COMMUNICATIONS

2001 NOVEMBER
VOLUME 40 NUMBER 4